藥 學 博 士 學 位 論 文

Glutaminyl cyclase 저해제로 *N*-(5-methyl-1*H*-imidazol-1-yl)propyl thiourea 골격계 화합물의 구조-활성 연구

강력한 TRPV1 길항제로서 α-Substituted 2-(3-Fluoro-4-methylsulfonamidophenyl)acetamides 화합물의 연구

Part I: Structure-activity relationship of human glutaminyl cyclase inhibitors having an *N*-(5-methyl-1*H*-imidazol-1-yl)propyl thiourea template.

Part II: α-Substituted 2-(3-Fluoro-4-methylsulfonamidophenyl)acetamides as Potent TRPV1 Antagonists.

2015 年 8 月

College of Pharmacy
Seoul National University

By

Tran Phuong Thao

Part I: Structure-activity relationship of human glutaminyl cyclase inhibitors having an *N*-(5-methyl-1*H*-imidazol-1-yl)propyl thiourea template.

Part II: α-Substituted 2-(3-Fluoro-4-methylsulfonamidophenyl)acetamides as Potent TRPV1 Antagonists.

지도교수 이지우

이 논문을 약학박사학위논문으로 제출함
2015 년 8 월

서울대학교 대학원
약학과 약품화학전공
TRAN PHUONG THAO

TRAN PHUONG THAO 의 박사학위논문을 인준함
2015 년 8 월

위 원 장 _____ (인)

부 위 원 장 _____ (인)

위 원 _____ (인)

위 원 _____ (인)

위 원 _____ (인)

Abstract

PART I: Structure-activity relationship of human glutaminyl cyclase inhibitors having an *N*-(5-methyl-1*H*-imidazol-1-yl)propyl thiourea template.

In an effort to design inhibitors of the human glutaminyl cyclase (QC), we have synthesized a library of *N*-aryl *N*-(5-methyl-1*H*-imidazol-1-yl)propyl thioureas and investigated the contribution of the aryl region of these compounds to their structure-activity relationships as cyclase inhibitors. Our design was guided by the proposed binding mode of the preferred substrate for the cyclase.

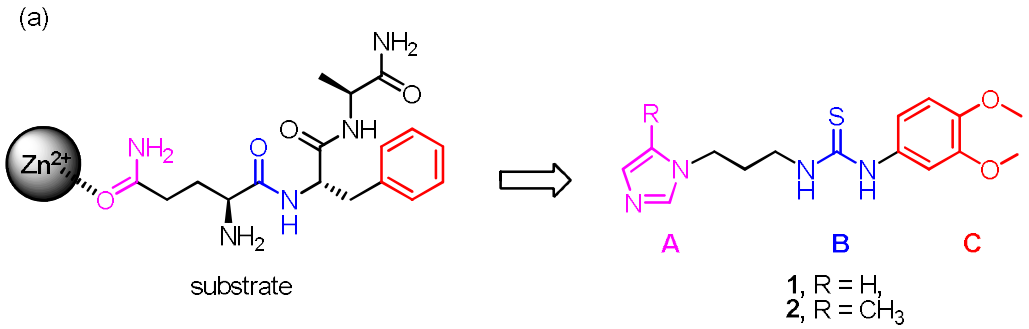

We have developed a new series of QC inhibitors with various constrained analogs of heterocycles and aromatic rings in the C-region. We evaluated their enzyme inhibitory activities and investigated the structure-activity relationships of these derivatives. Compounds with hydrogen-bond acceptors such as oxygen and nitrogen atoms appeared to be more potent than compounds lacking hetero atoms or containing delocalized aromatic rings. Our results indicate that having hydrogen-bond acceptors within the C-region is essential for inhibitory effect. Further exploration of structure-

activity relationships looking at non-aromatic heterocycles should help to identify the crucial interactions within the active site.

PART II: α-Substituted 2-(3-Fluoro-4-methylsulfonamidophenyl)-acetamides as Potent TRPV1 Antagonists.

The transient receptor potential vanilloid 1 channel (TRPV1) has emerged as a very promising therapeutic target, reflecting its central role in nociception and its involvement in a range of diseases. Capsaicin and resiniferatoxin provided early structural leads for understanding the vanilloid pharmacophore, and it was soon recognized that appropriately modified derivatives were able to achieve antagonism. Of particular importance, hyperthermia represents a common side effect of TRPV1 antagonists and the pattern of antagonistic activities for different agonists has been suggested to be related to the ability of an antagonist to cause hyperthermia. Further, different antagonists are differentially affected by the signaling pathways that regulate TRPV1. The availability of novel antagonists will be critical for optimizing such characteristics.

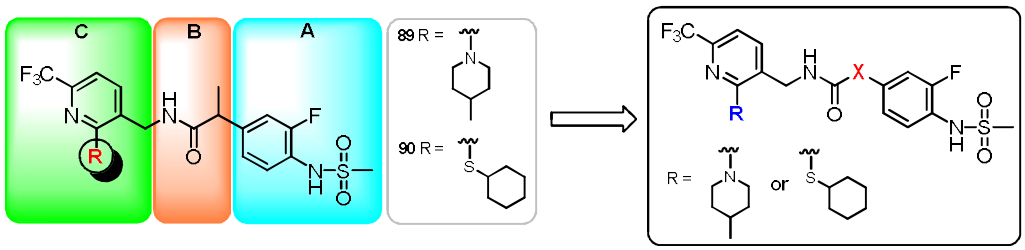

The structure of capsaicin (CAP) has been divided into three pharmacophoric regions. Correspondingly, the antagonistic template was subdivided into the same three pharmacophoric regions, namely the A-region (3-fluoro-4-methylsulfon amidophenyl), the B-region (propanamide), and the C-region ((6-trifluoromethyl-pyridin-3-yl)methyl).

In order to gain better positioning of the C-region with the receptor through α-substitution in the B-region, with consequent enhancement of activity, we have extensively investigated the structure activity relationships of α-substituted acetamide derivatives for *h*TRPV1 antagonism. We describe incorporation of various alkyl, dialkyl and aryl groups at the α-position in the B-region, with 4-methylpiperidinyl and cyclohexylthio groups at the 2-position in the pyridine C-region, and we have evaluated their antagonism of CAP stimulation of *h*TRPV1 expressed in CHO cells.

Key words: Glutaminyl cyclase QC, Alzheimer's disease, Enzyme inhibitor, TRPV1 Antagonist, Analgesis, Capsaicin, Molecular Modeling.

Student ID No. 2010-22881

Table of Contents

List of Tables

List of Figures

List of Schemes

I. PART I: STRUCTURE-ACTIVITY RELATIONSHIP OF HUMAN GLUTAMINYL CYCLASE INHIBITORS HAVING AN *N*-(METHYL-1*H*-IMIDAZOL-1-YL)PROPYL THIOUREA TEMPLATE.

1. Introduction

1.1. Alzheimer's disease (AD)

1.1.1. What is AD?

Dementia is a syndrome caused by damage to nerve cells in the brain, which are called neurons. Because of the damage, neurons can no longer function normally and may die. This, in turn, can lead to a decline in memory or other thinking skills that affects a person's behavior and the ability to perform everyday activities.

Alzheimer's disease (AD), the most common form of dementia, accounts for an estimated 60 percent to 80 percent of cases and currently afflicts more than 44 million persons worldwide.[1] AD was first identified in 1906 by Alois Alzheimer, a German neurologist and psychiatrist,[2] but research into its symptoms, causes, risk factors and treatment has gained momentum only in the last 30 years. Research has reported a great deal about Alzheimer's, however the precise biologic changes that cause Alzheimer's, why it progresses at different rates among affected individuals, and how the disease can be prevented, slowed or stopped is still a challenge. According to 2014 Alzheimer's Disease Facts and Figures, approximately 469,000 people age 65 or older will develop AD in the United States in 2014. The number of new cases of Alzheimer's increases dramatically with age: in 2014, there will be approximately 59,000 new cases among

people age 65 to 74, 172,000 new cases among people age 75 to 84, and 238,000 new cases among people age 85 and older (the "oldest-old"). The prevalence of AD varies among many different factors, including age, family history, genetic (heredity), and education level. A brain autopsy is only method of definitively diagnosing AD. There is no cure for AD, however promising research and development for early detection and treatment is underway.

The symptoms of AD vary among individuals. Early symptoms of Alzheimer's include: difficulty remembering recent conversations, names or events; apathy and depression. Impaired communication, disorientation, confusion, poor judgment, behavior changes and, ultimately, difficulty speaking, swallowing and walking are often later symptoms.

1.1.2. What causes AD?

The causes of AD are not yet fully understood, however many theories have been advanced as to its causes. These include: (1) aggravation of aging, (2) degeneracy of anatomical pathways, including the cholinergic and cortico-cortical pathways, (3) an environmental factor such as aluminium exposure, head injury, or malnutrition, (4) genetic factors including mutations of amyloid precursor protein (APP) and presenilin (PSEN) genes and allelic variation in apolipoprotein E (Apo E), (5) dysfunction of mitochondrial and/or immune system, (6) a compromised blood brain barrier, and (7) infectious agents.[3]

There are two hallmark pathologies of AD: extracellular deposition of beta amyloid-Aβ and intracellular accumulation of tau protein. Both these compounds are insoluble. Aβ is the main component of senile plaques; its deposition is specific for AD and is thought to be primary. Tau is the component of neurofibrillary tangles; its

accumulation is also seen in other degenerative diseases and is thought to be secondary.[4]

What is beta amyloid? Aβ is a 36 to 43 amino acid peptide, which is a small fragment of a transmembrane protein, called the Amyloid Precursor Protein (APP). APP made by neurons and other brain cells. It is also found in extra-neural tissues and is especially abundant in platelets. Its function is unknown. The Aβ amyloid residue is derived from cleavage of APP by the enzymes β-and γ-secretase. Aβ monomers and oligomers are further degraded by other enzymes. Defective clearance of Aβ from aberrant cleavage of APP and other mechanisms results in its accumulation. Aβ monomers polymerize initially into soluble oligomers and then larger insoluble fragments such as $A\beta_{42}$, which precipitate as amyloid fibrils.

Aβ is toxic to neurons. In brain slice preparations, it causes loss of long term potentiation, damages synapses, and kills neurons. Moreover, it shows selective neurotoxicity for the hippocampus and entorrhinal cortex (areas that are severely affected in AD) while sparing cerebellar neurons. This damage is mediated by free radicals, which are generated when soluble Aβ is complexed with Zn^{2+}, Cu^{2+}, and Fe^{3+}. There is a high correlation between the amount of soluble Aβ and the severity of the neurological dysfunction in AD. In transgenic AD models, severe neurological deficits occur in absence of amyloid deposits in tissue.

What is tau? Tau proteins are proteins perform the function of stabilizing microtubules. They are produced through alternative splicing of a single gene called microtubule-associated protein tau (MAPT). The deposition in the neuronal body and processes of insoluble polymers of over-phosphorylated MAPT can describe the neurofibrillary degeneration. A pairs of filaments formed by Tau aggregation is called paired helical filaments that are twisted around one another. By displacing organelles, these deposits interfere with cellular functions. They impair the axonal transport thus

affecting the nutrition of axon terminals and dendrites by distorting the spacing of microtubules. There is no mutation of the tau gene occurring in AD. The sequence of an appearance of an abnormal tau is as follows: Firstly it appears in the entorhinal cortex, then in the hippocampus, and final stages in association cortex. Recent observations in transgenic mice are the evidences indicating that the spread of the pathology to anatomically linked areas occurs by passage of abnormal tau across synapses.

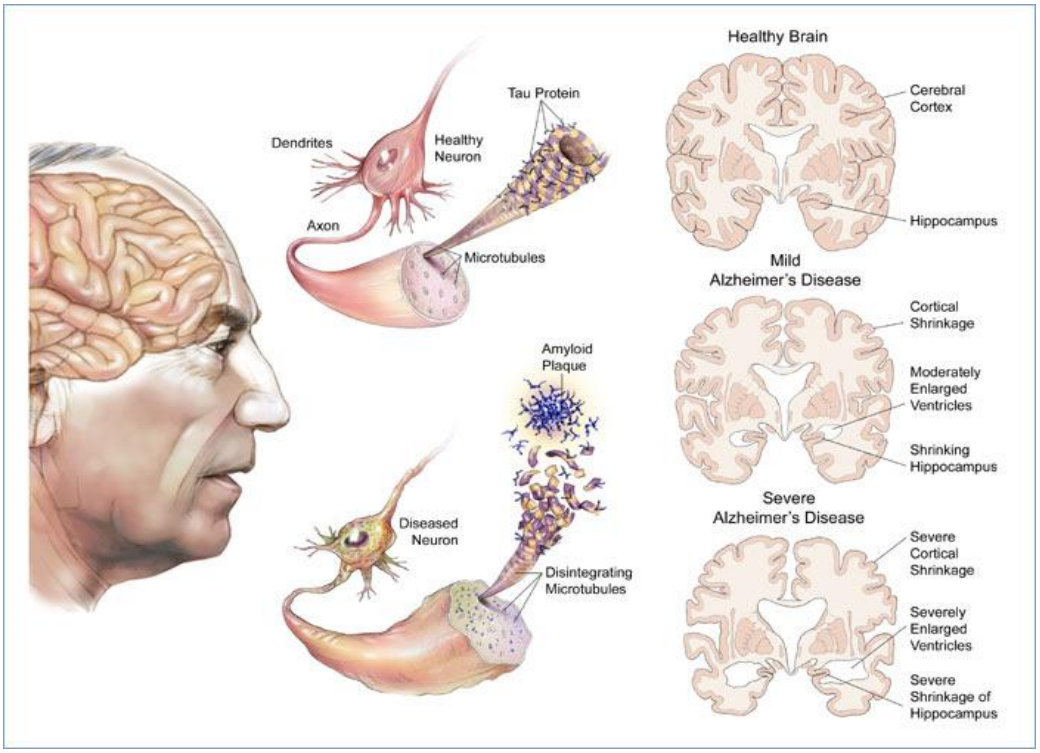

Figure 1. Alzheimer's disease pathological hallmarks and spatio-temporal progression of the disease.[5]

1.1.3. Treatment of AD

The fact that AD is currently incurable but there are multiple drugs that have been proven to slow disease progression and treat symptoms. When initiating treatment for AD patients, "cognitive" and "behavioral and psychiatric" are two symptom categories[2]

which are divided by physicians. While cognitive symptoms affect memory, language, judgment, and thought processes, behavioral symptoms alter a patient's actions and emotions. Using the two categories, we can enable treatment that is specific to the symptoms being experienced. Some treatments for cognitive symptoms and behavioral symptoms are presented as follows.

A. Treatment for Cognitive Symptoms

Treatment of cognitive symptoms focuses on altering the effect of chemical messengers in the brain. For this task, the Food and Drug Administration (FDA) has approved two types of medication.[2] The first type is called a cholinesterase inhibitor that involves in learning and memory. The cholinesterase inhibitor hinders the enzyme responsible for the breakdown of acetylcholine in the brain, in which acetylcholine is an important neurotransmitter involved in learning and memory. While normal aging causes a slight decrease in acetylcholine concentration, the concentration can be decreased by as much as ninety-percent in AD. Consequently, normal aging only leads to periodic forgetfulness but AD can cause significant memory and behavioral decline.[6] To increase the concentration of acetylcholine, the main objective of these drugs is to support communication between nerve cells. There are currently three cholinesterase inhibitors commonly prescribed: donepezil, galantamine, and rivastigmine.

In addition to cholinesterase inhibitors, a medication called Memantine, which has also been approved for the treatment of AD, regulate the activity of glutamate in the brain because glutamate is an excitatory neurotransmitter involved in learning and memory.[7] Glutamate causes overstimulation of nerves which may lead to the neuron degeneration seen in AD, called excitotoxicity.[8] Glutamate binds to N-methyl-D-aspartate (NMDA) receptors on the surface of brain cells. By blocking the NMDA receptors, Memantine protects the nerves from excessive glutamate stimulation.[9] Relying upon these functions, Memantine is indicated in the treatment of moderate to

severe AD and can temporarily delay worsening of cognitive symptoms. Beside of Mematine, there are many medications for AD and the overview of potential treatments for AD is presented in Table 1 as follows.

Table 1: Overview of Potential Treatments for AD[10]

Drug Name	Indication	Action*	Dose
Donepezil (Brand Name: Aricept)	Mild to severe AD	Prevents the breakdown of acetylcholine (ACh) by inhibiting the action of acetylcholinesterase	✓ 5 mg taken once daily ✓ Over time, may increase to 10 mg daily
Galantamine (Brand Name: Nivalin)	Mild to moderate AD	Prevents the breakdown of acetylcholine and stimulates receptors to release excess ACh	✓ 4 mg taken twice daily ✓ Over time, may increase to a maximum of 24 mg daily
Rivastigmine (Brand Name: Exelon)	Mild to moderate AD Also used to treat dementia from Parkinson's Disease	Prevents the breakdown of acetylcholine by inhibiting the enzymes that degrade ACh	✓ 1.5 mg taken twice daily ✓ Over time, may increase to a maximum of 12 mg daily
Memantine (Brand Name: Namenda)	Moderate to severe AD	Blocks glutamatergic (NMDA) receptors and regulates the action of glutamate	✓ 5 mg taken once daily ✓ Over time, may increase to a maximum of 10 mg daily

* All of drugs treat cognitive symptoms of AD

B. Treatment for Behavioral and Psychiatric Symptoms

AD can cause severe behavioral and psychiatric symptoms leading to reduction of cognitive and functionality. These symptoms include anxiety, sleeplessness, agitation, hallucinations, and delusions.[11] To these symptoms, there are possible treatment methods involving non-drug interventions and medications. For example, an effective

non-drug approach is altering the environment to eliminate obstacles and increase security.[2] Another possible approach is investigating any potential interactions between the patient's medications that could cause adverse effects to behavior or psychiatric health. Medication is needed if interventions do not improve the symptoms. Depending on the symptoms, different medications could be chosen. For example, an antidepressant such as Prozac or Zoloft can be prescribed in case of depression while antipsychotics and anxiolytics may be taken to reduce hallucinations and anxiety, respectively.[2]

1.2. Glutaminyl Cyclase (QC) (EC 2.5.2.3)

1.2.1. Overview of QC

Glutaminyl Cyclases (QCs) (EC 2.5.2.3) are acyltransferases that catalyze the cyclization of peptide or protein N-terminal glutaminyl residues into pyroglutamic acid (5-oxoproline) (**Figure 2**). The formation of pyroglutamic acid (p-Glu) is a reaction that serves to stabilize peptides and proteins by preventing N-terminal degradation, but under the physiological conditions of the cell, the spontaneous reaction occurs at a negligible rate.[12]

Aside from the increased molecular stability of p-Glu, the cyclization of N-terminal glutamine (Gln) has also been suggested to serve two important biological functions. First, the presence of p-Glu on several mammalian signaling peptides, hormones, and neurotransmitters (e.g. TRH, GRH)[13,14] appears to enhance the affinity of these ligands for their specific protein receptors.[15] Second, p-Glu residues are thought to serve a protective function by inhibiting the N-terminal proteolysis of polypeptides via aminopeptidases.[15,16]

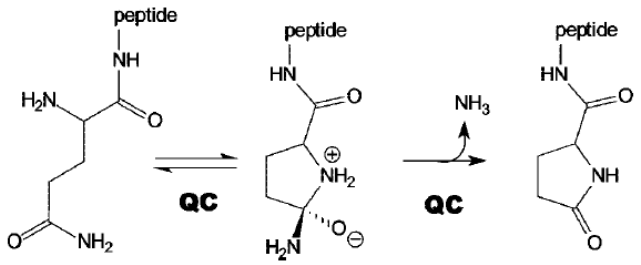

Figure 2. N-terminal cyclization of glutaminyl peptides by QC.[12]

QC is located in mammalian pituitary, hypothalamus, other parts of the brain, adrenal medulla, and B lymphocytes,[17,18] and are highly conserved from yeast to human. Animal QCs were shown to have distinct structure and protein stability from plant QCs despite their similar molecular masses [i.e., 33–40 kDa].[19,20] No bacterial QCs have been reported thus far; however, the mammalian QCs were predicted to exhibit remarkable homology to the bacterial double-zinc aminopeptidases.[21,22]

The structure of human QC was showed in **Figure 3**.[23]

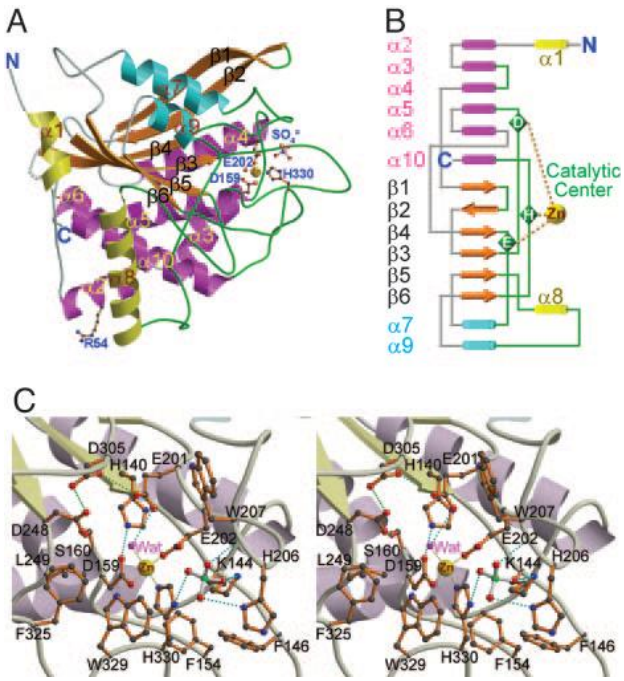

Figure 3. Structure of human QC.
(*A*) A ribbon diagram of the overall structure of human QC. The central six β-strands are colored orange. The α-helices located on the top, bottom, and edge are colored cyan, magenta, and yellow respectively. The zinc ion is shown as a yellow sphere. The zinc-coordinated residues, Arg-54 (genetic mutation to Trp residue occurred frequently in adult women with osteoporosis), and a sulfate ion are depicted with a ball-and-stick model. The coils and loops adjacent to the catalytic center are painted green, whereas those distant from the active site are colored gray. Gray dots represent the disordered region of residues 183–188. (*B*) A topology diagram of the human QC structure. The color codes for secondary structural elements are identical to those in *A*. (*C*) A stereoview of the human QC catalytic region. The active-site residues in conf-A are shown and labeled. Possible hydrogen and coordination bonds are represented with dotted lines colored cyan and yellow, respectively. The green dotted lines depict the possibly unusual hydrogenbonds between D305 and E201 (3.06 Å) and between D305 and D248 (2.53 Å).

1.2.2. Role of QC

In humans, QCs have been implicated in several pathological conditions including amyloidosis,[24] osteoporosis,[25] rheumatoid arthritis,[26] and melanoma.[27] Some peptide hormones, such as tyrotropin releasing hormone (TRH) and gonadotropin releasing hormone (GnRH), require the pGlu on the N-terminus for their biological activity.[28,29] The co-localization of QC and its putative products within the regulated secretory pathway suggests a potential involvement of the enzyme in the final maturation of these peptide hormones.[30]

Recently, it was reported that human QC catalyzes cyclization of the N-terminal glutamate of β-amyloid peptides (Aβ) into pGlu.[31] The resulting pGlu-Aβ peptides become more hydrophobic and resistant to proteolysis. Therefore, they rapidly aggregate and accumulate into neuritic plaques causing neurotoxicity.[32,33] It was demonstrated that pGlu-Aβ peptides are more toxic than other Aβ species such as $A\beta_{1-42}$ and $A\beta_{1-40}$, and they may act as initiators of Alzheimer's disease.[34] Finally, inhibition of QC reduced the amount of both pGlu-Aβ and Aβ plaques in transgenic mouse models of AD indicating that QC is a therapeutically important target in AD.[35]

Hence, besides the crucial role in hormone maturation, human QC might be involved in the pathophysiological process of AD, evoking its qualification as a new potential drug target.

2. Result and Dicussion

2.1. Design

Despite the significant potential role of QC in AD pathology, only a few QC-specific inhibitors have been developed thus far.[36,37] These QC-specific inhibitors have been designed based on two distinct structural characteristics of human QCs. First, the structure of human QC is closely related to that of aminopeptidases and has one zinc ion in the active site.[23] Second, human QC prefers substrates with a large hydrophobic side chain on the position penultimate to the *N*-terminal glutamine.[38] Therefore, previously reported QC-specific inhibitors contain an aromatic ring tethered to an imidazole as a zinc-binding moiety. Based on these findings, we have divided the common structural features of the reported QC-selective inhibitors (**1, 2**) into three regions as shown in **Figure 4**. The A-region represents a zinc-binding imidazole with a methyl substituent on the 5-position to enhance potency.[36] The B-region contains a hydrogen bond donor that matches the C-terminal amide nitrogen of glutamine. The C-region accommodates the hydrophobic side chain penultimate to the N-terminus of the preferred substrate, H-Gln-Phe-Ala-NH_2. Among these three regions, the C-region appears to be the most promising for further modification, because it accommodates various functional groups implying great structural flexibility in that region. Therefore, we decided to focus on modifying the C-region to investigate the structure–activity relationships of QC inhibitors.[39]

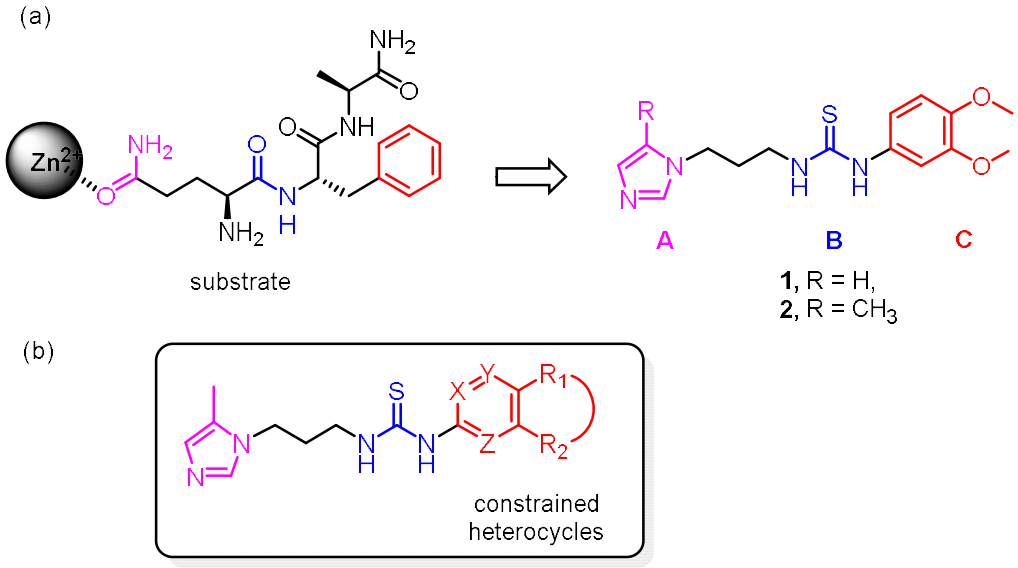

Figure 4. (a) Structures of the previously reported hQC inhibitors; (b) Newly designed scaffold based on the proposed binding mode of the preferred substrate shown in (a).

In this report, we have developed a new series of QC inhibitors with various constrained analogs of heterocycles and aromatic rings in the C-region. We evaluated their enzyme inhibitory activities and investigated the structure–activity relationships of these derivatives.

2.2. Chemistry

The C-region fragments with various aromatic rings and heterocycles were synthesized as shown in **Scheme 1** through **Scheme 4.**

All other amine fragments not listed in the scheme were obtained commercially. Benzofuran and chromane fragments were synthesized from

commercially available coumaran and chromanone, respectively, as shown in **Scheme 1**.

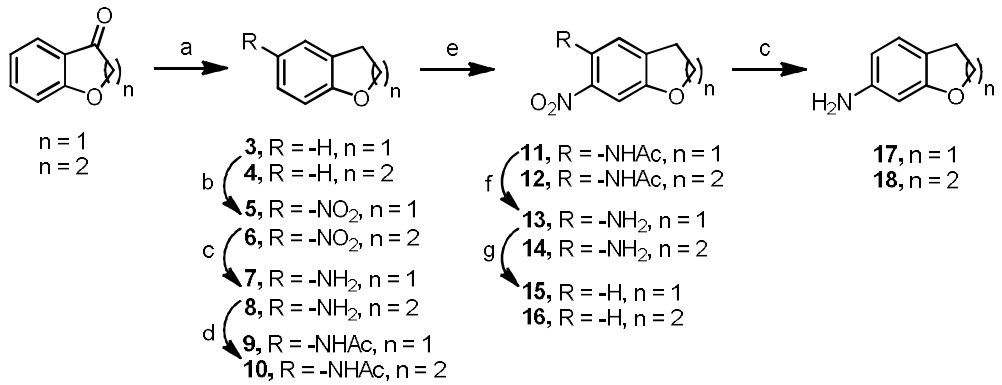

Scheme 1. Syntheses of 5 (or 6)-amino-2,3-dihydrobenzofuran and 6 (or 7)-aminochroman.
Reagents and conditions: (a) $LiAlH_4$, $AlCl_3$, diethyl ether, 0°C to reflux, 1 h; (b) $AgNO_3$, acetyl chloride, MeCN, 1 h, 0°C for **6**, or HNO_3 63%, -10°C, 1 h for **7**; (c) 10% Pd/C, H_2, MeOH:THF (1:1), 2 h, r.t; (d) Ac_2O, 1,4-dioxane, pyridine, 50°C, 2 h, r.t; (e) conc. HNO_3, AcOH, 1.5 h, r.t; (f) conc.HCl, EtOH, 2 h, reflux; (g) isoamylnitrite, THF, 3 h, reflux.

Each ketone was reduced by using $LiAlH_4$ and $AlCl_3$ and then nitrated. Subsequent reduction to the amine yielded fragments **7** and **8**, which were further subjected to another round of acetylation, nitration, deacetylation, deamination and reduction to provide fragments **17** and **18**. Benzoxazine fragments were constructed from 4- or 5-nitro-2-aminophenol as shown in **Scheme 2**. Each aminophenol was cyclized by using chloroacetyl chloride in biphasic media to obtain benzoxazinone intermediates in high yields (95–55%). Subsequent reduction of the ketone and nitro group yielded benzoxazine fragments **25** and **26**.

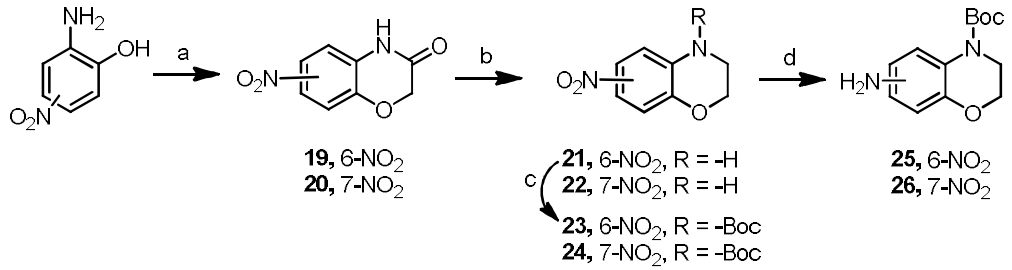

Scheme 2. Syntheses of N-Boc aminobenzoxazine derivatives.
Reagents and conditions: (a) Chloroacetyl chloride, isobutylmethyl ketone:water (1:1), $NaHCO_3$, 0°C (30 mins) to reflux (7 h); (b) BH_3.THF, reflux, 2 h, MeOH, reflux, 1 h; (c) $(Boc)_2O$, $NaHCO_3$, CH_2Cl_2, r.t, 12 h; (d) H_2, 10% Pd/C, MeOH, r.t, 2 h.

Indazole and imidazole fragments were synthesized from commercially available starting material as shown in **Schemes 3 and 4**.

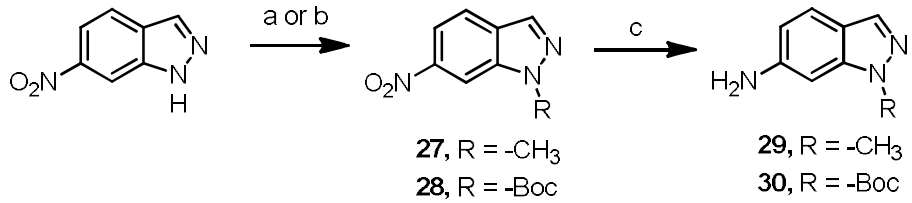

Scheme 3. Syntheses of 1-methyl-5-amino-1*H*-indazole and 1-boc-6-amino-1*H*-indazole.
Reagents and conditions: (a) 60% NaH, iodomethane, DMF, r.t, 1 h; (b) Boc_2O, $NaHCO_3$, THF, r.t, 2 h, (c) 10% Pd/C, H_2, MeOH:THF (2:1), 2 h, r.t.

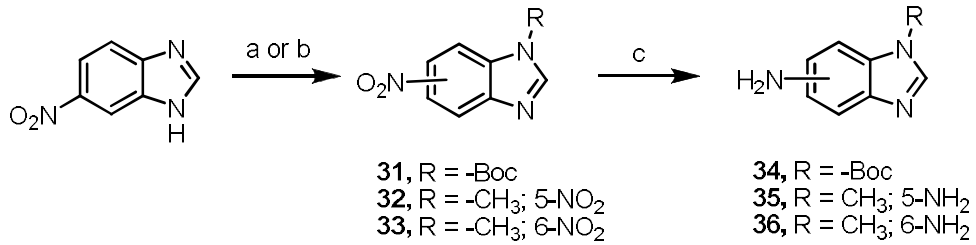

Scheme 4. Syntheses of 1-methyl amino-1*H*-benzimidazole and 1-boc amino-1*H*-benzimidazole derivatives.

Reagents and conditions: (a) Boc_2O, $NaHCO_3$, THF, r.t, 2 h; (b) 60% NaH, iodomethane, DMF, r.t, 1 h; (c) 10% Pd/C, H_2, MeOH, 2 h, r.t.

The A-region fragment with 5-methyl imidazole was synthesized by applying an optimized Gabriel synthesis based on the previously reported procedure[36] as described in **Scheme 5**. The isothiocyanate fragment **41** was synthesized from commercially available 4(5)-methylimidazole in 5 steps to give an overall yield of 36%.

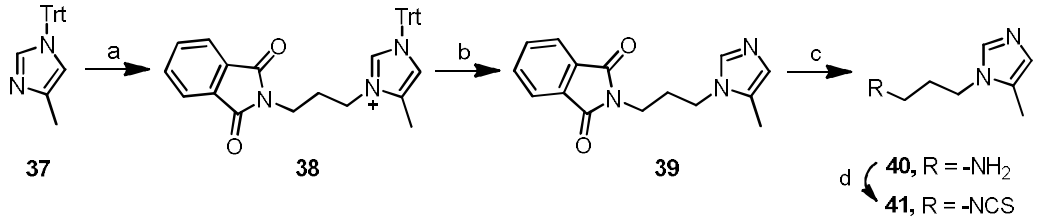

Scheme 5. Syntheses of C-region.
Reagents and conditions: (a) *N*-(3-bromopropyl)phthalimide, MeCN, overnight, reflux; (b) TFA, MeOH, 3 h, reflux; (c) hydrazine monohydrate, EtOH, r.t, 3 h; (d) di-2-pyridyl-thionocarbonate, CH_2Cl_2, 3 h, r.t.

Final coupling steps with all the C-region fragments and isothiocyanate **41** were carried out as demonstrated in **Scheme 6** by using an optimized co-solvent system to obtain thiourea compounds **42–47**, **52–55**, **58–60**, and **65–85** as final products. Bocprotected thiourea compounds **48**, **49**, **61**, and **63** were further subjected to deprotection in 6 N HCl to obtain final compounds **50**, **51**, **62**, **64**. Final products containing tetralone, **54** and **55**, underwent another reduction step with sodium borohydride to afford compounds **56** and **57**.

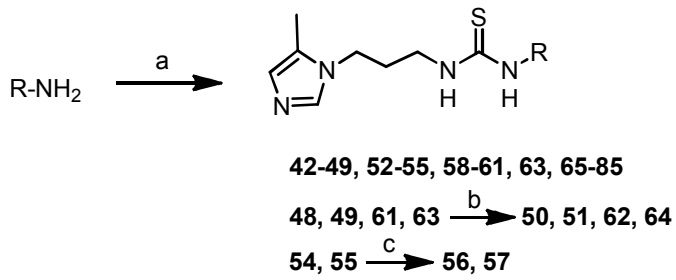

Scheme 6. Thiourea coupling reaction.
Reagents and conditions: (a) **41**, NEt_3, CH_2Cl_2:MeCN (1:1), 2 h, 0°C-r.t; (b) 6N HCl, EtOH, 100°C, overnight; (c) $NaBH_4$, MeOH, r.t, 3 h.

Finally, a reverse quinazolinedione derivative **88** was synthesized from commercially available 2*H*-1,3-benzoxazine-2,4-(1*H*)-dione as shown in **Scheme 7**. The 5-methyl imidazole fragment **40** was added first, and then the quinazolinedione core was cyclized in two steps to provide **88** as final product.

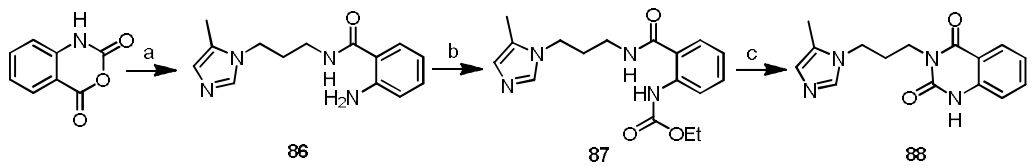

Scheme 7. Synthesis of 3-(3-(5-methyl-1*H*-imidazole-1-yl)propyl)quinazoline-2,4(1*H*,3*H*)-dione.
Reagents and conditions: (a) **40**, THF r.t, overnight; (b) EtOCOCl, EtOH, reflux, 3 h; (c) KOH, EtOH, reflux.

2.3. Biological Activity

Glutaminyl cyclase is expressed in various cell lines including HEK293.[40] In this study, we lysed HEK293 cells expressing endogeous QC with RIPA-buffer and used the lysates as the source of QC for our *in vitro* assays.[40] QC activity was assayed as described by Schilling *et al.*[41] and IC_{50} values (**Table 2** and **Table 3)** were determined from the inhibitory dose response curves. The IC_{50} value of the previously reported compound **2** was measured for comparison.

Compounds **42-57** and compound **88** containing various 5- and 6-membered ring constrained analogs exhibited IC_{50} values ranging from 58 nM to low micromolar concentrations (**Table 2**). Compound **52** was the most potent compound reported to date being twice as potent as the reference compound **2**, the best QC inhibitor so far.[36,37] When one of the oxygen atoms in the fused dioxane was replaced with either nitrogen or carbon, as shown with compounds **46-51**, the IC_{50} value was significantly increased. Additionally, when the ether group was replaced with a ketone, inhibitory potency decreased slightly (**54** and **55**), and reduction of the ketone to an alcohol reduced potency even further (**56** and **57**), yielding IC_{50} values 10-fold weaker than that of **52**. Furthermore, when the position of the dioxane ring was moved as shown in **53**, the compound completely lost its activity. Based on these observations, possible hydrogen bonding interactions exist in this specific region, and the presence of hydrogen bond acceptors appears to be crucial for binding.

When the fused dioxane was replaced with a dioxolane (compound **42**), the IC_{50} value increased up to three-fold. Again, inhibitory effects decreased further when the oxygen atoms were replaced with carbon (**43-45**) as was observed with the dioxane analogs. Interestingly, a reverse quinazolinedione analog **88** demonstrated comparable potency (IC_{50} = 123 nM), which warrants further investigation with various analogs. Significant activity changes within this series indicate that the electronic properties and spatial arrangements in the C-region are critical for inhibitory activity.

Table 2. IC_{50} values for inhibition of hQC by benzocyclic compounds

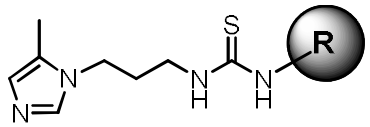

R	IC_{50} (nM)[a]	R	IC_{50} (nM)

2	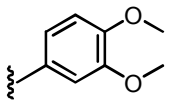	119	**51**	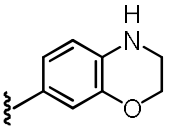	1070
42	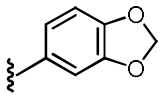	185	**52**	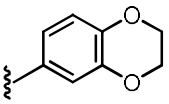	58
43	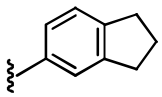	WE[b]	**53**	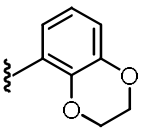	NE[b]
44	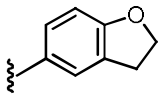	437	**54**	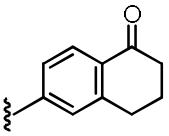	482
45	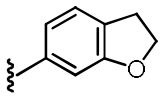	405	**55**	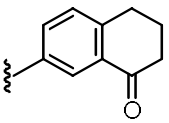	788
46	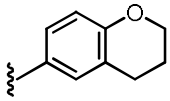	208	**56**	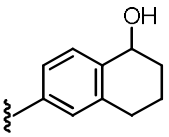	519
47	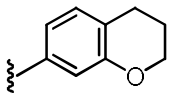	479	**57**	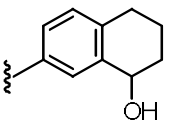	812
50	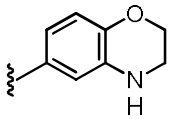	492	**88**	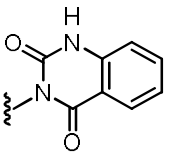	123

a The values indicate the mean of at least three experiments.
b WE: weakly effective, NE: not effective.

IC_{50} values of compounds with various 5-and 6-membered aromatic heterocycles are presented in **Table 3**. Compounds **60** and **78** demonstrated comparable potency having IC_{50} values of 239 nM and 158 nM respectively. Compounds in this series showed slightly weaker inhibitory potencies compared to the non-aromatic heterocycles in **Table 2**, suggesting that these planar aromatic rings may not fit well inside the active site. Additionally, compounds lacking hydrogen-bond acceptors demonstrated poor inhibition whereas compounds having more electron-withdrawing atoms at specific positions appeared to exhibit higher inhibitory effects. Again, these findings support our initial observations that hydrogen-bonding interactions are critical in the C-region for specific inhibition.

Table 3. IC_{50} values for inhibition of hQC by heterocyclic compounds

	R	IC_{50} (nM)[a]		R	IC_{50} (nM)
2	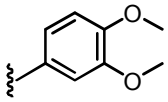	119	**73**	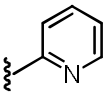	453
58	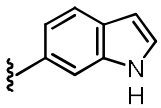	WE[b]	**74**	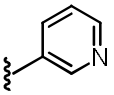	WE[b]
59	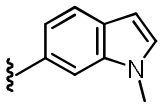	1613	**75**	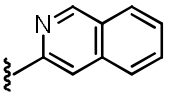	518
60	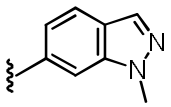	239	**76**	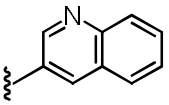	WE[b]
62	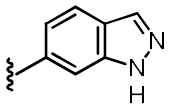	381	**77**	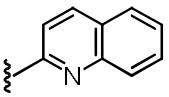	337

64	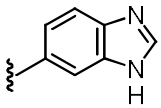	463	**78**	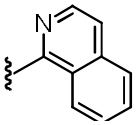	158
65	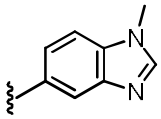	711	**79**	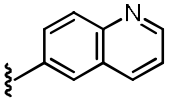	293
66	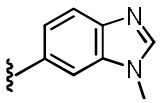	461	**80**	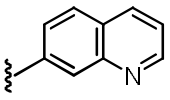	768
67	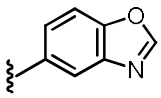	475	**81**	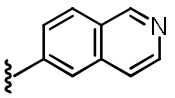	WE[b]
68	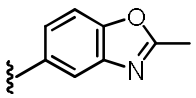	524	**82**	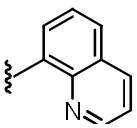	WE[b]
69	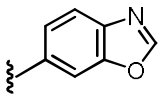	1070	**83**	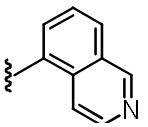	546
70	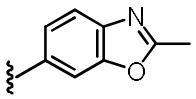	329	**84**	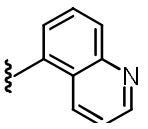	375
71	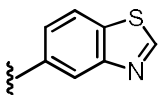	1220	**85**	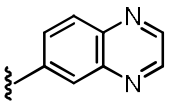	3050
72	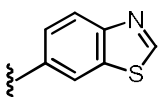	488			

a The values indicate the mean of at least three experiments.
b WE: weakly effective.

3. Conclusion

We have developed a series of potent hQC inhibitors and determined IC_{50} values against recombinant hQC. Among the compounds of this series, compound **52** is the most potent hQC inhibitor developed to date, two-fold more potent than the previously reported inhibitor. Several other compounds, **42**, **78** and **88**, demonstrated potencies close to the reference compound **2**. Compounds with hydrogen-bond acceptors such as oxygen and nitrogen atoms appeared to be more potent than compounds lacking hetero atoms or containing delocalized aromatic rings. Our results indicate that having hydrogen-bond acceptors within the C-region is essential for inhibitory effect. Further exploration of structure-activity relationships looking at non-aromatic heterocycles should help to identify the crucial interactions within the active site. Compound **52** emerged as the most promising candidate for future evaluation to monitor its ability to reduce the formation of pGlu-Aβ and Aβ plaques in cells and transgenic animals.

4. Experiment section

4.1. General Experimental

All chemical reagents were commercially available. Melting points were determined on a melting point Buchi B-540 apparatus and are uncorrected. Silica gel column chromatography was performed on silica gel 60, 230–400 mesh, Merck. PLC plates were used PLC silica gel 60 F_{254}, 1mm, Merck. Proton NMR spectra were recorded on a JEOL JNM-LA 300 at 300 MHz, Bruker Analytik, DE/AVANCE Digital 400 at 400 MHz, and Bruker Analytik, DE/AVANCE Digital 500 at 500 MHz. Chemical shifts are reported in ppm units with Me_4Si as a reference standard. Mass spectra were recorded on a VG Trio-2 GC-MS.

4.2. Syntheses of Human glutaminyl cyclase inhibitors having an *N*-(5-methyl-1*H*-imidazol-1-yl)propyl thiourea template

4.2.1. General procedure for thiourea coupling

Procedure A: The isothiocyanate compound (1 equiv.) was added to the solution of amine (1 equiv.) in 5 ml of a mixture of dichloromethane and acetonitrile (1:1, v/v). The mixture was cooled to 0°C. Then, triethylamine (2 equiv.) was added gradually. The mixture was stirred at 0°C for 15 minutes, after which stirring was continued at room temperature for 2-10 h. The reaction mixture was concentrated, extracted with dichloromethane, and washed with brine. The organic layer was dried over $MgSO_4$ and purified by column chromatography ($MeOH:CH_2Cl_2$) or by preparative TLC ($MeOH:CH_2Cl_2$) to afford the desired product.

4.2.2. General procedure for reduction of the nitro group to the amine

Procedure B: The nitro-group containing compound was dissolved in MeOH (or a mixture of MeOH and tetrahydrofuran) and then 10% Pd/C was added. The mixture was stirred at room temperature under hydrogen gas until the starting material had been consumed. The crude mixture was filtered through Celite, washed with methanol, and then concentrated. The product was carried on to the next step without further purification or was purified by column chromatography.

4.2.3. General procedure for Boc-protection

Procedure C: $NaHCO_3$ (3.3 equiv.) was added to the solution of the amine (1 equiv.) at 0 ^oC, stirred for 30 minutes, and then di-*tert*-butyl dicarbonate (1.1 equiv.) was added to the reaction mixture. The reaction was continued at room temperature for 2 h and then diluted with ethyl acetate. It was washed with H_2O and then with brine. Finally, it was

dried over $MgSO_4$, concentrated, and purified by column chromatography to give the desired product.

4.2.4. General procedure for Boc-deprotection

Procedure D: The Boc-protected compound was treated in ethanol with 6N HCl (4 equiv.). The reaction mixture was heated at 100°C until the starting material was consumed. It was then basified with K_2CO_3 to pH >8 and extracted with ethyl acetate. The organic layers were combined and concentrated under reduced pressure. The crude residue was purified by column chromatography or PLC to give the desired product.

4.2.5. General procedure for *N*-methylation

Procedure E: NaH (1.1 equiv) was added to the solution of amine (1 equiv.) in anhydrous *N*,*N*-dimethylformamide. Iodomethane (1.1 equiv.) was added dropwise to the reaction mixture at 0°C. The reaction was continued at room temperature until the starting material was consumed. The resulting mixture was diluted with ethyl acetate and washed with water and brine. The organic layer was dried over $MgSO_4$ and concentrated under reduced pressure. The product was carried on to the next reaction without further purification or was isolated by column chromatography.

Chroman (4).

To a solution of chroman-4-one (10 g, 1 equiv.) in diethyl ether was slowly added aluminum chloride (31.5 g, 3.5 equiv.) at 0°C, followed by lithium aluminium hydride (4.35 g, 1.75 equiv.) added portionwise. The reaction mixture was stirred for 1 h at boiling temperature. The reaction was cooled, and a solution of NH_4HCO_3 was added slowly, after which the solution was filtered through a plug of Celite and extracted with ethyl acetate (3×200 mL). The combined organic extracts were washed with water

(3×100 mL), and brine (100 mL), dried over $MgSO_4$, and purified by chromatography on a silica gel column (EA:n-hexane = 1:9) to give **4** (4.88 g, 54%) as a light yellow oil.

5-Nitro-2,3-dihydrobenzofuran (5).

Silver nitrate (1.41 g, 8.32 mmol) and coumaran **3** (0.59 mL, 8.32 mmol) were dissolved in acetonitrile (10 mL) and placed in a 100 mL three-necked flask equipped with a dropping funnel, condenser and drying tube, and thermometer. 0.59 mL (8.32 mmol) of acetyl chloride was added to the reaction mixture at 0°C. As the quantity of silver chloride increased, further dilution with acetonitrile and more vigorous stirring were used to help maintain reactant contact for one hour at 0-5^{o}C and for four hours at room temperature. 20 mL of water was added to the reaction flask at 0°C and then an additional 10 mL of water was added when the mixture was at room temperature. Exhaustive treatments of solid and liquid materials with ethyl acetate were used to extract the products. The organic layer was concentrated, dried over $MgSO_4$, and then purified by column chromatography (EA:n-hexan) to give 740 mg of **5** (54%) as a yellow solid.

6-Nitrochroman (6).

To chroman **4** (4.88 g) was added dropwise a solution of HNO_3 (8.5 mL, 63%) at -10^{o}C for 1 h. After the reaction was completed, the mixture was basified with a 10% solution of NaOH and extracted with dichloromethane (3×100 mL). The combined organic extracts were washed with water (3×50 mL) and brine, dried over $MgSO_4$, and purified by chromatography on a silica gel column (EA:n-hexane gradient) to give **6** (1.35 g, 19%) as a yellow solid.

5-Amino-2,3-dihydrobenzofuran (7) and 6-aminochroman (8).

Prepared from compound **5** or **6** respectively by following the general procedure B described above**.**

***N*-(2,3-nihydrobenzofuran-5-yl)acetamide (9) and *N*-(chroman-6-yl)acetamide (10).**

Ac_2O (2 equiv.) and pyridine (1 equiv.) were added dropwise to a stirred solution of compound **7** or **8**, respectively, (1 equiv.) in dioxane (4 mL) at 0°C and the solution was stirred at 20°C for 16 h. The solution was diluted with water (50 mL) and extracted with ethyl acetate (3×50 mL). The organic layer was washed with brine, dried over $MgSO_4$, and then evaporated to give **9** (99%) as a brown solid or **10** (86%) as a white solid.

***N*-(6-nitro-2,3-dihydrobenzofuran-5-yl)acetamide (11) and *N*-(7-nitrochroman-6-yl)acetamide (12).**

A solution of conc. HNO_3 (1.4 equiv.) in HOAc (1 mL) was added dropwise to a stirred solution of acetamide **9** or **10** (1 equiv.) in HOAc (10 mL) at 15°C. The mixture was stirred at 15°C for 1 h and then poured into ice/water (80 mL) and stirred for 30 min. The combined solvent was extracted with ethyl acetate, dried over $MgSO_4$, and then evaporated, purified by chromatography on a silica gel column (EA:n-hexane gradient) to give **11** in 64% yield as a brown solid or **12** in 33% yield as a yellow solid.

Nitroaniline (13) and 7-nitrochroman-6-amine (14).

A suspension of **11** or **12** (2.07 mmol) and conc. HCl (6.5 mL) in EtOH (25 mL) was heated at reflux temperature for 2 h. The solution was cooled, carefully neutralized with aqueous NH_3 solution, and the resulting precipitate was filtered and dried to give **13** (227 mg, 61%) as an orange solid or **14** (368.5 mg, 99%) as a brown solid.

6-Nitro-2,3-dihydrobenzofuran (15) and 7-nitrochroman (16).

Isoamylnitrite (3 equiv.) was added dropwise to a solution of **13** or **14** (1 equiv.) in anhydrous THF at 0°C. The reaction mixture was stirred at 0°C for 15 minutes and then refluxed for 3 h. The solution was cooled to room temperature, water (50 mL) was added, and the solution was extracted with ethyl acetate (3×50 mL). The organic layer was washed with brine, dried over $MgSO_4$, then evaporated and purified by column chromatography with a gradient eluent of EA:n-Hexane (2%-8%) to give **15** (70%) as a yellow solid or **16** (74%) as a yellow solid.

6-Amino-2,3-dihydrobenzofuran (17) and 7-aminochroman (18).

Prepared from nitro compounds **15** and **16** by following the general reduction procedure B with 56% and 83% yield, respectively.

6-Nitro-2*H*-benzo[*b*][1,4]oxazin-3(4*H*)-one (19) and 7-nitro-2*H*-benzo[*b*][1,4] oxazin-3(4*H*)-one (20).

To a solution of the 4- or 5-nitro-2-aminophenol (400 mg, 1 equiv.) in isobutyl methylketone (4 mL) was added $NaHCO_3$ (522 mg, 2.4 equiv.) and water (4 mL) and then the resulting mixture was cooled in an ice-bath. Chloroacetyl chloride (0.24 mL, 1.15 mL) was added dropwise with stirring and the cold mixture was set aside until it reached ambient temperature; it was then refluxed for 7 h. The mixture was extracted with ethyl acetate (3×30 mL), washed with water (2×30 mL), brine (30 mL) and dried over $MgSO_4$, and then it was concentrated under vacuum to give **19** (95% yield) or **20** (99% yield) as a brown solid.

6-Nitro-3,4-dihydro-2*H*-benzo[*b*][1,4]oxazine (21) and 7-nitro-3,4-dihydro-2*H*-benzo[*b*][1,4]oxazine (22).

To a solution of **19** or **20** (500 mg) in anhydrous THF was added dropwise boran tetrahydrofuran complex solution (1.0 M, 5.2 mL). The reaction mixture was heated to reflux for 2 h and then 4 mL MeOH was added. After 1 h, NH_4HCO_3 solution was added to the reaction mixture. The mixture was extracted with dichloromethane, washed with water, dried over $MgSO_4$, and concentrated under vacuum to give compound **21** or **22** with 53% or 62% yield, respectively, as an orange solid.

***Tert*-butyl 6-nitro-2*H*-benzo[*b*][1,4]oxazine-4(3*H*)-carboxylate (23) and *tert*-butyl 7-nitro-2*H*-benzo[*b*][1,4]oxazine-4(3*H*)-carboxylate (24).**

Prepared by following the general Boc-protection (procedure C) from the corresponding compounds **21** and **22**. Products **23** and **24** were obtained with 50% and 90% yields, respectively, as yellow solids.

***Tert*-butyl 6-amino-2*H*-benzo[*b*][1,4]oxazine-4(3*H*)-carboxylate (25) and *tert*-butyl 7-amino-2*H*-benzo[*b*][1,4]oxazine-4(3*H*)-carboxylate (26)**.

Synthesized from nitro compounds **23** or **24** by following the general procedure B.

1-Methyl-6-nitro-1*H*-indazole (27).

Prepared from commercially available 6-nitroindazole by following the general procedure E. Two isomers were obtained, 1-methyl-6-nitro-1*H*-indazole (**27**) as a yellow solid (59% yield) and 1-methyl-5-nitro-1*H*-indazole as an orange solid (38% yield).

***Tert*-butyl 6-nitro-1*H*-indazole-1-carboxylate (28).**

Prepared from commercially available 6-nitroindazole by following the general procedure C. Product as a yellow solid (99% yield) was carried on to the next step without further purification.

1-Methyl-6-amino-1*H*-indazole (29).

Synthesized from **27** by following the general procedure B.

***Tert*-butyl 6-amino-1*H*-indazole-1-carboxylate (30).**

Prepared from nitro compound **28** by following the general procedure B and purified by column chromatography with an EtOAc:n-hexane (1:1) system to give the desired product as a yellow solid (67% yield).

***Tert*-butyl 5-nitro-1*H*-benzo[*d*]imidazole-1-carboxylate or *tert*-butyl 6-nitro-1*H*-benzo[*d*]imidazole-1-carboxylate (31).**

Prepared from commercially available 6-nitrobenzimidazole by following the general procedure C. The mixture of 5-and 6-nitro compounds was not separated.

1-Methyl-5-nitro-1*H*-benzo[*d*]imidazole (32) and 1-methyl-6-nitro-1*H*-benzo[*d*]imidazole (33).

Prepared from commercially available 6-nitrobenzimidazole by following the general procedure E. The mixture of **32** and **33** was obtained as an orange solid (99% yield).

***Tert*-butyl 5-amino-1*H*-benzo[*d*]imidazole-1-carboxylate or *tert*-butyl 6-amino-1*H*-benzo[*d*]imidazole-1-carboxylate (34).**

Compound **34** was prepared from **31** by following the general procedure B to give the corresponding amine in 62% yield, as a yellow oil.

1-Methyl-5-amino-1*H*-benzo[*d*]imidazole (35) and 1-methyl-6-amino-1*H*-benzo[*d*]imidazole (36).

Prepared from the mixture of **32** and **33** by following the general procedure B to give amines **35** (45% yield) and **36** (40% yield) as brown solids.

4-Methyl-1-trityl-1*H*-imidazole (37).

4(5)-Methylimidazole (5 g, 60.94 mmol) was dissolved in 20 mL of *N*,*N*-dimethylformamide, and triethylamine (17 mL, 121.88 mmol) and trityl chloride (18.69 g, 67 mmol) were added. The mixture was stirred for 2 h. The precipitate was filtered off and then washed with ice-cooled *N, N*-dimethylformamide (3×50 mL) and water (3×50 mL). After the solvent was removed, the remaining product was dissolved in dichloromethane and then was washed with water. The organic layer was dried over $MgSO_4$ and was concentrated by rotary evaporation. Compound **37** as a white solid (18 g, 92%) was used without further purification.

2-(3-(5-Methyl-1*H*-imidazol-1-yl)propyl)isoindoline-1,3-dione (39).

Compound **37** (3 g, 9.26 mmol) was suspended in 30 mL acetonitrile and 2-(3-bromopropyl)phthalimide (1.48 g, 9.26 mmol) was added. The mixture was kept under reflux overnight and concentrated to give **38**. Crude mixture **38** was dissolved in a stirred solution containing methanol (20 mL) and trifluoroacetic acid (3 mL). The mixture was kept under reflux overnight. The solvent was removed, and the remaining oil was purified by flash chromatography using silica gel and a MC/MeOH gradient. Yield: 1.52 g (61%).

3-(5-Methyl-1*H*-imidazol-1-yl)propan-1-amine (40).

Compound **39** (300 mg, 1.11 mmol) was dissolved in 2 mL ethanol and hydrazine monohydrate (0.27 ml, 5.55 mmol) was added dropwise. The mixture was stirred at room temperature for 2 h. The formed precipitate was filtered off and washed with EtOH. The filtrate was collected and concentrated by rotary evaporation. The yellow oil product 3-(5-methyl-1*H*-imidazol-1-yl) propan-1-amine **40** (144 mg, 93%) was carried on to the next step without further purification. ^{1}H NMR (300 MHz, CD_3OD): δ 7.56 (d, J = 0.9 Hz, 1H), 6.67 (s, 1H), 4.01 (t, J = 7.14 Hz, 2H), 2.65 (t, J = 7.14 Hz, 2H), 2.22 (d, J = 0.93 Hz, 3H), 1.92 (quintet, J = 7.32 Hz, 2H). MS (FAB) *m/z*: 140 $[M+H]^+$.

1-(3-Isothiocyanatopropyl)-5-methyl-1*H*-imidazole (41).

Di-2-pyridylthionocarbonate (DPT) (834 mg, 3.59 mmol) in anhydrous dichloromethane was added to a solution of compound **40** (500 mg, 3.59 mmol) in anhydrous dichloromethane. The mixture was stirred at room temperature for 2 h until the starting material was consumed. The reaction mixture was evaporated and purified by column chromatography (MeOH:MC) to yield the product as an orange oil (418 mg, 64%). ^{1}H NMR (300 MHz, CD_3OD): δ 7.43 (d, J = 0.93 Hz, 1H), 6.8 (s, 1H), 4.04 (t, J = 6.78 Hz, 2H), 3.55 (t, J = 6.21 Hz, 2H), 2.23 (d, J = 0.93 Hz, 3H), 2.13 (quintet, J = 6.21Hz, 2H). MS (FAB) *m/z*: 182 $[M+H]^+$.

1-(Benzo[*d*][1,3]dioxol-5-yl)-3-(3-(5-methyl-1*H*-imidazol-1-yl)propyl)thiourea (42).

Prepared from commercially available 3,4-(methylenedioxy)aniline by following the general thiourea coupling procedure: 50% yield, white solid, mp = 92-93^{o}C; ^{1}H NMR (500 MHz, CD_3OD): δ 7.59 (s, 1H), 6.81(d, J = 8.2 Hz, 1H), 6.78 (d, J = 1.8 Hz, 2H), 6.67-6.65 (m, 2H), 5.96 (s, 2H), 4.54 (br, 1H), 3.98 (t, J = 4.1 Hz, 2H), 3.60 (t, J = 6.8 Hz, 2H), 2.21 (s, 3H), 2.06 (quintet, J = 7.1 Hz, 2H). MS (FAB) *m/z*: 319 $[M+H]^+$.

1-(2,3-Dihydro-1*H*-inden-5-yl)-3-(3-(5-methyl-1*H*-imidazol-1-yl)propyl)thiourea (43).

Prepared from commercially available 5-aminoindan by following the general thiourea coupling procedure: 65% yield, white solid, mp = 94-95°C; ^{1}H NMR (500 MHz, CD_3OD): δ 7.59 (s, 1H), 7.21 (d, J = 7.9 Hz, 1H), 7.09 (s, 1H), 6.97 (d, J = 7.85 Hz, 1H), 6.66 (s, 1H), 3.98 (t, J = 7.25 Hz, 2H), 3.61 (t, J = 6.8 Hz, 2H), 2.91-2.86 (m, 4H), 2.21 (s, 3H), 2.11-2.00 (m, 4H). MS (FAB) *m/z*: 315 $[M+H]^+$.

1-(2,3-Dihydrobenzofuran-5-yl)-3-(3-(5-methyl-1*H*-imidazol-1-yl)propyl)thiourea (44).

Prepared from amine **7** by following the general thiourea coupling procedure: 81% yield, white solid, mp = 151-152°C; ^{1}H NMR (300 MHz, CD_3OD): δ 7.59 (d, J = 1.08 Hz , 1H), 7.07 (s, 1H), 6.93 (dd, J_1 = 2.37 Hz, J_2 = 8.4 Hz, 1H), 6.74 (d, J = 8.43 Hz, 1H), 6.66 (s, 1H), 4.58 (t, J = 8.79 Hz, 2H), 3.96 (t, J = 7.32 Hz, 2H), 3.58 (t, J = 6.96 Hz, 2H), 3.20 (t, J = 8.61 Hz, 2H), 2.22 (d, J = 1.08 Hz, 3H), 2.07 (quintet, J = 7.14 Hz, 2H). MS (FAB) *m/z*: 317 $[M+H]^+$.

1-(2,3-Dihydrobenzofuran-6-yl)-3-(3-(5-methyl-1*H*-imidazol-1-yl)propyl)thiourea (45).

Prepared from amine **17** by following the general thiourea coupling procedure: 72% yield, white solid, mp = 60-61°C; ^{1}H NMR (300 MHz, CD_3OD): δ 7.59 (d, J = 1.08 Hz, 1H), 7.20 (d, J = 8.25 Hz, 1H), 6.69-6.66 (m, 3H), 4.59 (t, J = 8.61 Hz, 2H), 3.99 (t, J = 7.14 Hz, 2H), 3.20 (t, J = 6.78 Hz, 2H), 2.79 (t, J = 8.58 Hz, 2H), 2.22 (d, J = 0.93 Hz, 3H), 2.06 (quintet, J = 7.14 Hz, 2H). MS (FAB) *m/z*: 317 $[M+H]^+$.

1-(Chroman-6-yl)-3-(3-(5-methyl-1*H*-imidazol-1-yl)propyl)thiourea (46).

Prepared from amine **8** by following the general thiourea coupling procedure: 62% yield, white solid, mp = 171-172°C; ^{1}H NMR (300 MHz, CD_3OD): δ 7.59 (s, 1H), 6.91-6.88 (m, 2H), 6.75-6.72 (m, 2H), 6.66 (s, 1H), 4.17 (t, J = 5.31 Hz, 2H), 3.96 (t, J = 7.14 Hz, 2H), 3.61 (t, J = 6.78 Hz, 2H), 2.79 (t, J = 6.39 Hz, 2H), 2.22 (d, J = 0.9 Hz, 3H), 2.07-1.93 (m, 4H). MS (FAB) *m/z*: 331 $[M+H]^+$.

1-(Chroman-7-yl)-3-(3-(5-methyl-1*H*-imidazol-1-yl)propyl)thiourea (47).

Prepared from amine **18** by following the general thiourea coupling procedure: 30% yield, white solid, mp = 90-91°C; ^{1}H NMR (300 MHz, $CDCl_3$): δ 7.56 (s, 1H), 7.37 (s, 1H), 7.26 (d, J = 2.67 Hz, 1H,), 6.73 (s, 1H), 6.63 (s, 1H), 6.63 (d, J = 7.71 Hz, 2H), 6.60 (s, 1H), 4.21 (t, J = 5.49 Hz, 2H), 3.92 (t, J = 7.32 Hz, 2H), 3.69 (q, J = 6.96 Hz, 2H), 2.80 (t, J = 6.42 Hz, 2H), 2.18 (s, 3H), 2.11-2.00 (m, 4H). MS (ESI) *m/z*: 331 $[M+H]^+$.

1-(3,4-Dihydro-2*H*-benzo[*b*][1,4]oxazin-6-yl)-3-(3-(5-methyl-1*H*-imidazol-1-yl)propyl)thiourea (48) and 1-(3,4-dihydro-2*H*-benzo[*b*][1,4]oxazin-7-yl)-3-(3-(5-methyl-1*H*-imidazol-1-yl)propyl)thiourea (49).

Prepared from **25** or **26** by following the general thiourea coupling procedure: 40% and 65% yield, respectively, white solid.

1-(3,4-Dihydro-2*H*-benzo[*b*][1,4]oxazin-6-yl)-3-(3-(5-methyl-1*H*-imidazol-1-yl)propyl)thiourea (50).

Prepared from **48** by following the general Boc-deprotection (procedure D), white solid, 40% yield, mp = 230-231°C. ^{1}H-NMR (300MHz, $CDCl_3$): δ 7.50 (s, 1H), 6.60-6.56 (m, 2H), 6.37 (d, J = 2.19 Hz, 1H), 6.29 (dd, J_1 = 2.37 Hz, J_2 = 8.4 Hz, 1H), 4.08 (t, J =

4.38 Hz, 2H), 3.88 (t, J = 7.14 Hz, 2H), 3.51 (t, J = 6.78 Hz, 2H), 3.25-3.24 (m, 2H), 2.12 (t, J = 1.08 Hz, 3H), 1.94 (quintet, J = 7.14 Hz, 2H) . MS (FAB) *m/z*: 330 $[M-H]^+$.

1-(3,4-Dihydro-2*H*-benzo[*b*][1,4]oxazin-7-yl)-3-(3-(5-methyl-1*H*-imidazol-1-yl)propyl)thiourea (51).

Prepared from **49** by following the general Boc-deprotection (procedure D), white solid, 49% yield, mp = 94-95°C. ^{1}H-NMR (300MHz, $CDCl_3$): δ 7.50 (s, 1H), 7.40 (s, 1H), 6.74 (s, 1H), 6.62-6.58 (m, 3H), 5.97 (s, 1H), 4.27 (t, J = 4.59 Hz, 2H), 3.90 (t, J = 7.32 Hz, 2H), 3.68 (q, J = 6.60 Hz, 2H), 3.46 (t, J = 4.23 Hz, 2H), 2.18 (s, 1H), 2.09 (quintet, J = 6.75 Hz, 2H), 1.86 (s, 1H). MS (ESI) *m/z*: 332 $[M+H]^+$.

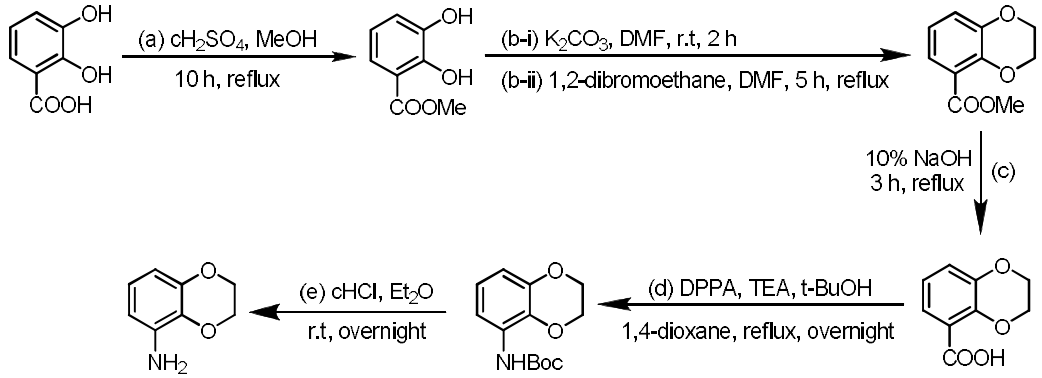

Scheme 8. Synthesis of 2,3-dihydrobenzo[b][1,4]dioxin-5-amine hydrochloride.

Step a: Synthesis of methyl 2,3-dihydroxybenzoate

A mixture of 2,3-dihydroxybenzoic acid (550 mg, 3.57 mmol), MeOH (10 mL), and sulfuric acid (0.2 mL) was refluxed for 10 h. After the solvent was removed under vacuum, the residue was crystallized by diethyl ether and EA (v/v=3:1) to give product as a pink solid (750 mg, 99%).

Step b: Synthesis of methyl 2,3-dihydrobenzo[1,4]dioxine-5-carboxylate

After a mixture of methyl 2,3-dihydroxybenzoate (750 mg, 4.55 mmol), potassium carbonate (1.89 g, 13.68 mmol), and DMF (3 mL) had been stirred at room temperature for 2 h, a solution of 1,2-dibromoethane (0.43 mL, 5.01 mmol) in DMF (5 mL) was added dropwise. After 5h of refluxing, water (10 mL) was added to the reaction mixture, followed by extraction with EA (3×50 mL). The organic layer was washed successively with water (50 mL) and brine (50 mL) and then dried over anhydrous $MgSO_4$. The organic solvent was removed under vacuum to give product as a white crystal (348 g, 51%).

Step c: Synthesis of 2,3-dihydrobenzo[1,4]dioxine-5-carboxylic acid

Methyl 2,3-dihydrobenzo[1,4]dioxine-5-carboxylate (348 mg, 1.79 mmol) and sodium hydroxide solution (2.2 mL, 10%) was refluxed for 3 h. After cooling to room temperature, the reaction mixture was neutralized with HCl (1 $molL^{-1}$) and then extracted with dichloromethane (3×20 mL). The organic layer was washed successively with water (30 mL) and brine (30 mL) and then dried over anhydrous $MgSO_4$. After the solvent was removed under vacuum, the residue was recrystallized from EA to give product as a white solid (281 mg, 87%).

Step d: Synthesis of tert-butyl 2,3-dimethoxyphenylcarbarmate

Triethylamine (0.23 mL) and *tert*-butanol (1.3 mL) were added to a solution of 2,3-dihydrobenzo[1,4]dioxine-5-carboxylic acid (1.56 mmol) and DPPA (0.35 mL) in 1,4-dioxane (4.4 mL) and the reaction mixture was heated at reflux for 16 h. The mixture was concentrated and the residue was diluted with EA (50 mL) and was washed with water. The resulting mixture was washed with satureated sodium carbonate (3×50 mL)

and brine (3×50 mL), dried ($MgSO_4$), and concentrated. The residue was purified by column chromatography (10% to 65% EA/n-hexane) to provide product in 50% yield as light yellow oil.

Step e: Synthesis of 2,3-dihydrobenzo[b][1,4]dioxin-5-amine hydrochloride

Prepared from *tert*-butyl 2,3-dimethoxyphenylcarbarmate (80 mg, 1.32 mmol) by following the general Boc-deprotection (procedure D). The preciated solids were collected by filtration, washed with ether, and dried to provide product in 96% yield as yellow oil.

1-(2,3-Dihydrobenzo[*b*][1,4]dioxin-6-yl)-3-(3-(5-methyl-1*H*-imidazol-1-yl)propyl)thiourea (52).

Prepared from commercially available 2,3-dihydrobenzo[b][1,4]dioxin-5-amine by following the general thiourea coupling procedure: 50% yield, white solid, mp = 73-74°C; ^{1}H NMR (300 MHz, $CDCl_3$): δ 7.63 (s, 1H), 7.37 (s, 1H), 6.91 (d, J = 8.4 Hz, 1H), 6.72 (d, J = 8.4 Hz, 2H), 6.67 (dd, J_1 = 2.37 Hz, J_2 = 8.4 Hz, 1H), 6.00 (br, 1H), 4.27 (s, 4H), 3.91 (t, J = 7.14 Hz, 2H), 3.68 (q, J = 6.24 Hz, 2H), 2,18 (d, J = 0.93 Hz, 3H), 2.10 (quintet, J = 7.14 Hz, 2H). MS (FAB) *m/z*: 333 $[M+H]^+$.

1-(2,3-Dihydrobenzo[*b*][1,4]dioxin-5-yl)-3-(3-(5-methyl-1*H*-imidazol-1-yl)propyl)thiourea (53).

Prepared from commercially available 5-amino-1,4-benzodioxane by following the general thiourea coupling procedure: 25% yield, white solid, mp = 94-95°C; ^{1}H NMR (300 MHz, CD_3OD): δ 7.48 (s, 1H), 6.60-6.56 (m, 2H), 6.37 (d, J = 2.19 Hz, 1H), 6.29 (dd, J_1 =2.37 Hz, J_2 = 8.4 Hz, 1H), 4.08 (t, J = 4.41 Hz, 2H), 3.85 (t, J = 7.14 Hz, 2H),

3.48 (t, J = 6.18 Hz, 2H), 3.25-3.24 (m, 2H), 2.25 (d, J = 1.08 Hz, 3H), 1.92 (t, J = 7.14 Hz, 2H). MS (FAB) *m/z*: 334 $[M+H]^+$.

1-(3-(5-Methyl-1H-imidazol-1-yl)propyl)-3-(5-oxo-5,6,7,8-tetrahydronaphthalen-2-yl)thiourea (54).

Prepared from commercially available 6-amino-1-tetralone by following the general thiourea coupling procedure: 40% yield, white solid, mp = 67-68°C; ^{1}H NMR (300 MHz, CD_3OD): δ 7.93 (d, J = 8.61 Hz, 1H), 7.63 (s, 1H), 7.47 (s, 1H), 7.35 (dd, J_1 = 2.01 Hz, J_2 = 8.43 Hz, 1H), 6.69 (s, 1H), 4.05 (t, J = 7.14 Hz, 2H), 3.65 (t, J = 6.96 Hz, 2H), 2.98 (t, J = 6.03 Hz, 2H), 2.63 (t, J = 5.85 Hz, 2H), 2.24 (d, J = 0.93 Hz, 3H), 2.15-2.04 (m, 4H). MS (ESI) *m/z*: 344 $[M+H]^+$.

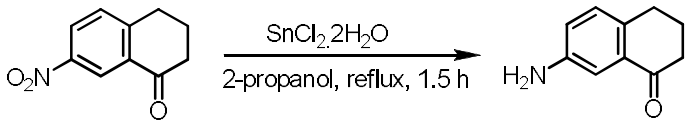

Scheme 9. Synthesis of 7-amino-1-tetralone.

A solution of commercially available 7-nitro-1-tetralone (1 equiv.) and $SnCl_2.2H_2O$ (3 equiv.) in 4 mL of 2-propanol was added concentrated HCl (0.2 mL). The mixture reaction was heated to reflux for 1.5 h. After the reaction was completed, the solution was cooled and basified by 5% solution of K_2CO_3, extracted with EA (3×30 mL). The combined organic extracts were washed with water (2×30 mL), brine (30 mL) and dried over $MgSO_4$, concentrated under vacuum to give 7-amino-1-tetralone (80 mg, 95% yield) as a red solid.

1-(3-(5-Methyl-1*H*-imidazol-1-yl)propyl)-3-(8-oxo-5,6,7,8-tetrahydronaphthalen-2-yl)thiourea (55).

Prepared from 7-amino-1-tetralone synthesized above by following the general thiourea coupling procedure: 48% yield, white solid, mp = 165-166°C. ^{1}H NMR (300 MHz, CD_3OD): δ 7.86 (d, J = 2.37 Hz, 1H), 7.61 (d, J = 1.29 Hz, 1H), 7.54 (dd, J_1 = 2.37 Hz, J_2 = 8.04 Hz, 1H), 7.34 (d, J = 8.22 Hz, 1H), 6.67 (s, 1H), 4.03 (t, J = 7.14 Hz, 2H), 3.63 (t, J = 6.6 Hz, 2H), 2.99 (d, J = 5.88 Hz, 2H), 2.66 (d, J = 6.03 Hz, 2H), 2.24 (d, J = 1.11 Hz, 3H), 2.16-2.01 (m, 4H). MS (ESI) *m/z*: 343 $[M+H]^+$.

1-(5-Hydroxy-5,6,7,8-tetrahydronaphthalen-2-yl)-3-(3-(5-methyl-1*H*-imidazol-1-yl)propyl)thiourea (56).

$NaBH_4$ (16.6 mg, 3 equiv.) was added slowly to a solution of ketone compound **54** in MeOH (5 mL). The reaction mixture was stirred for 3 h at room temperature. The reaction was quenched with saturated NH_4Cl, and the mixture was extracted with dichloromethane, washed with water (2×30 mL), dried over $MgSO_4$, and purified by column chromatography (MeOH:MC=1:9) to give **56** (21 mg, 45%) as a white solid, mp = 90-91°C. ^{1}H-NMR (300 MHz, CD_3OD): δ 7.62 (s, 1H), 7.42 (d, J = 8.43 Hz, 1H), 7.08 (dd, J_1 = 2.19 Hz, J_2 = 8.25 Hz, 1H), 7.00 (s, 1H), 6.68 (s, 1H), 4.69 (br, 1H), 4.01 (t, J = 7.14 Hz, 2H), 3.63 (t, J = 7.14 Hz, 2H), 2.78-2.73 (m, 2H), 2.23 (d, J = 0.99 Hz, 3H), 2.09-1.96 (m, 5H), 1.86-1.81 (m, 2H). MS (ESI) *m/z*: 345 $[M+H]^+$.

1-(8-Hydroxy-5,6,7,8-tetrahydronaphthalen-2-yl)-3-(3-(5-methyl-1*H*-imidazol-1-yl)propyl)thiourea (57).

Prepared from ketone compound **55** by following the method described for the synthesis of compound **56**, 23.7 mg, 47% yield, white solid, mp = 95-96°C. ^{1}H NMR (300 MHz, CD_3OD): δ 7.60 (s, 1H), 7.28 (d, J = 2.0 Hz, 1H), 7.13 (d, J = 8.25 Hz, 1H), 7.07 (dd, J_1 = 2.19 Hz, J_2 = 8.22 Hz, 1H), 6.67 (s, 1H), 4.71 (m, 1H), 4.01 (t, J = 7.14

Hz, 2H), 3.62-3.61 (m, 2H), 2.78-2.73 (m, 2H), 2.23 (d, J = 0.93Hz, 3H), 2.09-2.02 (m, 4H), 1.85-1.83 (m, 2H). MS (ESI) *m/z*: 345 $[M+H]^+$.

1-(1*H*-indol-6-yl)-3-(3-(5-methyl-1*H*-imidazol-1-yl)propyl)thiourea (58).

Prepared from commercially available 6-aminoindole by following the general thiourea coupling procedure: 48% yield, white solid, mp = 177-178°C; ^{1}H NMR (300 MHz, CD_3OD): δ 7.59-7.56 (m, 2H), 7.28 (s, 1H), 7.27 (d, J = 3.12 Hz, 1H), 6.87 (dd, J_1 = 2.01 Hz, J_2 = 8.4 Hz. 1H), 6.64 (s, 1H), 6.46 (d, J = 3.3 Hz, 2H), 3.97 (t, J = 7.5 Hz, 2H), 3.62 (t, J = 6.96 Hz, 2H), 2.20 (d, J = 0.9 Hz, 3H), 2.06 (quintet, J = 7.14 Hz, 2H). MS (FAB) *m/z*: 314 $[M+H]^+$.

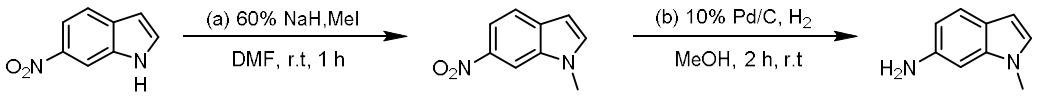

Scheme 10. Synthesis of 1-methyl-1*H*-indol-6-amine.

Step a: Synthesis of 1-methyl-6-nitro-1H-indole

Prepared from commercially available 6-nitroindole by procedure E. The product as a brown solid (99% yield) was carried on next step without further purification.

Step b: Synthesis of 1-methyl-1H-indol-6-amine

Synthesized from 1-methyl-6-nitro-1H-indole by procedure B, 90% yield, brown solid

1-(3-(5-Methyl-1*H*-imidazol-1-yl)propyl)-3-(1-methyl-1*H*-indol-6-yl)thiourea (59).

Prepared from 1-methyl-1*H*-indol-6-amine synthesized above by following the general thiourea coupling procedure: 40% yield, white solid, mp = 159-160°C; ^{1}H NMR (300 MHz, CD_3OD): δ 7.58 (d, J = 8.61 Hz, 2H), 7.29 (s, 1H), 7.20 (d, J = 3.12 Hz, 1H),

6.89 (dd, J_1 = 1.83 Hz, J_2 = 8.25 Hz, 1H), 6.64 (s, 1H), 6.44 (d, J = 1.17 Hz, 1H), 3.98 (t, J = 7.32 Hz, 2H), 3.78 (s, 3H), 3.63 (t, J = 6.96 Hz, 2H), 2.20 (d, J = 0.93 Hz, 3H), 2.04 (p, J = 7.14 Hz, 2H). MS (FAB) *m/z*: 328 $[M+H]^+$.

1-(3-(5-Methyl-1*H*-imidazol-1-yl)propyl)-3-(1-methyl-1*H*-indazol-6-yl)thiourea (60).

Prepared from amine **29** by following the general thiourea coupling procedure: 73% yield, white solid, mp = 175-176°C; ^{1}H NMR (300 MHz, CD_3OD): δ 7.96 (s, 1H), 7.74 (d, J = 8.61 Hz, 1H), 7.63 (d, J = 7.5 Hz, 2H), 7.03 (d, J = 8.43 Hz, 2H), 6.67 (s, 1H), 4.03 (s, 3H), 4.00 (t, J = 7.32 Hz, 2H), 3.66 (t, J = 6.96 Hz, 2H), 2.23 (d, J = 0.9 Hz, 3H), 2.09 (quintet, J = 6.96 Hz, 2H). MS (FAB) *m/z*: 329 $[M+H]^+$.

***Tert*-butyl 6-(3-(3-(5-methyl-1*H*-imidazol-1-yl)propyl)thioureido)-1*H*-indazole-1-carboxylate (61).**

Compound **30** was treated with isothiocyanate compound **41** by following the general thiourea coupling procedure to give **61** as a white solid, 59% yield.

1-(1*H*-indazol-6-yl)-3-(3-(5-methyl-1*H*-imidazol-1-yl)propyl)thiourea (62).

Prepared from compound **61** by following the general procedure D. The crude residue was purified by PLC to give **62** as a white solid (38% yield), mp = 240-241°C; ^{1}H NMR (300 MHz, CD_3OD): δ 8.01 (d, J = 0.9 Hz, 1H), 7.76 (d, J = 8.58 Hz, 1H), 7.62-7.60 (m, 2H), 7.02 (dd, J_1 = 1.65 Hz, J_2 = 8.61 Hz, 1H), 6.66 (s, 1H), 4.02 (t, J = 7.14 Hz, 2H), 3.64 (t, J = 6.96 Hz, 2H), 2.23 (d, J = 0.9 Hz, 3H), 2.11 (quintet, J = 6.96 Hz, 2H). MS (ESI) *m/z*: 315 $[M+H]^+$.

***Tert*-butyl 5-(3-(3-(5-methyl-1*H*-imidazol-1-yl)propyl)thioureido)-1*H*-benzo[*d*]imidazole-1-carboxylate or *tert*-butyl 6-(3-(3-(5-methyl-1*H*-imidazol-1-yl)propyl)thioureido)-1*H*-benzo[*d*]imidazole-1-carboxylate (63).**

Compound **34** was treated with isothiocyanate compound **41** by following the general thiourea coupling procedure to give **63**: 51% yield, yellow solid.

1-(1*H*-benzo[*d*]imidazol-6-yl)-3-(3-(5-methyl-1*H*-imidazol-1-yl)propyl)thiourea or 1-(1H-benzo[*d*]imidazol-5-yl)-3-(3-(5-methyl-1*H*-imidazol-1-yl)propyl)thiourea (64).

Prepared from compound **63** by following the general procedure D. white solid (15% yield), mp = 190-191°C; ^{1}H NMR (300 MHz, CD_3OD): δ 8.1 (s, 1H), 7.58-7.57 (m, 3H), 7.16 (d, J = 8.61 Hz, 1H), 6.65 (s, 1H), 3.97 (t, J = 7.14 Hz, 2H), 3.60 (t, J = 6.96 Hz, 2H), 2.22 (d, J = 1.08 Hz, 3H), 2.06 (quintet, J = 6.96 Hz, 2H). MS (ESI) *m/z*: 316 $[M+H]^+$.

1-(1-Methyl-1*H*-benzo[*d*]imidazol-5-yl)-3-(3-(5-methyl-1*H*-imidazol-1-yl)propyl) thiourea (65).

Prepared from amine **35** by following the general thiourea coupling procedure: 50% yield, white solid, mp = 200-201°C; ^{1}H NMR (300 MHz, CD_3OD): δ 8.15 (s, 1H), 7.58-7.56 (m, 3H), 7.24 (dd, J_1 = 2.01 Hz, J_2 = 8.43 Hz, 1H), 6.65 (s, 1H), 4.00 (t, J = 7.32 Hz, 2H), 3.95 (s, 3H), 3.63 (t, J = 6.75 Hz, 2H), 2.22 (d, J = 0.93 Hz, 3H), 2.09 (quintet, J = 6.96 Hz, 2H). MS (ESI) *m/z*: 329 $[M+H]^+$.

1-(1-Methyl-1*H*-benzo[*d*]imidazol-6-yl)-3-(3-(5-methyl-1*H*-imidazol-1-yl)propyl) thiourea (66).

Prepared from amine **36** by following the general thiourea coupling procedure: 50% yield, white solid, mp = 181-182°C; ^{1}H NMR (300 MHz, CD_3OD): δ 8.14 (s, 1H), 7.67 (d, J = 8.61 Hz, 1H), 7.60 (d, J = 1.11 Hz, 1H), 7.56 (d, J = 1.44 Hz, 1H), 7.14 (dd, J_1 = 1.83 Hz, J_2 = 8.43 Hz, 1H), 6.66 (s, 1H), 4.01 (t, J = 7.14 Hz, 2H), 3.88 (s, 3H), 3.64 (t, J = 6.96 Hz, 2H), 2.22 (d, J = 1.08 Hz, 3H), 2.09 (quintet, J = 6.96 Hz, 2H). MS (FAB) *m/z*: 329 $[M+H]^+$.

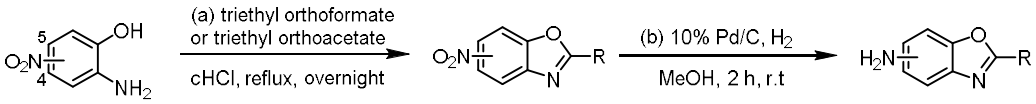

Scheme 11. Syntheses of amino-benzoxazole derivatives.

Step a: Synthesis of 5-nitrobenzo[d]oxazole

To a solution of 2-amino-4-nitrophenol (150 mg) was added $CH(OEt)_3$ (triethyl orthoformate, 3 mL) and HCl 1 drop at room temperature. The mixture was stirred at reflux until the starting material was consumed. The resulting mixture was diluted with EA and washed with water. The organic layer was dried over $MgSO_4$ and concentrated under reduced pressure to afford crude which was purified by column chromatography under EA:n-hexane (1:4) system to provide the pure compound (142 mg, 89%).

Step b: Synthesis of 5-aminobenzo[d]oxazole

Prepared from 5-nitrobenzo[*d*]oxazole by using procedure B.

1-(Benzo[*d*]oxazol-5-yl)-3-(3-(5-methyl-1*H*-imidazol-1-yl)propyl)thiourea (67).

Prepared from 5-aminobenzoxazole synthesized above by following the general thiourea coupling procedure: 27% yield, pink solid, mp = 74-75 °C; ^{1}H NMR (300 MHz, CD_3OD): δ 8.49 (s, 1H), 7.74 (d, J = 2.01 Hz, 1H), 7.68 (d, J = 8.61 Hz, 1H), 7.60 (s,

1H), 7.36 (dd, J_1 = 2.19 Hz, J_2 = 8.79 Hz, 1H), 6.67 (s, 1H), 4.02 (t, J = 7.14 Hz, 2H), 3.64 (t, J = 6.96 Hz, 2H), 2.23 (d, J = 0.93 Hz, 3H), 2.11 (quintet, J = 6.96 Hz, 2H). MS (ESI) *m/z*: 316 $[M+H]^+$.

Synthesis of 2-methyl-5-nitrobenzo[d]oxazole

Prepared by the same method with compound 5-nitrobenzo[*d*]oxazole from two starting materials, 2-amino-4-nitrophenol, and $CCH_3(OEt)_3$ (triethyl orthoacetate), 91% yield.

Synthesis of 2-methyl-5-aminobenzo-[d]oxazole

Prepared from 2-methyl-5-nitrobenzo[*d*]oxazole by using procedure B.

1-(3-(5-Methyl-1*H*-imidazol-1-yl)propyl)-3-(2-methylbenzo[*d*]oxazol-5-yl)thiourea (68).

Prepared from 2-methylbenzo[*d*]oxazol-5-amine synthesized above by following the general thiourea coupling procedure: 57% yield, white solid, mp = 58-59 ^oC; ^1H NMR (300 MHz, CD_3OD): δ 7.59 (s, 1H), 7.58 (d, J = 2.04 Hz, 1H), 7.56 (d, J = 8.58 Hz, 1H), 7.26 (dd, J_1 = 8.61 Hz, J_2 = 2.04 Hz, 1H), 6.67 (s, 1H), 4.01 (t, J = 6.96 Hz, 2H), 3.63 (t, J = 6.78 Hz, 2H), 2.63 (s, 3H), 2.23 (d, J = 0.9 Hz, 3H), 2.11 (quintet, J = 7.14 Hz, 2H). MS (ESI) *m/z*: 331 $[M+H]^+$.

Synthesis of 6-nitrobenzo[d]oxazole

Prepared by the same method with compound 5-nitrobenzo[*d*]oxazole from two starting materials 2-amino-5-nitrophenol, and $CH(OEt)_3$ (triethyl orthoformate), 136 mg, 85% yield.

Synthesis of 6-aminobenzo[d]oxazole

Prepared from 6-nitrobenzo[*d*]oxazole by using procedure B.

1-(Benzo[*d*]oxazol-6-yl)-3-(3-(5-methyl-1*H*-imidazol-1-yl)propyl)thiourea (69).

Prepared from 6-aminobenzoxazole synthesized above by following the general thiourea coupling procedure: 40% yield, pink solid, mp = 59-60^{o}C; ^{1}H NMR (300 MHz, CD_3OD): δ 8.46 (s, 1H), 7.83 (d, J = 2.01 Hz, 1H), 7.72 (d, J = 8.4 Hz, 1H), 7.60 (d, J = 1.08 Hz, 1H), 7.30 (dd, J_1 = 2.01 Hz, J_2 = 8.58 Hz, 1H), 6.67 (s, 1H), 4.03 (t, J = 7.14 Hz, 2H), 3.65 (t, J = 7.14 Hz, 2H), 2.25 (d, J = 1.08 Hz, 3H), 2.14 (quintet, J = 7.32 Hz, 2H). MS (ESI) *m/z*: 316 $[M+H]^+$.

Synthesis of 2-methyl-6-nitrobenzo[d]oxazole

Prepared by the same method with compound 5-nitrobenzo[*d*]oxazole from two starting materials, 2-amino-5-nitrophenol, and $CCH_3(OEt)_3$ (triethyl orthoacetate), 90% yield.

Synthesis of 2-methyl-6-aminobenzo-[d]oxazole

Prepared from 2-methyl-6-nitrobenzo[*d*]oxazole by using procedure B.

1-(3-(5-Methyl-1*H*-imidazol-1-yl)propyl)-3-(2-methylbenzo[*d*]oxazol-6-yl)thiourea (70).

Prepared from 2-methylbenzo[*d*]oxazol-6-amine synthesized above by following the general thiourea coupling procedure: 51% yield, white solid, mp = 75-76^{o}C; ^{1}H NMR (300 MHz, CD_3OD): δ 7.68 (d, J = 1.83 Hz, 1H), 7.60 (d, J = 1.08 Hz, 1H), 7.58 (d, J = 8.43 Hz, 1H), 7.22 (dd, J_1 = 1.83 Hz, J_2 = 8.43 Hz, 1H), 6.67 (s, 1H), 4.02 (t, J = 7.32 Hz, 2H), 3.64 (t, J = 7.14 Hz, 2H), 2.62 (s, 3H), 2.23 (d, J = 0.93 Hz, 3H), 2.11 (quintet, J = 6.96 Hz, 2H). MS (ESI) *m/z*: 331 $[M+H]^+$.

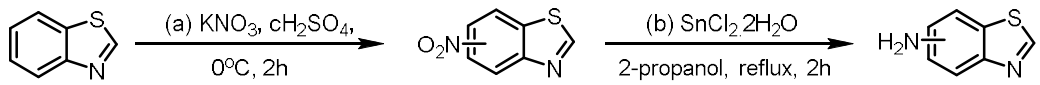

Scheme 12. Syntheses of aminobenzothiazole analogues.

Step a: Syntheses of 5-nitrobenzothiazole and 6-nitrobenzothiazole

To a solution of benzothiazole (500 mg) in concentrated H_2SO_4 (8 mL) was added portionwise postassium nitrate (374 mg, 1 equiv.) at 0°C. After 2 h, the reaction was quenched by ice, basified with solution of 10% NaOH, extracted by dichloromethane (3×30 mL). The combined organic extracts were washed by water and dried over $MgSO_4$. The solvent was removed under reduced pressure to give mixture of 5- and 6-nitrobenzothiazole (430 mg), which was used in the next step without further purification.

Step b: Syntheses of 5-aminobenzothiazole and 6-aminobenzothiazole

Prepared from 430 mg mixture of 5- and 6-nitrobenzothiazole (430 mg) and $SnCl_2.2H_2O$ (3 equiv.) in 4 mL of 2-propanol was added concentrated HCl (0.2 mL). The mixture reaction was heated to reflux for 1.5 h. After the reaction was completed, the solution was cooled and basified by 5% solution of K_2CO_3, extracted with EA (3×30 mL). The combined organic extracts were washed with water (2×30 mL), brine (30 mL), dried over $MgSO_4$, concentrated, and purified by chromatography on a silica gel column (EA: n-hexan gradient) to afford 55 mg of 5-aminobenzothiazole and 100 mg of 6-aminobenzothiazole.

1-(Benzo[*d*]thiazol-5-yl)-3-(3-(5-methyl-1*H*-imidazol-1-yl)propyl)thiourea (71).

Prepared from 5-aminobenzothiazole synthesized above by following the general thiourea coupling procedure: 29% yield, white solid, mp = 78-79°C. ^{1}H NMR (300 MHz, CD_3OD): δ 9.26 (s, 1H), 9.00 (s, 1H), 8.22 (d, J = 1.83 Hz, 1H), 8.04 (d, J = 8.61 Hz, 1H), 7.50 (dd, J_1 = 1.65 Hz, J_2 = 8.22 Hz, 1H), 7.30 (s, 1H), 4.30 (t, J = 6.96 Hz, 2H), 3.72 (t, J = 6.18 Hz, 2H), 2.38 (d, J = 1.08 Hz, 3H), 2.24-2.20 (m, 2H). MS (ESI) *m/z*: 333 $[M+H]^+$.

1-(Benzo[*d*]thiazol-6-yl)-3-(3-(5-methyl-1*H*-imidazol-1-yl)propyl)thiourea (72).

Prepared from 6-aminobenzothiazole synthesized above by following the general thiourea coupling procedure: 44% yield, white solid, mp = 72-73°C. ^{1}H NMR (300 MHz, CD_3OD): δ 9.20 (s, 1H), 8.13 (d, J = 2.19 Hz, 1H), 8.04 (d, J = 8.61 Hz, 1H), 7.60 (s, 1H), 7.46 (dd, J_1 = 2.04 Hz, J_2 = 8.79 Hz, 1H), 6.67 (s, 1H), 4.03 (t, J = 7.14 Hz, 2H), 3.65 (t, J = 6.78 Hz, 2H), 2.23 (d, J = 1.08 Hz, 3H), 2.14 (quintet, J = 7.14 Hz, 2H). MS (ESI) *m/z*: 333 $[M+H]^+$.

1-(3-(5-Methyl-1*H*-imidazol-1-yl)propyl)-3-(pyridin-2-yl)thiourea (73).

Prepared from commercially available 2-aminopyridine by following the general thiourea coupling procedure: 53% yield, white solid, mp = 146-147°C; ^{1}H NMR (300 MHz, CD_3OD): δ 8.23-8.20 (m, 1H), 7.75-7.69 (m, 1H), 7.62 (d, J = 0.93 Hz, 1H), 7.03-6.99 (m, 1H), 6.97 (d, J = 8.43 Hz, 1H), 6.65 (s, 1H), 4.13 (t, J = 7.14 Hz, 2H), 3.76 (t, J = 6.96 Hz, 2H), 2.23 (d, J = 0.93 Hz, 3H), 2.19 (quintet, J = 7.14 Hz, 2H). MS (FAB) *m/z*: 276 $[M+H]^+$.

1-(3-(5-Methyl-1*H*-imidazol-1-yl)propyl)-3-(pyridin-3-yl)thiourea (74).

Prepared from commercially available 3-aminopyridine by following the general thiourea coupling procedure: 55% yield, white solid, mp = 51-52°C; ^{1}H NMR (300

MHz, CD_3OD): δ 8.55 (d, J = 2.55 Hz, 1H), 8.30 (dd, J_1 = 1.29 Hz, J_2 = 4.77 Hz, 1H), 8.00-7.96 (m, 1H), 7.61 (s, 1H), 7.42-7.37 (m, 1H), 6.69 (s, 1H), 4.04 (t, J = 7.14 Hz, 2H), 3.64 (t, J = 6.96 Hz, 2H), 2.24 (d, J = 0.72 Hz, 3H), 2.08 (quintet, J = 6.96 Hz, 2H). MS (FAB) *m/z*: 276 $[M+H]^+$.

1-(Isoquinolin-3-yl)-3-(3-(5-methyl-1*H*-imidazol-1-yl)propyl)thiourea (75).

Prepared from commercially available 3-aminoisoquinoline by following the general thiourea coupling procedure: 21% yield, white solid, mp = 184-185°C. ^1H NMR (300 MHz, CD_3OD): δ 9.04 (s, 1H), 8.01 (d, J = 8.22 Hz, 1H), 7.79 (d, J = 8.04 Hz, 1H), 7.70 (d, J = 7.71 Hz, 1H), 7.64 (s, 1H), 7.52-7.47 (m, 1H), 7.31 (s, 1H), 6.64 (s, 1H), 4.11 (t, J = 7.14 Hz, 2H), 3.81 (t, J = 6.78 Hz, 2H), 2.25 (s, 3H), 2.23-2.10 (m, 2H). MS (FAB) *m/z*: 326 $[M+H]^+$.

1-(3-(5-Methyl-1*H*-imidazol-1-yl)propyl)-3-(quinolin-3-yl)thiourea (76).

Prepared from commercially available 3-aminoquinoline by following the general thiourea coupling procedure: 62% yield, white solid, mp = 85-86°C. ^1H NMR (300 MHz, CD_3OD): δ 8.88 (d, J = 2.37 Hz, 1H), 8.38 (s, 1H), 7.97 (d, J = 8.4 Hz, 1H), 7.90 (d, J = 8.07 Hz, 1H), 7.74-7.68 (m, 1H), 7.62 (s, 1H), 7.59-7.57 (m, 1H), 6.69 (s, 1H), 4.06 (t, J = 7.14 Hz, 2H), 3.65 (t, J = 7.14 Hz, 2H), 2.25 (d, J = 1.08 Hz, 3H), 2.13 (quintet, J = 6.96 Hz, 2H). MS (FAB) *m/z*: 326 $[M+H]^+$.

1-(3-(5-Methyl-1*H*-imidazol-1-yl)propyl)-3-(quinolin-2-yl)thiourea (77).

Prepared from commercially available 2-aminoquinoline by following the general thiourea coupling procedure: 64% yield, white solid, mp = 221-222°C. ^1H NMR (500 MHz, CD_3OD): δ 8.19 (d, J = 8.9 Hz, 1H), 7.82 (t, J = 9.25 Hz, 2H), 7.70 (t, J = 7.25 Hz, 1H), 7.62 (s, 1H), 7.47 (t, J = 7.45 Hz, 1H), 7.12 (d, J = 8.85 Hz, 1H), 6.63 (s, 1H),

4.13 (t, J = 7.00 Hz, 2H), 3.84 (t, J = 6.7 Hz, 2H), 2.29 (quintet, J = 6.9 Hz, 2H), 2.21 (s, 3H). MS (FAB) *m/z*: 326 $[M+H]^+$.

1-(Isoquinolin-1-yl)-3-(3-(5-methyl-1*H*-imidazol-1-yl)propyl)thiourea (78).

Prepared from commercially available 1-aminoisoquinoline by following the general thiourea coupling procedure: 45% yield, white solid, mp = 136-137°C. ^{1}H NMR (300 MHz, CD_3OD): δ 8.34 (d, J = 8.61 Hz, 1H), 8.10 (d, J = 5.85 Hz, 1H), 7.91 (d, J = 8.22 Hz, 1H), 7.81 (t, J = 6.96 Hz, 1H), 7.71 (t, J = 7.14 Hz, 1H), 7.63 (s, 1H), 7.46 (d, J = 6.21 Hz, 1H), 6.64 (s, 1H), 4.12 (t, J = 7.14 Hz, 2H), 3.83 (t, J = 6.78 Hz, 2H), 2.25 (d, J = 0.9 Hz, 3H), 2.25-2.21 (m, 2H). MS (FAB) *m/z*: 326 $[M+H]^+$.

1-(3-(5-Methyl-1*H*-imidazol-1-yl)propyl)-3-(quinolin-6-yl)thiourea (79).

Prepared from commercially available 6-aminoquinoline by following the general thiourea coupling procedure: 46% yield, white solid, mp = 57-58°C. ^{1}H NMR (300 MHz, CD_3OD): δ 8.79 (dd, J_1 = 1.65 Hz, J_2 = 4.38 Hz, 1H), 8.32 (d, J = 7.68 Hz, 1H), 8.01 (s, 1H), 7.97 (d, J = 8.97 Hz, 1H), 7.77 (dd, J_1 = 2.37 Hz, J_2 = 8.97 Hz, 1H), 7.64 (s, 1H), 7.54 (dd, J_1 = 4.38 Hz, J_2 = 8.22 Hz, 1H), 6.69 (s, 1H), 4.06 (t, J = 7.14 Hz, 2H), 3.67 (t, J = 6.96 Hz, 2H), 2.25 (d, J = 0.93 Hz, 3H), 2.10 (quintet, J = 6.96 Hz, 2H). MS (FAB) *m/z*: 326 $[M+H]^+$.

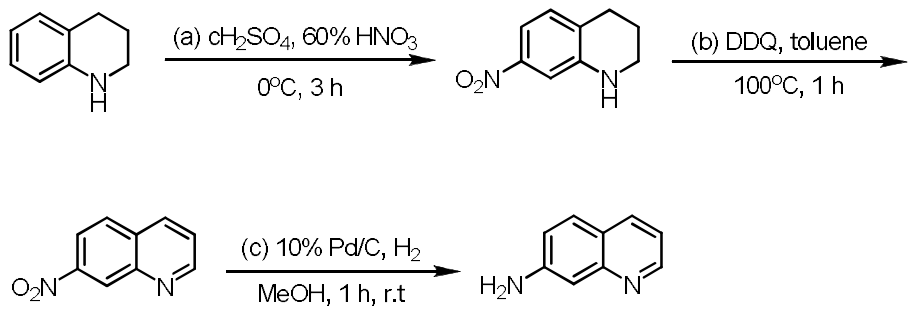

Scheme 13. Synthesis of 7-aminoquinoline.

Step a: Synthesis of 7-nitro-1,2,3,4-tetrahydroquinoline

To a solution of commercially available 1,2,3,4-tetrahydroquinoline (488 mg, 3.66 mmol) in H_2SO_4 (4 mL) was slowly added HNO_3 (60%) (0.29 mL, 3.85 mmol) at 0°C. After finishing adding nitric acid, the reaction mixture was stirred at 0°C for another 2 h. The reaction mixture was basified by using K_2CO_3 to pH >8, then extracted with EA. The organic layer was combined and concentrated under reduced pressure. The crude was purified by column chromatography to give product as a red solid (236 mg, 36%).

Step b: Synthesis of 7-nitroquinoline

7-Nitro-1,2,3,4-tetrahydroquinoline (100 mg, 0.56 mmol) and 2,3-dichloro-5,6-dicyano-1,4-benzoquinone (DDQ, 267 mg, 1.18 mmol) were dissolved in 14 mL toluene. The reaction mixture was heated at 100 °C for 1 h. After cooling to room temperature, the mixture was filtered through Celite bed and the filtrate was concentrated under reduced pressure. The crude was purified by column chromatography to give product as a yellow solid (90 mg, 92%).

Step c: Synthesis of 7-aminoquinoline

Prepared from 7-nitroquinoline by procedure B to give amine product as a yellow solid (60 mg, 80%).

1-(3-(5-Methyl-1*H*-imidazol-1-yl)propyl)-3-(quinolin-7-yl)thiourea (80).

Prepared from 7-aminoquinoline synthesized above by following the general thiourea coupling procedure: 30% yield, white solid, mp = 100-101°C. ^{1}H NMR (300 MHz, CD_3OD): δ 8.80 (dd, J_1 = 1.65 Hz, J_2 = 4.38 Hz, 1H), 8.33 (d, J = 7.86 Hz, 1H), 8.13 (s,

1H), 7.92 (d, J = 8.97 Hz, 1H), 7.69-7.63 (m, 2H), 7.49-7.44 (m, 1H), 6.68 (s, 1H), 4.07 (t, J = 7.14 Hz, 2H), 3.68 (t, J = 6.57 Hz, 2H), 2.25 (d, J = 0.9 Hz, 3H), 2.14 (quintet, J = 7.14 Hz, 2H). MS (ESI) *m/z*: 326 $[M+H]^+$.

1-(Isoquinolin-6-yl)-3-(3-(5-methyl-1*H*-imidazol-1-yl)propyl)thiourea (81).

Prepared from commercially available 6-aminoisoquinoline by following the general thiourea coupling procedure: 68% yield, white solid, mp = 95-96°C. ^{1}H NMR (300 MHz, CD_3OD): δ 9.10 (s, 1H), 8.35 (d, J = 5.85 Hz, 1H), 8.12 (s, 1H), 8.04 (d, J = 8.79 Hz, 1H), 7.72-7.69 (m, 2H), 7.63 (s, 1H), 6.68 (s, 1H), 4.06 (t, J = 7.14 Hz, 2H), 3.68 (t, J = 6.78 Hz, 2H), 2.24 (s, 3H), 2.17 (quintet, J = 6.96 Hz, 2H). MS (FAB) *m/z*: 326 $[M+H]^+$.

1-(3-(5-Methyl-1*H*-imidazol-1-yl)propyl)-3-(quinolin-8-yl)thiourea (82).

Prepared from commercially available 8-aminoquinoline by following the general thiourea coupling procedure: 64% yield, white solid, mp = 142-143°C. ^{1}H NMR (300 MHz, CD_3OD): δ 8.98 (d, J = 7.53 Hz, 1H), 8.85 (dd, J_1 = 1.83 Hz, J_2 = 4.2 Hz, 1H), 7.63 (d, J = 1.17 Hz, 1H), 7.60 (d, J = 1.26 Hz, 1H), 7.56 (s, 1H), 7.54-7.51 (m, 1H), 6.68 (s, 1H), 4.08 (t, J = 7.14 Hz, 2H), 3.69 (t, J = 6.96 Hz, 2H), 2.25 (d, J = 1.11 Hz, 3H), 2.17 (quintet, J = 7.14 Hz, 2H). MS (FAB) *m/z*: 326 $[M+H]^+$.

1-(Isoquinolin-5-yl)-3-(3-(5-methyl-1*H*-imidazol-1-yl)propyl)thiourea (83).

Prepared from commercially available 5-aminoisoquinoline by following the general thiourea coupling procedure: 49% yield, white solid, mp = 117-118°C. ^{1}H NMR (300 MHz, CD_3OD): δ 9.29 (s, 1H), 8.49 (d, J = 6.06 Hz, 1H), 8.11 (dd, J_1 = 3.12 Hz, J_2 = 6.03 Hz, 1H), 7.85 (d, J = 6.03 Hz, 1H), 7.76 (s, 1H), 7.74-7.70 (m, 1H), 7.57 (s, 1H),

6.65 (s, 1H), 3.97 (t, J = 6.96 Hz, 2H), 3.61 (t, J = 6.96 Hz, 2H), 2.19 (s, 3H), 2.04 (quintet, J = 6.93 Hz, 2H). MS (FAB) *m/z*: 326 $[M+H]^+$.

1-(3-(5-Methyl-1*H*-imidazol-1-yl)propyl)-3-(quinolin-5-yl)thiourea (84).

Prepared from commercially available 5-aminoquinoline by following the general thiourea coupling procedure: 47% yield, white solid, mp = 187-188°C. ^{1}H NMR (300 MHz, CD_3OD): δ 8.89 (dd, J_1 = 1.65 Hz, J_2 = 4.2 Hz, 1H), 8.42 (d, J = 7.89 Hz, 1H), 8.05 (d, J = 8.61 Hz, 1H), 7.81 (t, J = 7.32 Hz, 1H), 7.61-7.50 (m, 3H), 6.65 (s, 1H), 3.95 (t, J = 7.14 Hz, 2H), 3.59 (t, J = 7.14 Hz, 2H), 2.19 (s, 3H), 2.02 (quintet, J = 7.32 Hz, 2H). MS (FAB) *m/z*: 326 $[M+H]^+$.

1-(3-(5-Methyl-1*H*-imidazol-1-yl)propyl)-3-(quinoxalin-6-yl)thiourea (85).

Prepared from commercially available 6-aminoquinoxaline by following the general thiourea coupling procedure: 34% yield, yellow solid, mp = 74-75°C. ^{1}H NMR (300 MHz, CD_3OD): δ 8.80 (d, J = 1.83 Hz, 1H), 8.79 (d, J = 2.01 Hz, 1H), 7.62 (s, 1H), 6.68 (s, 1H), 4.07 (t, J = 7.32 Hz, 2H), 3.68 (t, J = 6.93 Hz, 2H), 2.26 (d, J = 0.93 Hz, 3H), 2.17 (quintet, J = 7.14 Hz, 2H). MS (ESI) *m/z*: 327 $[M+H]^+$.

2-Amino-*N*-(3-(5-methyl-1*H*-imidazol-1-yl)propyl)benzamide (86).

A mixture of isatoic anhydride (0.553 mmol) and amine **40** (0.052 mmol) in THF (3 mL) was stirred overnight at room temperature and concentrated *in vacuo*. The residue was shaken with dichloromethane and 3 mL of 1 N NaOH, and the layers were separated. The organic layer was washed twice with H_2O, dried over $MgSO_4$, and concentrated. The residue was triturated with ethyl acetate, and the product was recovered by filtration.

3-(3-(5-Methyl-1*H*-imidazol-1-yl)propyl)quinazoline-2,4(1*H*,3*H*)-dione (88).

Ethylchloroformate (1.4 mL) was added to benzamide **86** (0.35 mmol) at 0°C. The reaction mixture was heated at reflux temperature for 3 h to give crude ethyl 2-(3-(5-methyl-1*H*-imidazol-1-yl)propylcarbamoyl)phenylcarbamate **(87)**. The crude **87** was dissolved in EtOH and then concentrated, after which EtOH (4 mL) and KOH (72 mg) were added. The mixture was heated at reflux temperature for 3 h and again concentrated. The residue was diluted with H_2O, HOAc was added to a pH of 6-7, dichloromethane was added, and the layers were separated. The organic layer was washed with H_2O, dried over $MgSO_4$, and concentrated. The residue was triturated with ethyl acetate, and the product **88** was isolated by column chromatography with a MeOH:MC (1:9) system in 74% yield, mp = 192-193°C; ^{1}H NMR (300 MHz, CD_3OD): δ 8.04 (dd, J_1 = 1.47 Hz, J_2 = 8.07 Hz, 1H), 7.66-7.60 (m, 2H), 7.25-7.13 (m, 2H), 6.66 (s, 1H), 4.09-4.01 (m, 4H), 2.22 (d, J = 0.9 Hz, 3H), 2.17 (quintet, J = 7.32 Hz, 2H). MS (ESI) *m/z*: 285 $[M+H]^+$.

5. References

1. Alzheimer's Disease International (ADI), London. **2014**, *World Alzheimer Report 2014- Dementia and Risk Reduction: An analysis of protective and modifiable factors*, http://www.alz.co.uk/research/world-report-2014, October 2014.
2. Alzheimer's Association, "2010 Alzheimer's Disease Facts and Figures", *Alzheimers Dement.* **2010**, 6 (2), 158-94.
3. Armstrong, R. A. *Folia Neuropathol.***2013**, 51, 169-188.
4. Agamanolis, D. P. 2014, Chapter 9: Degenerative diseases, http://neuropathology-web.org/chapter9/chapter9bAD.html , June 2014.

5. Sierram. **2011**, *Caffeine and Alzheimer's Disease*, http://sierram.web.unc.edu/2011/04/22/caffeine-and-alzheimers-disease/, 22 April 2011.

6. Ramirez, J. J. *J Undergrad Neurosci Educ*., **2003** Spring, 1 (2), R9.

7. Riedel, G.; Platt, B.; Micheau, J. *Behav. Brain Res.*, **2003**, 140, 1-47.

8. Reisberg, B.; Doody, R.; Stöffler, A.; Schmitt, F.; Ferris, S.; Möbius, H. J. *N. Engl. J. Med.*, **2003**, 348, 1333-41.

9. Saltiel, Emmanuel. **2003**, *Memantine (Namenda)* http://www.medicinenet.com/memantine/article.html, 12 Nov. 2010.

10. Lippincott, Williams, Wilkins. **2010,** "Alzheimer Disease Drugs". *Nursing 2010 Drug Handbook*, **2010,** 546-551.

11. Alzheimer's Disease Education & Referral (ADEAR) Center, National Institute on Aging, "Alzheimer's Disease Fact Sheet", *NIH Publication No. 08-6423*. **2008**.

12. Arri, K.; Kobayashi, H.; Kai, T.; Kokuba, Y. *Eur. J. Pharma. Sci.*, **1999,** 9, 75-78.

13. Pohl, T.; Zimmer, M.; Mugele, K.; Spiess, J. *Proc. Natl. Acad. Sci. USA,* **1991,** 88, 10059-10063.

14. Song, I., Chuang, C., Bateman, R. *J. Mol. Endocrinol.,* **1994**, 445-453.

15. Van Coillie, E.; Proost, P.; Van Aelst, I.; Struyf, S.; Polfliet, M.; De Meester, I.; Harvey, D.; Van Damme, U.; Opdenakker, G. *Biochem.,* **1998**, 37, 12672-12680.

16. Hinke, S.; Pospisilik, J.; Demuth, H.; Mannhart, S.; Kuhn-Wache, K.; Hoffman, T.; Nishimura, E.; Pederson, R.; McIntosh, C. *J. Biol. Chem.,* **2000**, 275, 3827-3834.

17. Busby, W. H. J.; Quackenbush, G. E., Humm, J.; Youngblood, W. W.; Kizer, J. S. *J. Biol. Chem.,* **1987**, 262, 8532–8536.

18. Vale, W.; Spiess, J.; Rivier, C.; Rivier, J. *Science*., **1981**, 213, 1394- 1397.

19. Oberg, K. A.; Ruysschaert, J. M.; Azarkan, M.; Smolders, N.; Zerhouni, S.; Wintjens, R.; Amrani, A.; Looze, Y. *Eur. J. Biochem.,* **1998**, 258, 214–222.

20. Schilling, S.; Hoffmann, T.; Rosche, F.; Manhart, S.; Wasternack, C.; Demuth, H. U. *Biochemistry,* **2002**, 41, 10849–10857.

21. Schilling, S.; Niestroj, A. J.; Rahfeld, J. U.; Hoffmann, T.; Wermann, M.; Zunkel, K.; Wasternack, C.; Demuth, H. U. *J. Biol. Chem.* **2003**,278, 49773–49779.

22. Booth, R. E.; Lovell, S. C.; Misquitta, S. A.; Bateman, R. C.; *BMC Biol.* **2004**, 2, 2.

23. Huang, K-F.; Liu, Y-L.; Cheng, W-J.; Ko, T-P.; Wang, A. H-J. *Proc. Natl. Acad. Sci. USA,* **2005**, 102, 13117–13122.

24. Schilling, S.; Zeitschel, U.; Hoffmann, T.; Heiser, U.; Francke, M.; Kehlen, A.; Holzer, M.; Hutter-Paier, B.; Prokesch, M.; Windisch, M.; Jagla, W.; Schlenzig, D.; Lindner, C.; Rudolph, T.; Reuter, G.; Cynis, H.; Montag, D.; Demuth, H. U.; Rossner, S. *Nat. Med.* **2008**, 14, 1106-1111.

25. Ezura, Y.; Kajita, M.; Ishida, R.; Yoshida, S.; Yoshida, H.; Suzuki, T.; Hosoi, T.; Inoue, S.; Shiraki, M.; Orimo, H.; Emi, M. *J. Bone Miner. Res.* **2004**, 19, 1296-1301.

26. Batliwalla, F. M.; Baechler, E. C.; Xiao, X.; Li, W.; Balasubramanian, S.; Khalili, H.; Damle, A.; Ortmann, W. A.; Perrone, A.; Kantor, A. B.; Gulko, P. S.; Kern, M.; Furie, R.; Behrens, T. W.; Gregersen, P. K. *Genes Immun.* **2005**, 6, 388-397.

27. Muthusamy, V.; Duraisamy, S.; Bradbury, C. M.; Hobbs, C.; Curley, D. P.; Nelson, B.; Bosenberg, M. *Cancer Res.* **2006**, 66, 11187-11193.

28. Awade, A. C.; Cleuziat, P.; Gonzales, T.; Robert-Baudouy, J. *Proteins.* **1994**, 20, 34-51.

29. Garavelli, J. S. *Nucleic Acids Res.* **2000**, 28, 209-211.

30. Bockers, T. M.; Kreutz, M. R.; Pohl, T. *J Neuroendocrinol.* **1995**, 7, 445-453.

31. Cynis, H.; Scheel, E.; Saido, T. C.; Schilling, S.; Demuth, H. U. *Biochemistry.* **2008**, 47, 7405-7413.

32. Russo, C.; Violani, E.; Salis, S.; Venezia, V.; Dolcini, V.; Damonte, G.; Benatti, U.; D'Arrigo, C.; Patrone, E.; Carlo, P.; Schettini, G. *J. Neurochem.* **2002**, 82, 1480-1489.

33. Harigaya, Y.; Saido, T. C.; Eckman, C. B.; Prada, C. M.; Shoji, M.; Younkin, S. G. *Biochem. Biophys. Res. Commun.* **2000**, 276, 422-427.

34. Nussbaum, J. M.; Schilling, S.; Cynis, H.; Silva, A.; Swanson, E.; Wangsanut, T.; Tayler, K.; Wiltgen, B.; Hatami, A.; Ronicke, R.; Reymann, K.; Hutter-Paier, B.; Alexandru, A.; Jagla, W.; Graubner, S.; Glabe, C. G.; Demuth, H. U.; Bloom, G. S. *Nature,* **2012**, 485, 651-655.

35. Schilling, S.; Appl, T.; Hoffmann, T.; Cynis, H.; Schulz, K.; Jagla, W.; Friedrich, D.; Wermann, M.; Buchholz, M.; Heiser, U.; von Hörsten, S.; Demuth, H. U. *J. Neurochem.*. **2008**, 106, 1225-1236.

36. Buchholz, M.; Hamann, A.; Aust, S.; Brandt, W.; Böhme, L.; Hoffmann, T.; Schilling, S.; Demuth, H.-U.; Heiser, U. *J. Med. Chem.* **2009**, 52, 7069-7080.

37. Buchholz, M.; Heiser, U.; Schilling, S.; Niestroj, A. J.; Zunkel, K.; Demuth, H.-U. *J. Med. Chem.* **2006**, 49, 664-677.

38. Schilling, S.; Manhart, S.; Hoffmann, T.; Ludwig, H.-H.; Wasternack, C.; Demuth, H.-U. *Biol. Chem.* **2003**, 384, 1583–1592.

39. Tran, P-T.; Hoang, V-H.; Thorat, S. A.; Chang, Y. J.; Nam, D. W.; Song, H.; Mook-Jung, I.; Lee, J.; Lee, J. *Bioorg. Med. Chem.* **2013**, 21, 3821–3830.

40. Cynis, H.; Schilling, S.; Bodnar, M.; Hoffmann, T.; Heiser, U.; Saido, T. C.; Demuth, H. U. *Biochim. Biophys. Acta* **2006**, 1764, 1618-1625.

41. (a) Schilling, S.; Hoffmann, T.; Wermann, M.; Heiser, U.; Wasternack, C.; Demuth, H. U. *Anal. Biochem.* **2002**, 303, 49-56. (b) QC activity was fluorometrically

evaluated using H-Gln-βNA (L-glutaminyl-β-naphthylamine, BACHEM, Switzerland). The samples were prepared in a total volume of 200 ul of assay buffer (20 mM Tris-Cl (pH 8.0), 200 mM potassium chloride) containing the fluogenic substrate (0.05 mM), 0.025U pGAPase (pyroglutaminyl aminopeptidase, QUIAZEN, Germany), 50 ug of HEK293 cell lysate, and variable amounts of the test inhibitory compounds. The assay reaction was initiated by addition of the cell lysate and incubated for 1 h at 37°C. Excitation/emission wavelengths were 320/415 nm. QC activity was determined from the standard curves of β-naphthlyamine under assay conditions (Sigma). IC_{50} values of compounds were collected from 3 independent experiments.

PART II: α-SUBSTITUTED 2-(3-FLUORO-4-METHYLDULFONAMIDOPHENYL)-ACETAMIDES AS POTENT TRPV1 ANTAGONISTS.

1. Introduction

1.1. Overview about Pain

1.1.1. What is Pain?

The International Association for the Study of Pain (IASP) defines pain is "An unpleasant sensory and emotional experience associated with actual or potential tissue damage, or described in terms of such damage".[42]

There are three classes of pain. First, nociceptive pain is protective, it concerned with excessive stimulation of the pain conducting fibers (nociceptors) innervating the skin, viscera and other organs. The second type of pain is inflammatory pain which is also adaptive and protective by activation of immune system by tissue injury or infection. The third kind of pain is not protective, but maladaptive due to damage of nerves in central nervous system or at periphery (neuropathic) or by its abnormal function (dysfunction), it is called pathological pain.[43]

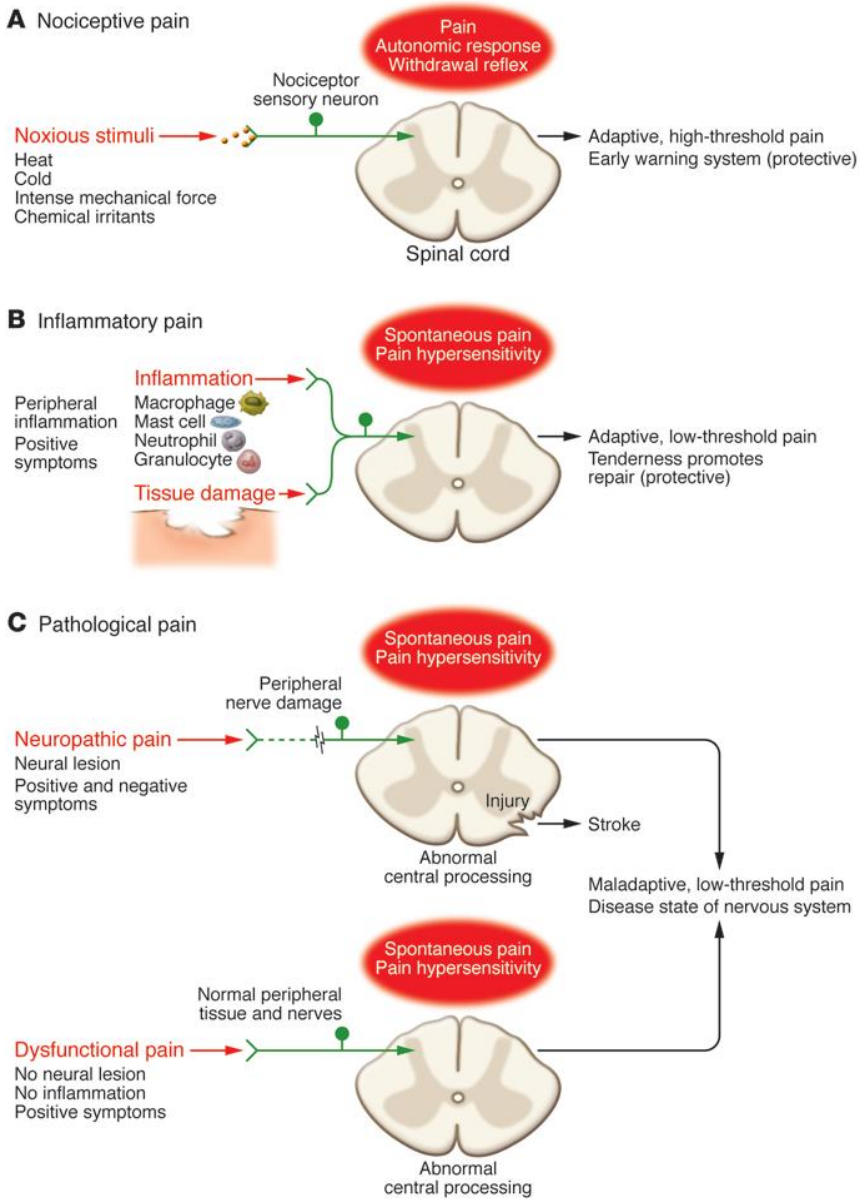

Figure 5. Pain classification.

Pain can be broadly divided into three classes. (A) Nociceptive pain represents the sensation associated with the detection of potentially tissue-damaging noxious stimuli and is protective. (B) Inflammatory pain is associated with tissue damage and the infiltration of immune cells and can promote repair by causing pain hypersensitivity

until healing occurs. (C) Pathological pain is a disease state caused by damage to the nervous system (neuropathic) or by its abnormal function (dysfunctional).[43]

Pain also can be classified by its duration into acute pain and chronic pain. Acute pain generally comes on suddenly and has a limited duration. The causes of acute pain can be from disease, inflammation, or injury to tissues and it usually goes away when the injury heals. Chronic pain lasts much longer than acute pain and usually somewhat resistant to medical treatment. It can be mild, moderate, or intense (severe) and generally associated with a long-term illness, such as osteoarthritis. It is frequently caused by damage to nerve, but can be the result of damaged tissue.[44]

1.1.2. Treatment of Pain

Treatment of pain is an unmet medical need costing billions of dollars every year. Successful pain treatment is highly dependent on successful resolution of the pain's cause.[45] Pain medications, also known as analgesics or pain killers, are a type of drugs used to relieve pain. Analgesic drugs act in various ways on the peripheral and central nervous systems. They prevent the brain from processing pain signals, yet do not rely on anesthesia or loss of consciousness to achieve their pain-killing effect. There are two primary types of analgesics: drugs aimed at preventing or treating pain, include: A) Opioid drugs also known as narcotic analgesics; B) Non-opioid analgesics (non-narcotic analgesics). Drugs from different classes may be combined to handle certain types of pain.

A. Opioid drugs (Narcotic analgesics)[46-50]

These drugs used to alleviate moderate to severe pain are either opiates (derived from the opium poppy plant), such as morphine, codeine; or opiate-like (synthetic drugs) as fentanyl, meperidine, methadone,...

Opioids are most effective analgesics available today. These drugs act by acting to opioid receptors, which are found in the brain, spinal cord, and gastrointestinal tract. Opioids can effectively change the way a person experiences pain when they attach to certain opioid receptors in the brain and spinal cord.

Buprenorphine is thought to be a partial agonist of the opioid receptor, and tramadol is an opiate agonist with serotonin-norepinephrine reuptake inhibitor properties. Tramadol is structurally closer to venlafaxine than to codeine and delivers analgesia by not only delivering "opiate-like" effects but also by acting as a weak but fast-acting serotonin releasing agent and norepinephrine reuptake inhibitor.

The advantage of opioids is there is no maximum dose. Although opioids are effective in providing pain relief, many physicians fail to prescribe them because they fear their patients may become addicted to the substances. In August 2004, the Drug Enforcement Administration (DEA) issued new guidelines to help physicians prescribe narcotics appropriately without fear of being arrested for prescribing the drugs beyond the scope of their medical practice. DEA is trying to work with physicians to ensure that those who need to drugs receive them but to ensure opioids are not abused.

Opioid drugs are generally prescribed to manage pain associated with conditions and procedures such as: severe injury and trauma pain, severe musculoskeletal pain (e.g. back pain or neck pain), surgery, postpartum (after-labor) pain, severe dental pain. Narcotics are also used to block pain during numerous medical and dental procedures and may be used just before or during an operation to help anesthesia work more effectively.

The disadvantages of opioid drugs are some unpleasant side effects and their toxicity beside the drug tolerance such as: drowsiness, constipation, pruritus (itching), dizziness, lightheadedness, unclear thinking, nausea, vomiting, dry mouth, sedation, reduced sex drive, accelerated heart rate, depression of respiration and cough reflex,

gastrointestinal disorders, decreased motor response rate, urinary retention. In high doses, opioids can affect breathing and cause severe respiratory distress.

B. Non-opioid analgesics (non-narcotic analgesics)[51-57]

Non-opioid drugs are milder forms of analgesics and include acetaminophen, the most commonly used over the counter non-narcotic analgesic, which used to treat mild-to-moderate pain and reduce fever. Other drugs are not technically part of the analgesic family, but are nonetheless considered analgesics in practice. These include non-steroidal anti-inflammatory drugs (NSAIDs) such as aspirin, ibuprofen, naproxen,…

Acetaminophen is used to treat mild-to-moderate pain and reduce fever. Acetaminophen act as a painkiller by elevating the amount of pain you can tolerate before you experience the feeling of pain. The best known brand of acetaminophen is Tylenol, but there are also many generic versions available.

Non-steroidal anti-inflammatory drugs (NSAIDs) represent for most non-opioid analgesics NSAIDs are used to treat mild to moderate pain and may be combined with opioids to treat moderate to severe pain. NSAIDs not only relieve pain, but they also reduce the inflammation that often accompanies and worsens pain. All NSAIDs are taken by mouth. One NSAID, ketorolac, can also be given by injection into a vein (intravenously) or muscle (intramuscularly). Indomethacin can be given by suppository. The analgesic, anti-inflammatory, and antipyretic effects of NSAIDs, as well as their most notable side effects, are involved blockade of the production of prostaglandins by inhibition of the enzyme cyclooxygenase (COX) at the site of injury in the periphery, thus decreasing the formation pain mediators in the peripheral nervous system. Non-opioids do not bind to opioid receptors and are not classified under the Controlled Substances; they act primarily in peripheral tissues to inhibit the formation of pain-producing substances such as prostaglandins.

Although non-opioids are often the first choice for treating most types of chronic pain, they have two serious drawbacks. The first drawback has to do with ceiling effects. When non-opioids reach to the ceiling or the upper limit of pain relief, increasing the dosage will not provide any further pain relief. The second major drawback of the non-narcotics is their side effects. Although most non-opioids are quite safe when used for temporary acute pain, problems may increase when people take them over a long period of time (for chronic pain). NSAIDs are generally not applicable to people with stomach problems because they may have a higher risk for stomach bleeding. Except aspirin all NSAIDs raise the risk of serious adverse cardiovascular events, such as heart attack or stroke. Beside the common side effects such as: upset stomach, nausea, abdominal pain, diarrhea, heartburn, unusual bleeding, drowsiness, dizziness, skin rashes; there are more severe side effects of NSAIDs, for example: allergic reactions, high blood pressure, stomach bleeding, stomach ulcers (with long-term use), kidney or liver problems.

COX-2 inhibitors

COX-2 (Cyclo-oxygenase-2) inhibitors are unique type of non-steroidal anti-inflammatory drugs designed to relieve pain as effectively as other NSAIDs but without the gastric problems characteristic of these agents.[58-61] Conditions associated with COX-2 inhibitors include osteoarthritis, rheumatoid arthritis and some types of acute pain.

COX-2 inhibitors target only the pain-signaling prostaglandins, that make them differ from traditional NSAIDs. They relieve pain without causing stomach problems often associated with other NSAIDs because they do not affect cyclo-oxygenase-1 (COX-1), a chemical associated with protecting the stomach lining.

Oxicam and meloxicam, the relatively selective COX-2 inhibitors, were the first step towards developing a true COX-2 selective inhibitor. Coxibs, the newest class of NSAIDs, can be considered as true COX-2 selective inhibitors, and include celecoxib, rofecoxib, valdecoxib, parecoxib and etoricoxib.

Some COX-2 inhibitors (Vioxx and Bextra) have been withdrawn from the market by their manufacturers because they showed a statistically significant increased risk of serious side effects including heart attack, stroke and gastrointestinal bleeding. Consequently, celecoxib (Celebrex) is the only remaining COX-2 inhibitor available in the United States.[1]

COX-1 is a constitutively expressed enzyme with a "house-keeping" role in regulating many normal physiological processes. One of these is in the stomach lining, where prostaglandins serve a protective role, preventing the stomach mucosa from being eroded by its own acid. When nonselective COX-1/COX-2 inhibitors (such as aspirin, ibuprofen, and naproxen) lower stomach prostaglandin levels, these protective effects are lost and ulcers of the stomach or duodenum and potentially internal bleeding can result.

There are the other classes of drugs that can be used to relieve pain include: anticonvulsants, antidepressants and psychostimulants, marijuana-like cannabinoids, corticosteroids to reduce inflammation, disease-modifying antirheumatic drugs (DMARDs) to decrease damage to joints, and nerve blocks and other anesthetics. Many antidepressant drugs can relieve chronic pain in addition to relieving depression. These drugs also may improve sleep quality, which may in turn help reduce pain. In some cases, antidepressants work by treating accompanying depression that makes chronic pain more difficult to handle.[62]

1.2. TRPV1 Receptor. [63]

1.2.1. Structure and Mechanism

In 1997, TRPV1 (transient receptor potential vanilloid 1) was first emulated and characterized as a cation channel directly gated by capsaicin and noxious heat (>43°C)

by Caterina et al.[64] Since then, numerous studies about characterizing the biophysical and physiological properties were published, while its possible therapeutic use for pain treatment was pursued.[65-68] The TRPV1 also known as the capsaicin receptor and the vanilloid receptor 1.[69]

TRPV1 detects and regulates body temperature. It also provides sensation of scalding heat and pain (nociception). TRPV1 receptor is a molecular integrator of nociceptive stimuli, including protons, heat, inflammatory mediators such as anandamide and lipoxygenase products, and vanilloids such as capsaicin (CAP) and resiniferatoxin (RTX). The TRPV1 receptor can increase intracellular Ca^{2+} that leads to excitation of primary sensory neurons and ultimately the central perception of pain base on its functions as a non-selective cation channel with high Ca^{2+} permeability and its activation (**Figure 6**). As a result, TRPV1 could be a prime target for the development of novel pain reducers (analgesics).[65-68]

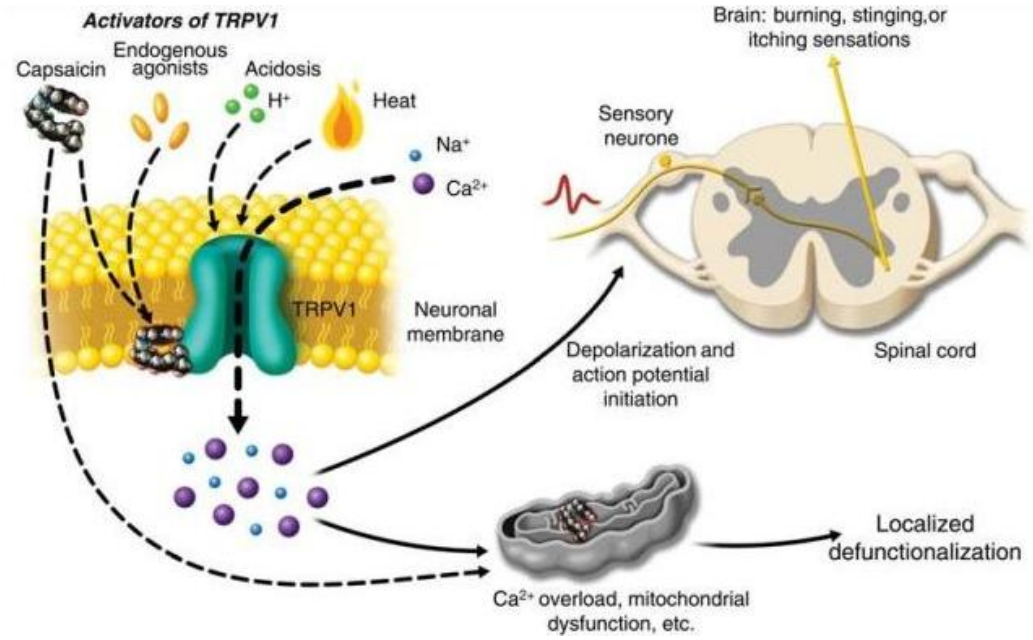

Figure 6. TRPV1 and pain mechanism.

(Source: Br J Anaesth © 2011 Oxford University Press)

The TRPV1 receptor is the first discovered mammalian member of the TRP superfamily. The members of this superfamily contain six transmembrane helices (TM1–TM6) with a pore domain between helices 5 and 6, and the N- and C-termini on the cytosolic side of cell membrane (**Figure 7**).[70] The single particle electron microscopy determined the first three-dimensional structure of TRPV1. It is a protein that has two distinct domains: first is a relatively compact domain which consists with a six-helix transmembrane protein structure; second is a large open basket-like domain which is resident in the intracellular compartment.[71]

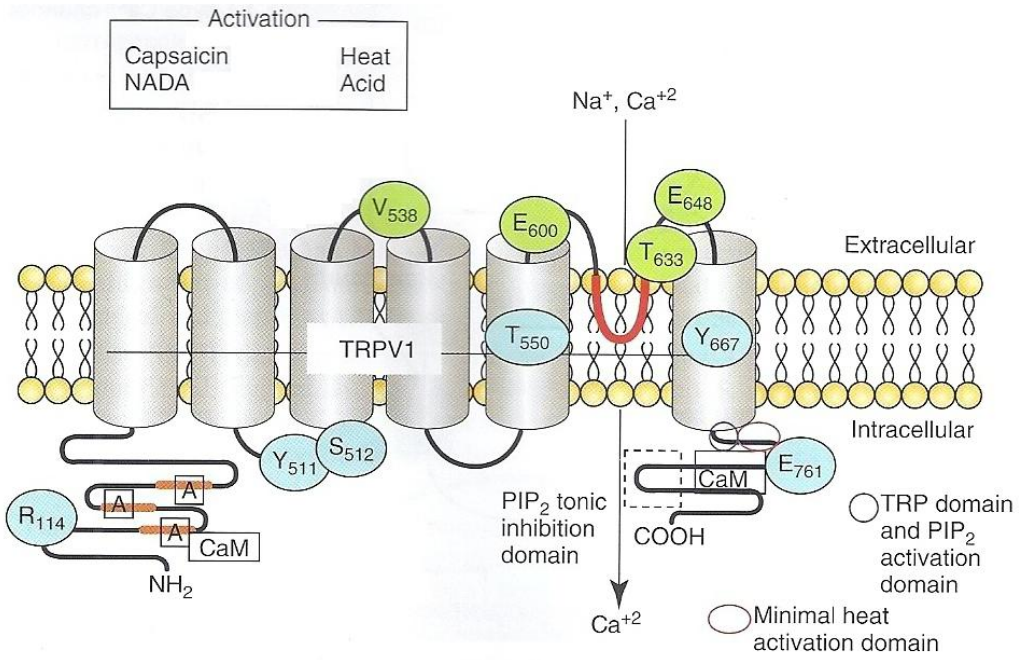

Figure 7. Six transmembrane helices of TRPV1 receptor.[72]

The important features of a group of ligands that are believed to bind to a common site can be presented by pharmacophore models of TRPV1 antagonists. The set of

possible pharmacophore models includes size and shape of the site and location of appropriate interacting sites on the protein has filtered by the homology model of the TRPV1 channel. The overlap volume of the ligands must fit in the binding site and there should be corresponding hydrogen-bond donors or acceptors located near the hydrogen-bonding features identified by the pharmacophore model (**Figure 8**).[70]

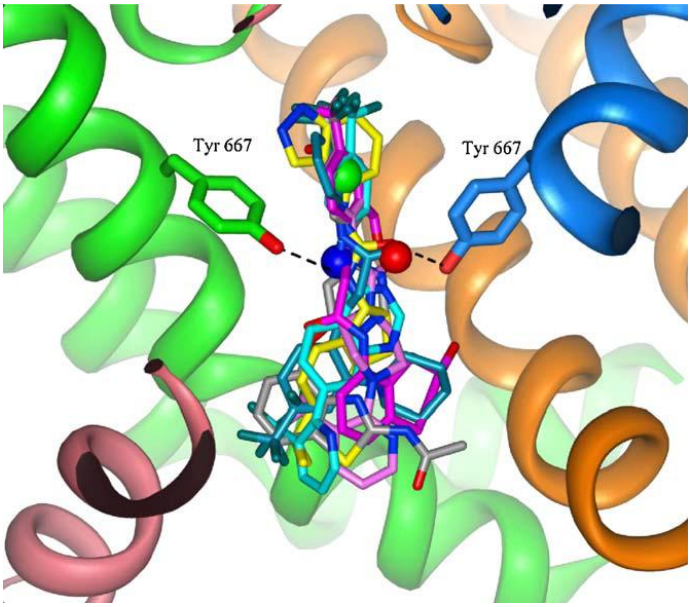

Figure 8. TRPV1 antagonist pharmacophore model.
Tyr 667 of blue monomer donates a hydrogen-bond to all ligands and Tyr 667 of green monomer accepts a hydrogenbond from most ligands. ABT-102 (yellow carbons) and other ligands occupy the binding site in the center of the pore. Pharmacophore model features are shown asspheres (red: acceptor; blue: donor; and green: ring).

Three fundamental features: a hydrogen-bond acceptor, a hydrogen-bond donor, and a ring feature are showed in TRPV1 antagonist pharmacophore model. In addition, the TRPV1 antagonists have been superimposed in such a way that they could fit in the volume of the TRPV1 pore (**Figure 8**).[70]

1.2.2. TRPV1 Agonists

What is an agonist? An **agonist** is a chemical that binds to a receptor of a cell. It triggers a response by that cell Agonists (i.e., capsaicin and resiniferatoxin activate TRPV1, and, upon prolonged application TRPV1 activity) would decrease by desensitization leading to alleviation of pain. Via a patch or an ointment, Agonists can be applied locally to the painful area of the body. With low concentrations of capsaicin (0.025-0.075%), a lots of capsaicin-containing creams are available over the counter. However, whether these preparations actually leading to TRPV1 desensitization is difficult to answer.[73] One possible explanation is that they act via counter-irritation. For higher capsaicin concentration (up to 10%), many novel preparations are under clinical trials.[73] Among them, 8% capsaicin patches have recently become available for clinical use, in which supporting evidence shows that a 30 minute treatment can provide up to 3 months analgesia. To achieve this result, 8% capsaicin patches cause regression of TRPV1 containing neurons in the skin.

1.2.3. TRPV1 antagonists

Drugs or receptor ligands that block or depress agonist-mediated responses are called antagonists. TRPV1 antagonists are promising drug candidates. Inhibiting the transmission of nociceptive signaling from the periphery to the CNS as well as blocking other pathological states associated with this receptor is applied in therapy. Thus, TRPV1 antagonists have showed as novel and promising analgesic and anti-inflammatory agents, particularly for chronic pain and inflammatory hyperalgesia. The antagonists has been increased in the number and extensively reviewed in clinical development.[74] Applying these agents systemically could be useful.[45] TRPV1 antagonists have shown efficacy in reducing nociception from inflammatory and neuropathic pain models in rats.[75] This provides evidence that TRPV1 is the capsaicin's

sole receptor. The pharmacophore model for TRPV1 antagonists was showed in **Figure 8**.

TRPV1 antagonists include competitive and non-competitive antagonists. The competitive antagonists are Antagonists that bind to the agonist binding site, and lock the channel in the closed, nonconductive state. In contrast, non-competitive antagonists are antagonists that interact with additional binding sites on the receptor structure preventing receptor opening by the agonist or blocking its aqueous pore. Non-competitive antagonists are recognized over-activated TRPV1 channels and act as open channel blockers, thus they can reduce the potential of unwanted side effects to become attractive therapies.[76]

1.2.4. Structure Activity Relationship

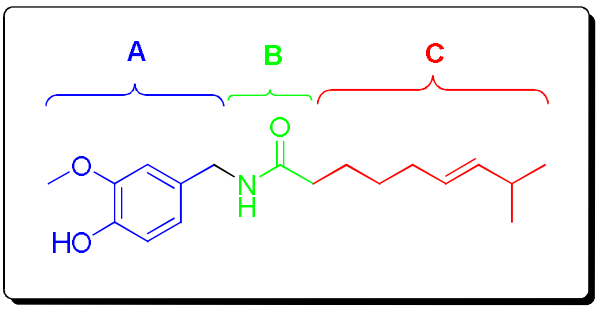

Figure 9. Capsaicin

Capsaicin (8-methyl-*N*-vanillyl-6-nonenamide) (**Figure 9**), a naturally occurring vanilloid was first isolated in 1846, is the best known TRPV1 agonist. Currently, it has been used as topical applications in some chronic pain syndromes such as postherpetic neuralgia, musculoskeletal pain, bladder dysfunction etc.[77] Capsaicin structure was conveniently divided into three functional regions: an aromatic "**A" region** where a parent homovanillyl (3-methoxy 4-hydroxybenzyl) group is optimal, a "**B" region** known as the ester or amide linker and the hydrophobic side-chain aliphatic "**C" region**

where a lipophilic octanyl moiety is associated with the highest potency. The dipolar groups in homovanillyl motif at A-region and amide bond at B-regions concern with hydrogen bonding interactions.[78] Phenolic hydroxide and amide moieties appear to be vital for inducing capsaicin responses. The potency of capsaicin analogues is reduced when remove the phenolic hydroxide or amide bond in A and B-regions. The lipophilic moiety in C-region interacts with a corresponding cleft of the vanilloid binding site on TRPV1. The longer fatty acids lead to reduction of potency, whereas the unsaturation restores and increases activity.[79]

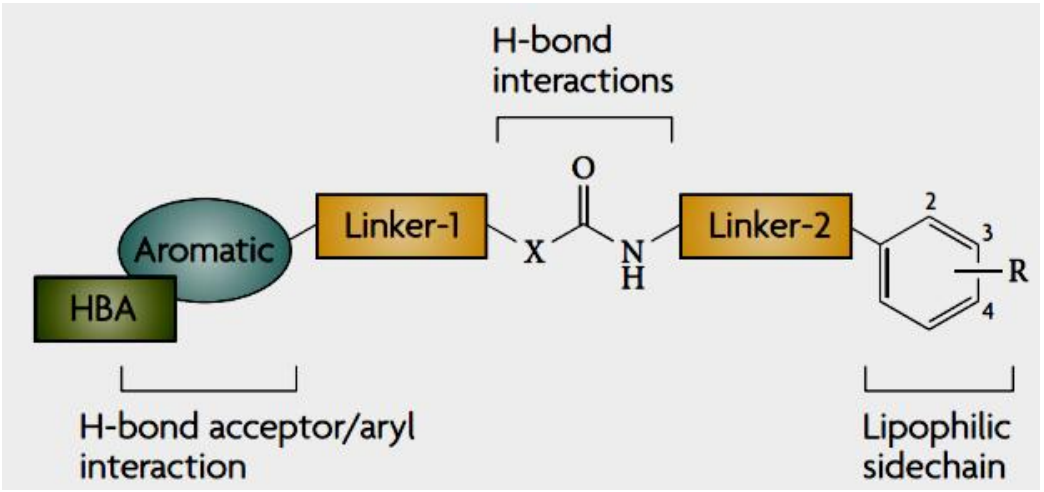

Figure 10. Hydrogen bonding interaction of TRPV1 Antagonist.[66]

The significant *in vitro* and/or *in vivo* data of recent TRPV1 antagonist analogues provide the basis for a developing structure-activity relationship (SAR) for small-molecule TRPV1 antagonists (**Figure 10**). Both H-bond donor and acceptor are considered to be important for optimal potency. There is a central hydrogen-bond acceptor/donor motif flanked by a lipophilic side chain on one side and an aromatic group that incorporates a hydrogen-bond acceptor on the other side. These are readily

provided by urea (X=N), thiourea, amide (X=C) or reverse-amide functionalities, among others. Both potency and drug-like properties of TRPV1 antagonists are improved by mono or bicyclic-aryl and heteroaryl rings with a properly positioned hydrogen-bond acceptor (HBA). Interactions (π–π) between this aryl ring and another on TRPV1 are possible, as has been suggested for the agonist capsaicin. The lipophilic side-chain interacts with a hypothetical hydrophobic binding site on TRPV1. Proper placement of lipophilic substituents (often 4-CF_3 or 4-*t*-Bu) is crucial for optimal TRPV1 potency.[66] The linkers can take many forms, such as direct bonds, single-atom or double atom spacers or ring systems, thus they serve as scaffolding for the proper positioning/spacing of the three interactions above.

1.2.5. Recent Developments

There is an evident of the progress of small-molecule drug discovery in the initiation of clinical trials of TRPV1 antagonists. **Table 4** shows that AstraZeneca, Daewoong Pharm., Amorepacific, GlaxoSmithKline and Neurogen/Merck have advanced TRPV1 antagonists into clinical testing.[80] While Phase I trials of AMG517 was initialized by Amgen in September 2004, and this compound was terminated the clinical trial in Phase Ib due to its hyperthermic response (up to 40.2^{o}C) in human volunteers;[81] Phase I trials of SB-705498 for dental pain and reached Phase II for acute migraine headache are proceeded by GlaxoSmithKline. Consequently, in May 2006, GlaxoSmithKline reported several results showing Phase I clinical data of SB-705498 in healthy volunteers. Furthermore, SB-705498 not only reduced capsaicin-evoked flare and acute heat-evoked pain on non-sensitized skin but also reduced heat-evoked pain after ultraviolet B (UVB)-evoked inflammation. In addition, the initiation of Phase II trials with NGD-8243/MK-2295 in acute pain was started by Neurogen/Merck in November 2006.[82]

Table 4. Recent development of TRPV1 agonists and anatagonists.[80,82]

Compound	Therapeutic indications	Stage of developments (status)
Agonists*		
ALGRX-4975	Analgesia after total knee replacement surgery and bunionectomy	Phase III trial (ongoing)
WN-1001	Cluster headache, osteoarthritis	Phase III trial (completed)
NGX-4010 (Qutenza; Astellas Pharma/ NeurogesX)	Postherpetic neuralgia post-hepatic	Phase III trial (ongoing)
Antagonists		
ABT-102	Pain associated with inflammation, tissue injury and ischaemia	Phase I trial (completed)
AMG-517	Pain	Phase I trial (terminated)
AZD-1386	Chronic nociceptive pain and GERD Pain and Capsaicin-evoked pain	Phase II trial (terminated) Phase II trial (completed)
DWP-05195	Neuropathic pain	Phase I trial (ongoing)
GRC-6211	Pain, migraine, urinary incontinence-associated pain and osteoarthritis	Phase II osteoarthritis trial (suspended)
JTS-653	Pain	Phase II trial (discontinued)
MK-2295	Post-operative pain (tooth extraction)	Phase II trial (completed)
PHE377	Neuropathic pain	Phase I trial (completed)
SB-705498	Pain, migraine and rectal pain	Phase II migraine and rectal pain trial (terminated) Phase II non-allergic intranasal rhinitis trial

		(ongoing)
PAC-14028	Skin pruritus and Rosacea	Phase II trial (completed)
XEN-D0501	Chronic idiopathic cough and COPD	Phase II trial (recruiting)
SYL-1001	Ocular pain, dry eye syndrome	Phase I trial (completed) Phase II trial (recruiting)
GSK-2798745	Pulmonary edema	Phase I trial (recruiting)
MR-1817	Oral treatment of pain	Phase I trial (completed)
JNJ-39439335	Pain Osteoarthritis, knee pain	Phase I trial (completed)

GERD, gastroesophageal reflux disease; COPD: Chronic obstructive pulmonary disease; *These agonists have been reviewed in Reference 83.

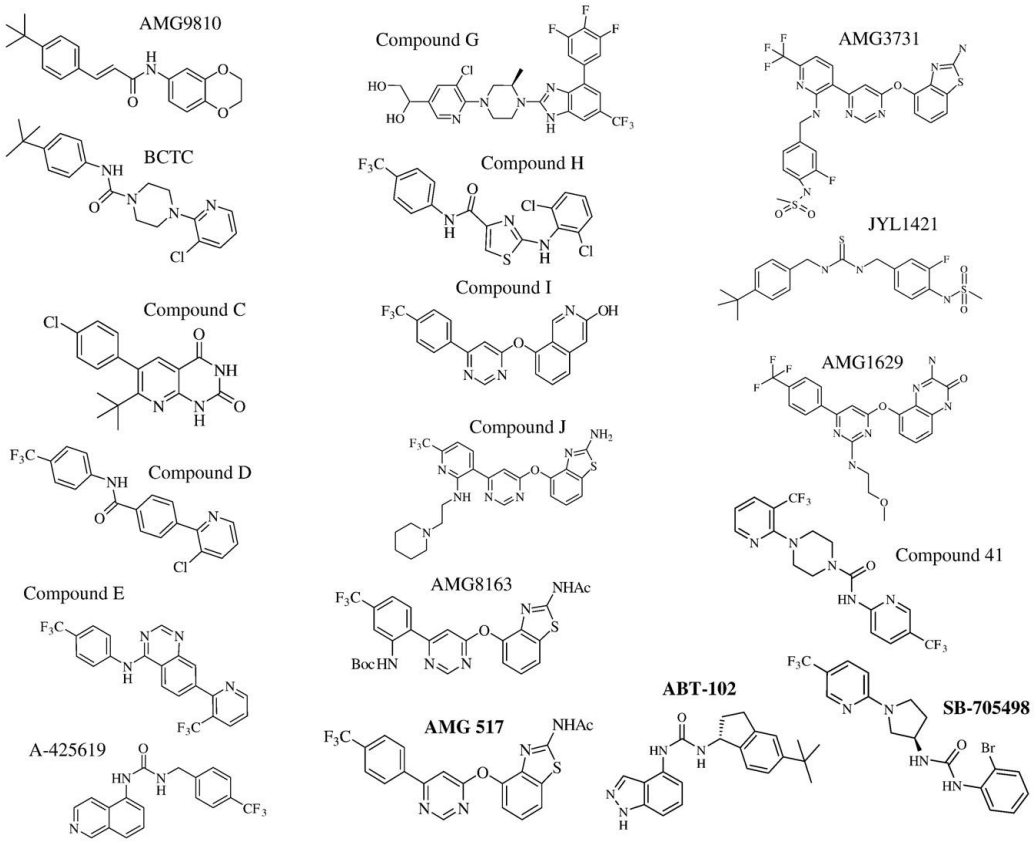

Figure 11. Chemical structures of antagonists[86]

The major obstacle using these drugs is their effect on body temperature (hyperthermia).[84] Recently, it showed that TRPV1 can play a role in the regulation of body temperature. Since there is a number of TRPV-selective antagonists' causing an increase in body temperature (**Table 5**),[85] TRPV1 is tonically active in vivo and can regulate body temperature by inducing the body to decrease its own temperature.[84] Otherwise, the body overheats if it do not utilize these signals. The propensity of capsaicin (a TRPV1 agonist) to cause sweating is explained in a similar manner (i.e.: a signal to reduce body temperature).

Table 5. In vitro profiles of select TRPV1 anagonists and their effects on rat body tempreture.[86]

Chemotype	**Cap (nM)**	**pH 5 (nM)**	**Heat 45°C (nM)**	**BCT Increase (°C)**	***p* value comparing BCT veh group**	**Dose mg/kg (route)**
AMG9810	79±9	349±66	9±1	0.6	0.0156	30 (i.p.)
BCTC	0.4±0.3	0.5±0.6	0.1±0.02	1.4	0.0015	3 (i.v.)
Compound C	42±6	10±1	24±8	1.1	0.0038	30 (p.o.)
Compound D	17±1	13±1	3±1	0.8	0.009	3 (i.v.)
Compound E	1±0.2	2±0.2	0.6±0.1	1.1	0.004	3 (p.o.)
A-425619	10±2	>4000	58±4	1	<0.0001	30 (p.o.)
Compound G	1±0.2	1±0.1	2±0.1	0.5*	0.0294	30 (p.o.)
Compound H	18±3	70±5	16±9	0.7*	0.0412	30 (p.o.)
Compound I	1±0.5	>4000	23±6	0.4	0.005	3 (i.v.)
Compound J	14±2	>4000	360±97	0.8	0.04	3 (i.v.)
AMG8163	0.6±0.3	0.59±0.3	0.15±0.1	1.1	<0.01	3 (p.o.)
AMG3731	5.8±5.2	6.6±1.0	4.8±0.4	1.3	<0.01	10 (p.o.)
AMG1629	0.6±0.4	1.1±0.1	<0.2	0.8	<0.01	3 (p.o.)

AMG0347	0.6±0.2	0.7±0.3	0.4±0.1	0.6	<0.0001	0.05 (i.v.)
AMG 517	1.1±0.7	0.5±0.23	1.5±0.7	1.3	<0.01	3 (p.o.)
JNJ-17203212	102±12	16±5[#]	Unknown	0.8	<0.0001	72 μ mol/kg (p.o.)

Body core temperature (BCT) increase compared to vehicle at 60 min after antagonist administration in shown. Asterisk indicates BCT increase at 90 min post administration of antagonist. # indicates IC_{50} value of JNJ-17203212 was determined at pH 5.8-6.

Recently, it was proposed that predominant function of TRPV1 is body temperature maintenance because tonically active TRPV1 channels are present in the viscera and keep an ongoing suppressive effect on body temperature. The evidences suggesting that TRPV1 is involved in body temperature maintenance are results of many experiments, in which TRPV1 blockade increases body temperature in multiple species, including rodents and humans.[85] It leads to the stopping in clinical trials of AMG 517, GRC 6211 and NGD 8243 due to its hyperthermia[87] and its phosphorylation,[88] respectively. NIH also suggested that Cdk5 mediated phosphorylation of TRPV1 is required for its ligand-induced channel opening.[88] Furthermore, SB-705498 was evaluated in the clinic but its effect on body temperature was not reported.[89]

Thus, development of novel and potent TRPV1 antagonist became a prime challenges for pharmaceutical companies as well as for the pharmaceutical research institutes. In next part, we will discuss our efforts to design, synthesis, and structure activity relationship of novel TRPV1 antagonist.[90]

2. Result and Dicussion

2.1. Design

Previously, we have described a series of *N*-(6-trifluoromethyl-pyridin-3-yl)methyl 2-(3-fluoro-4-methylsulfonamidophenyl)propanamides, originally designed based on a pharmacophoric combination approach, that showed potent *h*TRPV1 antagonism toward multiple activators.[93-97] The structure of capsaicin (CAP) has been divided into three pharmacophoric regions.[91] Correspondingly, the antagonistic template was subdivided into the same three pharmacophoric regions, namely the A-region (3-fluoro-4-methylsulfonamidophenyl), the B-region (propanamide), and the C-region ((6-trifluoromethyl-pyridin-3-yl)methyl) (**Figure 12**). The structure activity relationship (SAR) studies of the template were initiated by incorporating a variety of functional groups including amino[93], oxy[94], thio[95], alkyl[96] and aryl[97] groups into the 2-position in the pyridine C-region. In these series, multiple compounds showed highly potent and (*S*)-stereospecific antagonism of *h*TRPV1 activators including capsaicin, pH, heat (45^{o}C) and *N*-arachidonoyl dopamine (NADA). Their *in vitro* mechanism of action as TRPV1 antagonists was confirmed *in vivo* by their ability to block capsaicin-induced hypothermia. Most importantly, the selected compounds showed promising antinociceptive activity in neuropathic and inflammatory pain models.

In an effort to optimize the properties of the antagonistic template, our focus was next directed to the propanamide (or α-methylacetamide) B-region. The modeling analysis of the B-region using our established *h*TRPV1 homology model[92,93] indicated that the amide group made a hydrogen bond with Tyr511 and also contributed to the appropriate positioning of the C-region for hydrophobic interactions. In order to gain better positioning of the C-region with the receptor through α-substitution in the B-region, with consequent enhancement of activity, we have extensively investigated the structure activity relationships of α-substituted acetamide derivatives for *h*TRPV1 antagonism. Compounds **89** and **90**, previously described as highly potent and stereoselective antagonists, were selected as the parent compounds for this optimization

of the B-region **(Figure 12)**.[93,95] Here, we describe incorporation of various alkyl, dialkyl and aryl groups at the α-position in the B-region of **89** and **90**, with 4-methylpiperidinyl and cyclohexylthio groups at the 2-position in the pyridine C-region (**Figure 12**), respectively, and we have evaluated their antagonism of CAP stimulation of *h*TRPV1 expressed in CHO cells.

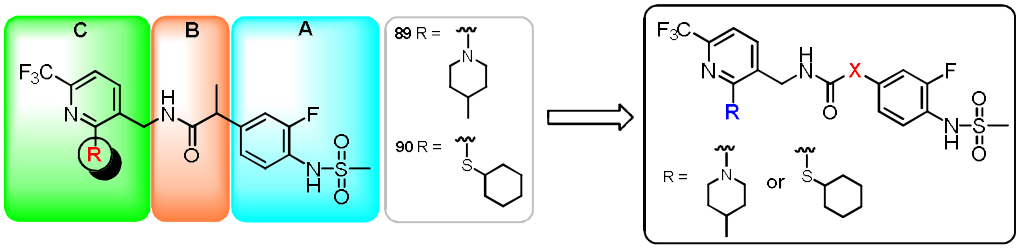

Figure 12. How to design the structure from previous research.

2.2. Chemistry

The syntheses of α-substituted acetamide derivatives were accomplished by one of four different synthetic routes (**Scheme 14-17**). For the synthesis of A/B-regions of the α-ethyl derivative **109**, the nucleophilic substitution of 2,4-difluoronitrobenzene **91** by diethyl malonate afforded the adduct **92**,[98] which was alkylated with ethyl iodide to provide **93**. Further elaboration by a known protocol provided the α-ethyl acetic acid **95** (**Scheme 14**).

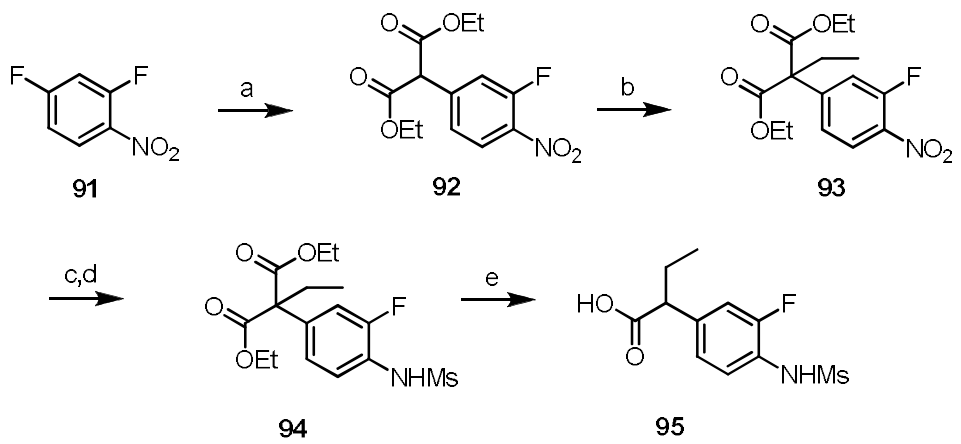

Scheme 14. Synthesis of the A/B-region for **109**.
Reagents and conditions: (a) Diethyl malonate, NaH, DMSO, 15°C, 52%; (b) EtI, TBAF, DMF, r.t, overnight, 65%; (c) Pd/C, H_2, EtOH, 80%; (d) MsCl, Pyridine, CH_2Cl_2, 0°C- r.t, 1 h, 86%; (e) 2N NaOH, EtOH, reflux, 8 h, 99%.

α-Substituted 2-phenylacetic acids as the A/B-regions of compounds **110-131** were prepared efficiently by vicarious nucleophilic substitution[99] from the corresponding ethyl 2-substituted 2-chloroacetates **96**, respectively, using the method previously reported for the synthesis of parent compounds **89** and **90** (**Scheme 15**).

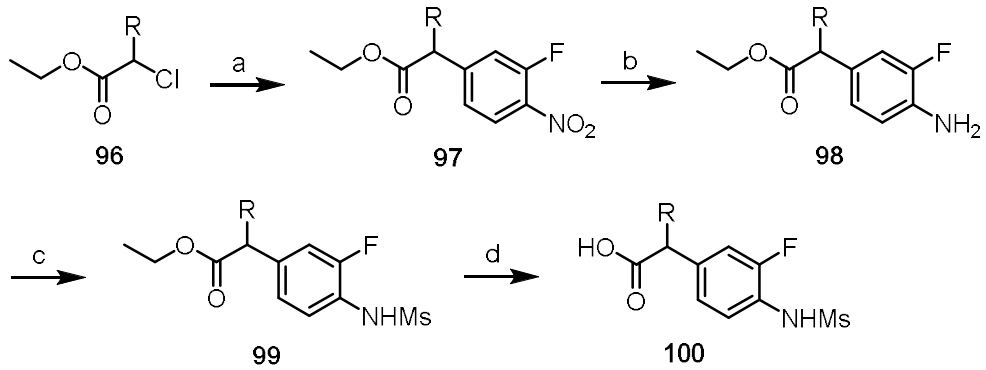

Scheme 15. Synthesis of the A/B-region for **110-131.**

Reagents and conditions: (a) 1-Fluoro-2-nitrobenzene, KO*t*Bu, DMF, -5-0°C; (b) H_2, Pd/C, EtOH-EtOAc (1:1); (c) MsCl, Pyridine, CH_2Cl_2, 0°C- r.t; (d) LiOH, THF-H_2O (2:1), reflux-r.t.

For the synthesis of the A/B-regions of the α,α'-dialkyl derivatives **132-135**, the α-methyl ethyl ester **101**[100] was alkylated with the corresponding alkyl iodides to provide the dialkyl intermediates **102**, which were converted to the respective α,α'-dialkylated acetic acids **103** (**Scheme 16**).

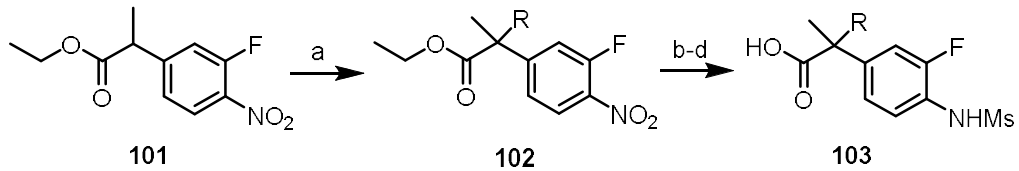

Scheme 16. Synthesis of the A/B-region for **132-135.**
Reagents and conditions: (a) NaH, MeI (or EtI), DMF, 0°C; (b) Pd/C, H_2, EtOH, 1 h, 82-90%; (c) MsCl, Pyridine, CH_2Cl_2, 0°C- r.t, 1 h, 78-89%; (d) LiOH, THF-H_2O, 45°C, 2 h.

For the synthesis of the A/B-regions of the cyclopentyl derivatives **136-137**, the ethyl 2-(3-fluorophenyl)acetate **104** was nitrated and then alkylated with 1,4-dibromobutane. Further three-step elaboration provided the α-cyclopentyl acetic acid **106** (**Scheme 17**).

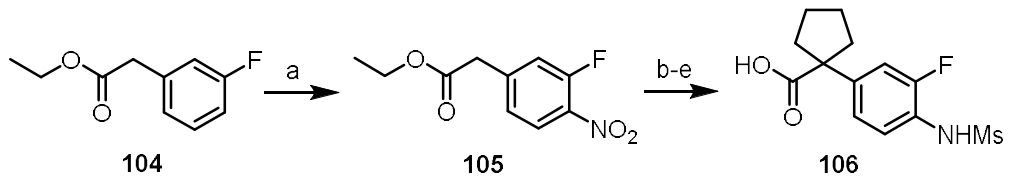

Scheme 17. Synthesis of the A/B-region for **136-137.**
Reagents and conditions: (a) HNO_3, H_2SO_4, 0°C, 2 h ; (b) NaH, 1,4-dibromobutane , THF, r.t, 30 min; (c) Pd/C, H_2, EtOH, 1 h, 92%; (d) MsCl, Pyridine, CH_2Cl_2, 0°C- r.t, 1 h, 82%; (e) LiOH, THF-H_2O, 45°C, 2 h.

The preparation of C-region amines **107,**[93] **108**[95] is carried out as illustrated in the following **scheme 18**.

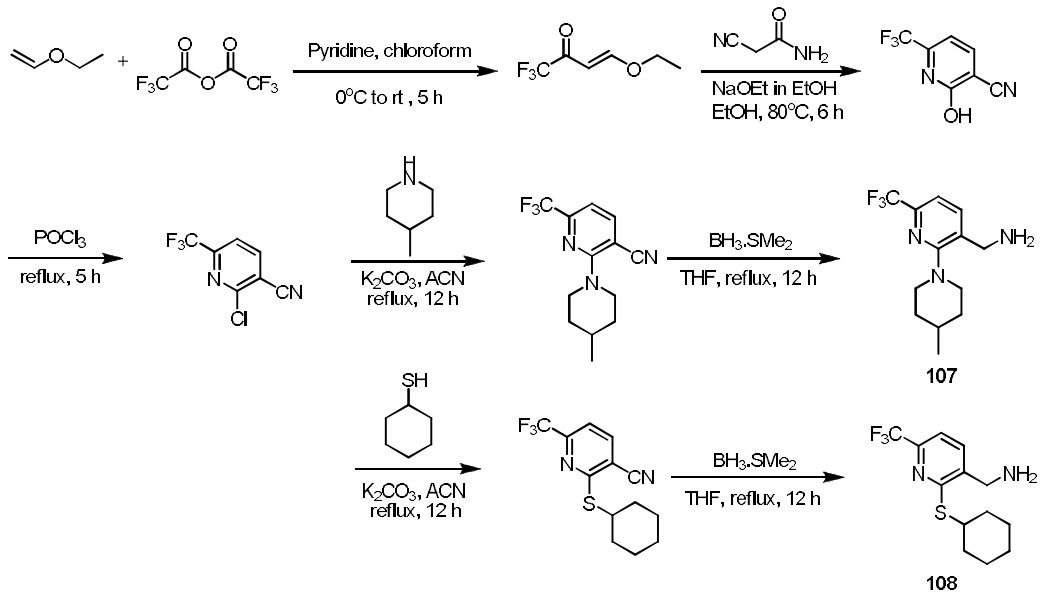

Scheme 18. Syntheses of C-region amines.

The prepared α- substituted 2-phenylacetic acids (**95**, **100**, **103**, **106**) as A/B-regions were coupled with the two C-regions, **107** and **108**, to provide the final compounds **109-137**, respectively (**Scheme 19**).

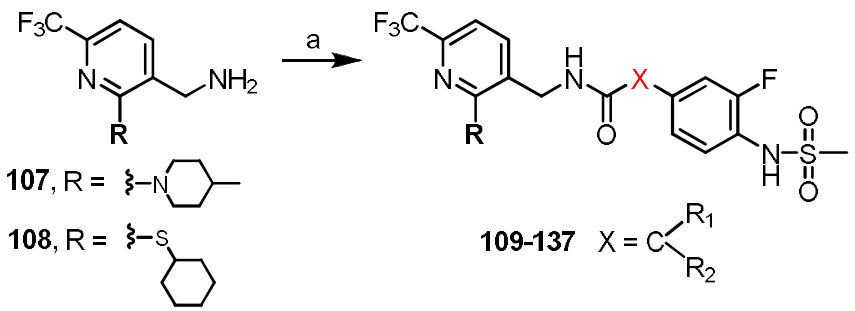

Scheme 19. Syntheses of α-substituted derivatives.

Reagents and conditions: (a) RCO_2H (**95**, **100**, **103**, **106**), TBTU, HOBt, DIPEA, THF-DMF, r.t, 70-90%.

2.3. Biological Activity

The synthesized TRPV1 ligands were evaluated *in vitro* for antagonism as measured by inhibition of activation by capsaicin (100 nM, CAP). The assays were conducted using a fluorometric imaging plate reader (FLIPR) with human TRPV1 heterologously expressed in Chinese hamster ovary (CHO) cells.[93] The results are summarized in **Table 6**, together with the potencies of the parent antagonists **89** and **90** as racemates with $K_{i(CAP)}$ = 0.3 and 0.9 nM, respectively.[93,95]

Table 6. *In vitro h*TRPV1 antagonistic activities for α-substituted acetamide derivatives

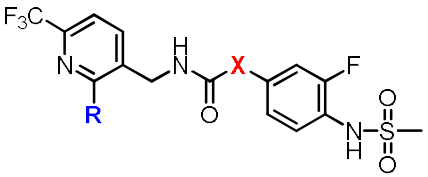

X	R= 		$K_{i(CAP)}$ (nM)	R= 	$K_{i(CAP)}$ (nM)
		**89**	0.3	**90**	0.9
		**109**	1.6	NS	
		**110**	88.7	**111**	103
		**112**	31.1	**113**	WE
		**114**	1.3	**115**	62.5

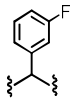	**116**	2.4	**117**	48.7
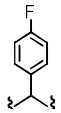	**118**	3.4	**119**	37.6
	**120**	42.9	**121**	WE
	**122**	0.1	**123**	56.4
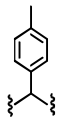	**124**	1.1	**125**	7.5
	**126**	65.9	**127**	WE
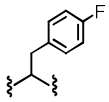	**128**	49.3	**129**	WE
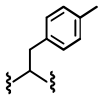	**130**	WE	**131**	40.3
	**132**	49	**133**	65.7
	**134**	124	**135**	WE
	**136**	WE	**137**	WE

WE: weakly active, NS: not synthesized

First, we examined the SAR of the α-alkyl derivatives (**109-113**). The α-ethyl derivative **109**, the one-carbon elongated surrogate of **89**, showed 5-fold less antagonistic potency compared to **89**. However, a further increase in size, such as

cyclopentyl (**110**, **111**) and cyclohexyl (**112**, **113**) groups, led to a dramatic loss in antagonism (>100-fold) compared to the parents **89** and **90**.

Next, the SAR of the α-phenyl derivatives (**114-125**) was examined. The α-phenyl derivatives **114** and **115** showed a moderate or a substantial reduction, respectively, in antagonism compared to the parents but still exhibited potent antagonism compared to the cyclohexyl derivatives (**112**, **113**) despite of a comparable size of the α-substituent. We therefore further investigated other phenyl derivatives substituted with small size groups such as fluoro and methyl. α-Fluorophenyl derivatives (**116-119**) displayed comparable potencies to the α-phenyl derivatives (**114-115**), respectively. However, there was a significant difference in potency with the α-tolyl derivatives (**120-125**) depending on the methyl position in the α-tolyl group as well as on the 2-substituent in the pyridine C-region. Whereas the α-*o*-tolyl derivatives (**120**, **121**) exhibited significant reductions (>140 fold) in potency, the α-*p*-tolyl derivatives (**124**, **125**) displayed moderate loss (3-8 fold) in potency compared to the parents **89** and **90**, respectively. Surprisingly, the α-*m*-tolyl derivative **122** with a 4-methylpiperidinyl group showed exceptionally excellent antagonism with $K_{i(CAP)}$ = 0.1 nM, which was even 3-fold more potent than the parent **89**. Contrary to this finding, the α-*m*-tolyl derivative **123** with a cyclohexylthio group was found to be 60-fold less potent than the parent **90**. The results indicated that the 2-substituent in the pyridine C-region contributed to the appropriate orientation of α-substituent in the B-region for optimal binding with the receptor. Compound **122** was found to be the only antagonist in this series which showed better potency than the corresponding parent and was the most potent antagonist in the series of 2-(3-fluoro-4-methylsulfonamidophenyl)propanamide antagonists reported so far.

Next we investigated the SAR of α-benzyl derivatives (**126-131**). Unfortunately, all of them showed much weaker potencies than the corresponding α-phenyl derivatives,

indicating that α-benzyl substituents appear to provide unfavorable steric interactions with the receptor.

Finally, we examined α,α'-dialkyl derivatives (**132-137**). They were found to be weak antagonist. The SAR analysis indicated that their antagonistic potencies became progressively poorer as the size of α,α'-dialkyl groups increased.

In order to examine its *in vitro* activity as an antagonist for multiple *h*TRPV1 activators, compound **122**, the most potent antagonist in this series, was evaluated for antagonism of TRPV1 activation by capsaicin, pH, heat (45°C) and *N*-arachidonoyl dopamine (NADA). Inhibitory potencies were compared to the respective values for the parent **89** (**Table 7**). Whereas compound **122** showed 3-fold better potency for antagonism of CAP, it exhibited 5-15 fold weaker potency toward the other activators compared to **89**.

Table 7. *In vitro h*TRPV1 antagonistic activities of **122** for multiple activators.

Activators, parameter	**89**	**122**
CAP (f)K_i (nM)	0.3	0.1
pH, IC_{50} (nM)	15.8	86.7
heat 45°C, IC_{50} (nM)	2.56	36.2
NADA (f)K_i (nM)	0.02	0.25

Molecular Modeling

Using our *h*TRPV1 model[93] built based on our *r*TRPV1 homology model[92], we performed a flexible docking study of compound **122**. Its predicted binding interactions are shown in **Figure 13**.[101] Since the active stereoisomer of the propanamide B-region

in this template was found to be the (*S*)-configuration in all cases in our previous reports, we performed the docking study with the (*S*)-**122**.

The A-region, 3-fluoro-4-methylsulfonamidophenyl group, occupied the deep bottom hole and formed hydrophobic interactions with Tyr511, Ile564, Ile569, and Met572. The sulfonamide S=O participated in hydrogen bonding with the backbone amide of Lys571, and the phenyl ring engaged in π-π stacking with the phenyl ring of Tyr511. In the B-region, the amide group formed hydrogen bonds with the side chains of Tyr511 and Lys571, contributing to the appropriate positioning of the C-region for its hydrophobic interactions. In addition, the *m*-tolyl ring as an α-substituent nicely fitted into the hydrophobic pocket composed of Tyr554, Tyr555, Ile564, and Ile569, contributing for the high potency of **122**. In the C-region, the 3-trifluoromethyl pyridine ring extended toward the upper hydrophobic area consisting of Met514 and Tyr511. Furthermore, the 4-methylpiperidine ring was involved in hydrophobic interactions with Thr550, Tyr554, and Phe587 of the adjacent monomer.

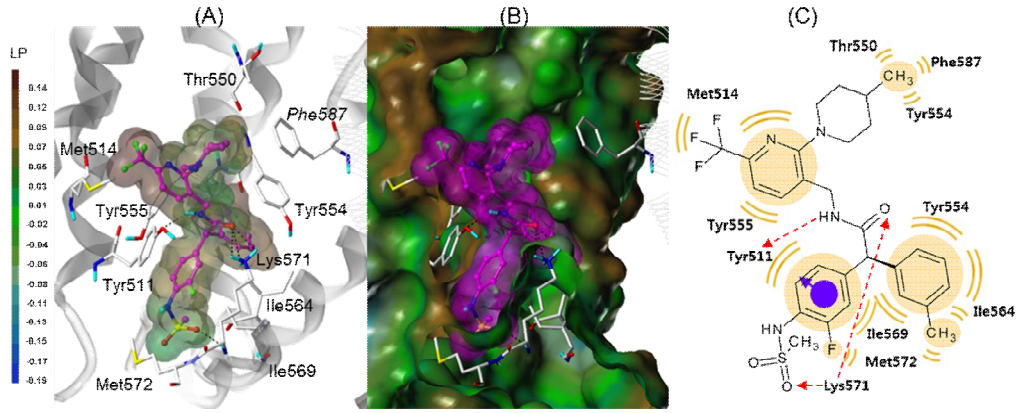

Figure 13. Docking result of (*S*)-**122** in the *h*TRPV1 mode.
(A) Binding mode and interactions of **122** at the binding site of *h*TRPV1. The key interacting residues are labeled and displayed as capped-stick with their carbon atoms in white color. The helices are colored by gray and the neighboring monomer helices

are shown in line ribbon. **122** is depicted in ball-and-stick with the carbon atoms in magenta color. The van der Waals surface representation of **122** is colored by the lipophilic potential property. Hydrogen bonds are shown in black dashed lines, and non-polar hydrogens are not shown for clarity. (B) The Fast Connolly surface representation of *h*TRPV1 and the van der Waals surface representation of the docked **122**. Molecular surface of *h*TRPV1 was generated by MOLCAD and presented with the lipophilic potential property. For clarity, the surface of *h*TRPV1 is Z-clipped and that of **122** is in magenta color. (C) 2-D representation of the interactions between **122** and *h*TRPV1. Hydrophobic, hydrogen bonding, and π-π stacking interactions are marked in light brown, red, and blue, respectively.

3. Conclusion

The structure activity relationship for *h*TRPV1 antagonism by α-substituted acetamide derivatives in the B-region of the 2-(3-fluoro-4-methylsulfonamidophenyl) propanamide template was investigated. Steric repulsion of the α-substituent emerged as a key determinant of antagonistic potency. In this series, compound **122** showed excellent antagonism with $K_{i(CAP)}$ = 0.1 nM. Compound **122** was thus 3-fold more potent than the parent **89**, which we previously had described as potent antagonist, and compound **122** is the most potent antagonist reported using this antagonistic template. Detailed *in vitro* analysis of antagonism by **122** of the response to multiple TRPV1 activators indicated that **122** exhibited preferential antagonism for capsaicin, with weaker potency for the other activators. The docking study of **122** indicated that its high potency might be attributed to a specific hydrophobic interaction of the *m*-tolyl group with the receptor.

4. Expriment section

4.1. General Experimental

All chemical reagents were commercially available. Melting points were determined on a melting point Buchi B-540 apparatus and are uncorrected. Silica gel column chromatography was performed on silica gel 60, 230–400 mesh, Merck. PLC plates were used PLC silica gel 60 F_{254}, 1mm, Merck. Proton NMR spectra were recorded on a JEOL JNM-LA 300 at 300 MHz, Bruker Analytik, DE/AVANCE Digital 400 at 400 MHz, and Bruker Analytik, DE/AVANCE Digital 500 at 500 MHz. Chemical shifts are reported in ppm units with Me_4Si as a reference standard. Mass spectra were recorded on a VG Trio-2 GC-MS.

4.2. Biological experiment

4.2.1. Functional Investigations on TRPV1

TEST COMPOUNDS are analyzed on CHO K1 cells stably transfected with human, rat or mouse recombinant TRPV1 in the FLIPR-3 (2×10^4 cells/well of a 96-well black, clear-bottom microtiterplate, calcium-sensitive dye, room temperature). Changes in fluorescence intensity upon COMPOUND administration are recorded over 6 minutes (i.e. determination of agonistic COMPOUND activity). Thereafter the reference agonist (i.e. capsaicin, 100 nM final concentration) is added and recording is continued for another 6 minutes (i.e. determination of antagonistic COMPOUND activity).

4.2.2. Method FLIPR-Capsaicin-Assay

The effect of TEST COMPOUNDS to inhibit a capsaicin stimulus acting on TRPV1 or to perform as agonist on calcium release in TRPV1 transfected eukaryotic cells is analysed.

Cell culture conditions: Chinese hamster ovary cells (CHO K1 cells, European Collection of Cell Cultures (ECACC), UK) stably expressing human, rat or mouse TRPV1 are plated on poly-D-lysine-coated, black 96-well plates with a clear bottom (BD Biosciences) at a density of 20,000 cells/well in avolume of 100µl Ham´s F12 medium with L-glutamine, 10% v/v fetal calf serum (Gibco Invitrogen) and 20 µg/ml L-proline (Sigma). The cells are then incubated overnight at 37°C and 5% CO_2 at approximately 98% relative humidity. The following day the cells are incubated with Fluo-4 (Molecular Probes) and 0.01 Vol% Pluronic F127 (Molecular Probes) in Hank's buffered saline solution (HBSS, Gibco Invitrogen) for 30 minutes at 37°C. The plates are then washed 3 times with HBSS buffer and, after a further incubation for 15 minutes at room temperature, used in the FLIPR assay for the Ca^{2+} measurement. The Ca^{2+}-dependent fluorescence is measured both before and after addition of the substances to be investigated (wavelength λ_{ex}= 488 nm, λ_{em}= 540 nm). The quantification is carried out by measuring the highest fluorescence intensity (FC, Fluorescence Counts) over time.

Indirect measurement of intracellular calcium using Fluo-4 dye: The FLIPR protocol consists of 2 additions of substances. To test for agonistic activity, the TEST COMPOUNDS (3x concentrated in 150 µl total volume, final screening concentration 10 µM, or dose-response curves from 0.01 µM to 25 µM) are added to the cells and the Ca^{2+} inflow is compared to the control (capsaicin 10 µM). To test for antagonistic activity, 100nM capsaicin is added 6 minutes after TEST COMPOUND addtition by the FLIPR pipettor, and the inflow of Ca^{2+} is determined again.

Desensitising agonists and antagonists lead to a suppression of the Ca^{2+} inflow after addition of Capsaicin. The inhibition [%] compared to the maximum achievable inhibition with the reference antagonist is calculated.

To test for non-specific inhibition of the fluorescence assay by the TEST COMPOUNDS, plates containing wild-type CHO-K1 cells are activated with ATP (50µl/well, 10µM final concentration). Each assay plate contains a reference standard (e.g. BCTC) as well as vehicle controls (HBSS-DMSO) and positive controls (10 µM capsaicin). A capsaicin dose response curve is generated on a separate plate, to determine the EC50 concentration.

Data analysis: FLIPR raw data (fluorescence units) are transferred to Excel, to determine %-stimulation (as compared to the response elicited by 10 µM capsaicin) in the first part of the experiment or %-inhibition (of the signal elicited by 100 nM capsaicin) in the second part of the experiment for the drugs under investigation.

EC_{50}/IC_{50} values are calculated using GraphPad Prism (GraphPad Software, San Diego, USA).

Functional (f)Ki-values are calculated according to the modified Cheng-Prusoff equation.[102]

***Composition of the cell culture media for CHO-K1 cells*:**

500 ml Ham's F12 medium (Gibco No. 21765-029)

10% FCS (PAA No. 10270-106)

18µg/ml L-Prolin (Sigma No. P5607)

9mg/ml G418 is added for the TRPV1-transfected cells

HBSS (1x) without phenole red (Gibco No. 14025-050)

2.5 mM Probenecid (Sigma No. P8761)

20mM HEPES (Sigma No. H7006)

4.2.3. Method FLIPR-TRPV1-pH-Assay

In the pH-assay, human TRPV1-transfected cells are activated with HBSS containing 60mM MES (instead of capsaicin) resulting in a final pH of 6.0 to 6.3 in the assay medium. Data are recorded and processed as described above.

MES sodium salt (Sigma No. M3058)

4.2.4. Method Temperature-Stimulation-Assay TRPV1

In the temperature assay, CHO-K1 cells expressing human TRPV1 are stimulated by a final medium temperature of 45°C.

Cell culture conditions: CHO-K1/humanTRPV1 or CHO-K1 wildtype cells are maintained in culture in complete HAM`s F12 Nutrient Mixture with L-Glutamin (Gibco No. 21765-029) supplemented with 10% FCS (Gibco REF: 10270-106), 90µg/ml Geneticin (Gibco Cat. 10131-027) and 0.02 mg/ml L-Proline (Sigma No. P5607, stock solution 100mg/ml, sterile filtered). Cells are cultured as a monolayer at 37°C with 5% CO_2 and are detached every 3 to 4 days by using of Accutase (PAA No. L11-007).

Ligands and ligand storage: TEST COMPOUNDS are prepared as 10 mM solutions in DMSO (Fluka No. 41647) and then diluted in buffer A. To keep the DMSO concentration below 0.1%, the highest used concentration of test compounds in the test is 10 µM.

Indirect measurement of intracellular calcium using Fluo-4 dye: CHO-K1/TRPV1 cells are seeded in 100 µl of complete HAM`s F12 Nutrient Mixture medium in clear bottom black 96 MTPs (Corning Cellbind Surface Assay Plates No. 3340) at 3.000 c/w 96 h before analysis.

The day of the experiment, medium is replaced and cells are loaded for 90 min at 37°C with 50 µl buffer B.

After loading the cells, buffer B is removed and 50 µl buffer A is added to the cells, the plate is then incubated for 15 min at room temperature in the dark.

25 µl of reference antagonist or TEST COMPOUND (3 fold concentrated in buffer A giving the final concentration in the wells) are added to start the experiment. The treated cells are incubated at room temperature for 5 min. During this incubation period, the baseline fluorescence prior to stimulation is measured at 485/528nm using the FLX800 Fluorescence Reader (Fa. Biotek). After 5 min, the plate is transferred into the PCR cycler PTC200, MJ Research (flat bottom insert) and the temperature cycling program is started (using heated lid, 2 min 57°C, 1 min 20°C). Directly after this temperature stimulus resulting in a final temperature 45°C (approx. EC80 of temperature stimulation response) in the wells, the fluorescence is measured again. The differences in fluorescence before and after temperature stimulation are calculated and used for the IC_{50} determination of the antagonists. Each experiment is also performed on CHO-K1 wildtype cells to detect unspecific drug interactions in this assay system.

Buffer A: HBSS +$CaCl_2$ + $MgCl_2$ (Gibco No. 14025-050) containing 2.5 mM probenecid and 10 mM HEPES, pH 7.4

Buffer B: HBSS + $CaCl_2$ + $MgCl_2$ (Gibco No. 14025-050) containing 2.17 µM fluo-4 AM (Molecular Probes No. F14201, 50 µg), 2.5 mM probenecid, 10 mM HEPES, pH 7.4

4.2.5. Method NADA-Assay TRPV1

The effect of TEST COMPOUNDS to inhibit a N-arachidonoyl-dopamine stimulus acting on TRPV1 or to perform as agonist on calcium release in TRPV1 transfected eukaryotic cells is analysed.

Cell culture conditions: CHO-K1/human TRPV1 or CHO-K1/rat TRPV1 cells are maintained in culture in complete HAM`s F12 Nutrient Mixture with L-Glutamin

(Gibco No. 21765-029) supplemented with 10% FCS (Gibco REF: 10270-106), 90µg/ml Geneticin (Gibco Cat. 10131-027) and 0.02 mg/ml L-Proline (Sigma No. P5607, stock solution 100mg/ml, sterile filtered) at 37°C with 5% CO_2, and are detached every 3 to 4 days by using of Accutase (PAA No. L11-007).

Ligands and ligand storage: NADA (N-arachidonoyl-dopamine, Tocris No. 1568, 5mg/ml ethanol) is dissolved at in ethanol to 10 mM stock concentration and stored at -20°C. Working solutions are freshly prepared by dilution in buffer A.

The TEST COMPOUNDS are freshly prepared as 10 mM solutions in DMSO (Fluka No. 41647) and then diluted in buffer B. To keep the DMSO concentration below 0.1%, the highest concentration of COMPOUNDS used in the test is 10 µM.

Indirect measurement of intracellular calcium by FLIPR3 using Fluo-4 dye: CHO-K1/TRPV1 cells are seeded in 100 µl of complete HAM`s F12 Nutrient Mixture medium in clear bottom black 96 MTP's (Corning Cellbind Surface Assay Plates No. 3340) at 20.000 c/w 24 h before analysis.

The day of experiment, medium is replaced and cells are loaded for 40 min at 37°C, with 50 µl buffer C.

After washing with buffer D (twice, automatic biotech device), 100 µl buffer D is added to the cells and the plate is incubated for 15 min at room temperature in the dark. Then, in the FLIPR machine, 50 µl of known antagonist or TEST COMPOUND (3 fold concentrated in buffer B, giving 0.1% BSA final concentration in the wells) are added to the cells followed by the addition of 50 µl of NADA as agonist (4 fold concentrated in buffer A, final BSA concentration 0.1%, final volume 200 µl). Use of FLIPR3 Tips (Molecular devices pipette tips, black, 96 type b) is essential.

Fluorescence measurement is performed for about 9 min before and for about 5 min after agonist injection. The obtained profiles have been analyzed by FLIPR software using Max - Min from image 78 to 148.

On each assay plate, the NADA dose-response curve (20000 nM – 19.5 nM, dilution factor 2) is included for calculating the agonist´s EC_{50} value for the respective plate. The NADA-concentration of the standard second agonist addition by the FLIPR pipettor is 5000nM (approx. EC90) to enable determination of the IC_{50} value of the TEST COMPOUNDS. The best concentration range of the test substances is always adapted. As result, the (f)Ki value can be calculated according to Cheng-Prusoff.

Buffer A: HBSS +$CaCl_2$ + MgCl (Gibco No. 14025-050) containing 2.5 mM probenecid, 0.1% BSA (PAA No. K05-013, 30% stock solution), 10 mM HEPES, pH 7.4

Buffer B: HBSS +$CaCl_2$ + $MgCl_2$ (Gibco No. 14025-050) containing 2.5 mM probenecid, 0.3% BSA (PAA No. K05-013, 30% stock solution), 10 mM HEPES, pH 7.4

Buffer C: HBSS + $CaCl_2$ + $MgCl_2$ (Gibco No. 14025-050) containing 2.17 µM fluo-4 AM (Molecular Probes No. F14201, 50 µg), 2.5 mM probenecid, 10 mM HEPES, pH 7.4

Buffer D: HBSS +$CaCl_2$ + $MgCl_2$ (Gibco No. 14025-050) containing 2.5 mM probenecid, 10 mM HEPES, pH 7.4

4.2.6. Molecular Modeling

Based on our rat TRPV1 tetramer homology model, the human TRPV1 (hTRPV1) model was constructed as a tetramer. In the binding site, five residues are different between rat and human, and they were mutated as Ile514Met, Val518Leu, Val525Ala, Ser526Thr, and Met547Leu. Then, the side chains and backbone within 6 Å of the mutated residues were energy minimized using the Protein Composition Tool in SYBYL 8.1.1 (Tripos Int., St. Louis, MO, USA). The ligand structure was generated with Concord and energy minimized using the MMFF94s force field and MMFF94

charge until the rms of the Powell gradient was 0.05 kcal $mol^{-1}A^{-1}$ in SYBYL. The flexible docking study on the hTRPV1 model was performed using GOLD v.5.0.1 (Cambridge Crystallographic Data Centre, Cambridge, UK). It uses a genetic algorithm (GA) and allows for full ligand flexibility and partial protein flexibility. The binding site was defined as 8 Å around capsaicin which was extracted from the docking result in the rTRPV1 model and merged into the aligned hTRPV1 model. The side chains of the important six residues for ligand binding (i.e., Tyr511, Ser512, Leu515, Leu547, Thr550, and Asn551) were set to be flexible with 'crystal mode'. The default parameters were used with the GoldScore scoring function, and 30 docking runs per ligand were performed. All computation calculations were undertaken on an Intel® Xeon™ Quad-core 2.5 GHz workstation with Linux Cent OS release 5.5.

4.3. Synthesis of the A/B-region for 109 (Scheme 14)

Diethyl 2-(3-fluoro-4-nitrophenyl)malonate (92)

To a suspension of NaH (60%, 5.49 g, 137.5 mmol) in dry DMSO (80 mL) under ice cooling was added dimethyl malonate (16.5 g, 125 mmol) dropwise over a period of 10 min followed by a solution of 2,4-difluoronitrobenzene **91** (9.9 g, 62.5 mmol) in dry DMSO (15 mL) under an Ar atmosphere. The resultant mixture was stirred at 15°C overnight. The reaction mixture was quenched with saturated NH_4Cl and extracted with ethyl acetate (4×200 mL). The combined organic extracts were washed with water, brine and dried (Na_2SO_4). The residue obtained upon evaporation of the solvents was purified on a column of silica gel to afford the nitro-diester **92** as a light yellow solid (9.7 g, 52%).

Diethyl 2-ethyl-2-(3-fluoro-4-nitrophenyl)malonate (93)

To 9,75 mL of 1.0M tetrabutylammonium fluoride solution in THF (9.75 mmol) in dry DMF (15 mL) under ice cooling was added a solution of the compound **92** (2 g, 6.96 mmol) in dry DMF (5 mL) dropwise over a period of 5 min under an Ar atmosphere followed by iodoethane (1. 6 g, 10.4 mmol). After stirring the resultant mixture at rt overnight, it was quenched with saturated NH_4Cl and extracted with ethyl acetate (4×60 mL). The combined organic extracts were washed with water, brine and dried. The residue obtained upon evaporation of the solvents was purified on column of silica gel to afford compound **93** as a colorless oil (1.48 g, 65%).

Diethyl 2-ethyl-2-(3-fluoro-4-(methylsulfonamido)phenyl)malonate (94)

Step c: Synthesis of diethyl 2-(4-amino-3-fluorophenyl)-2-ethylmalonate

Diethyl 2-ethyl-2-(3-fluoro-4-nitrophenyl)malonate **93** 9(1.48 g, 4.52 mmol) was dissolved in 150 mL of EtOH, then 10% Pd/C was added. The mixture was stirred at room temperature under hydrogen gas until the starting material had been consumed. The crude mixture was filtered through Celite, washed with ethanol, and then concentrated to afford desired product (1.07g, 80%).

Step d: Synthesis of diethyl 2-ethyl-2-(3-fluoro-4-(methylsulfonamido)-phenyl)malonate

The amino compound diethyl 2-(4-amino-3-fluorophenyl)-2-ethylmalonate (1.07 g, 3.62 mmol) was dissolved in 10 mL dichloromethane, cooled under a blanket of nitrogen to 0°C, and 3 mL of pyridine, 0.72 mL of methanesulfonyl chloride (0.54 mmol) were added, and stirring of the reaction mixture was continued at 0°C over a period of 1 h. To the reaction mixture there were added, with ice cooling, 15 mL of water, and the mixture was set to pH 1 with 16% strength aq. HCl. Following extraction of the mixture with dichloromethane (3 x 50 mL), the organic phases were combined, dried over $MgSO_4$ and concentrated in vacuo. Purification of the crude product was

carried out by column chromatography (eluent: 50% EA in n-hexane) and yielded 1.17 g (86%) of product.

2-(3-fluoro-4-(methylsulfonamido)phenyl)butanoic acid (95)

Diethyl 2-ethyl-2-(3-fluoro-4-(methylsulfonamido)phenyl)malonate **94** (1.17g, 3.12 mmol) was dissolved in EtOH (20 mL), 2N NaOH (9.36 mmol) were added and the mixture was heated under reflux over a period of 8 h and cooled to room temperature. To the reaction mixture there were added 15 mL of water and the phases were separated. The aqueous phase was acidified with HCl and extracted with dichloromethane (3 x 50 mL) a number of times. The combined organic phases were dried over $MgSO_4$, concentrated, and the residue purified by means of column chromatography. Yield 850 mg (99 %).

4.4. Synthesis of the A/B-region for 110-131 (Scheme 15)

4.4.1. General instructions for the synthesis of 2-cycloalkyl-2-(3-fluoro-4-(methyl-sulfonamido)phenyl)acetic acids

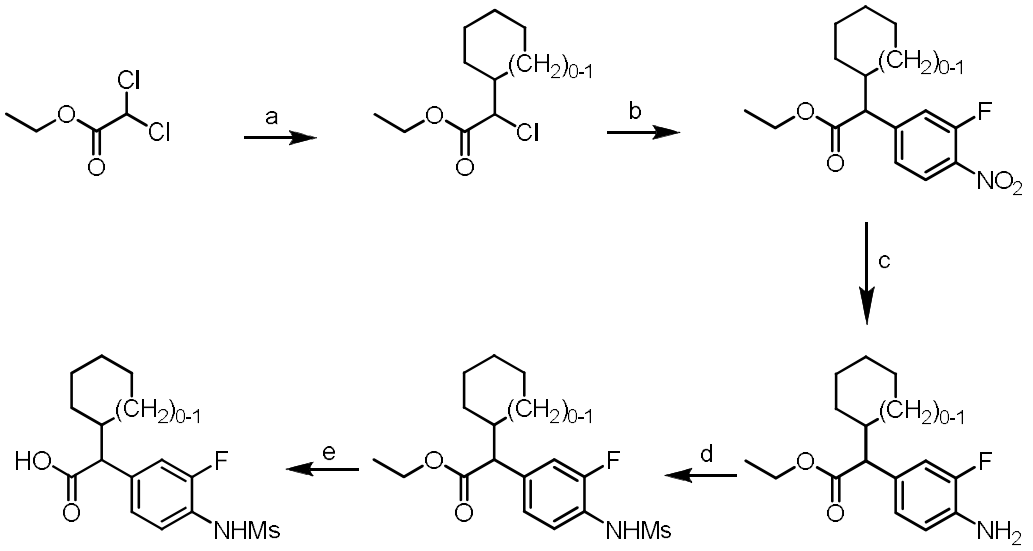

Scheme 20. Synthesis of A/B region for **112-113.**

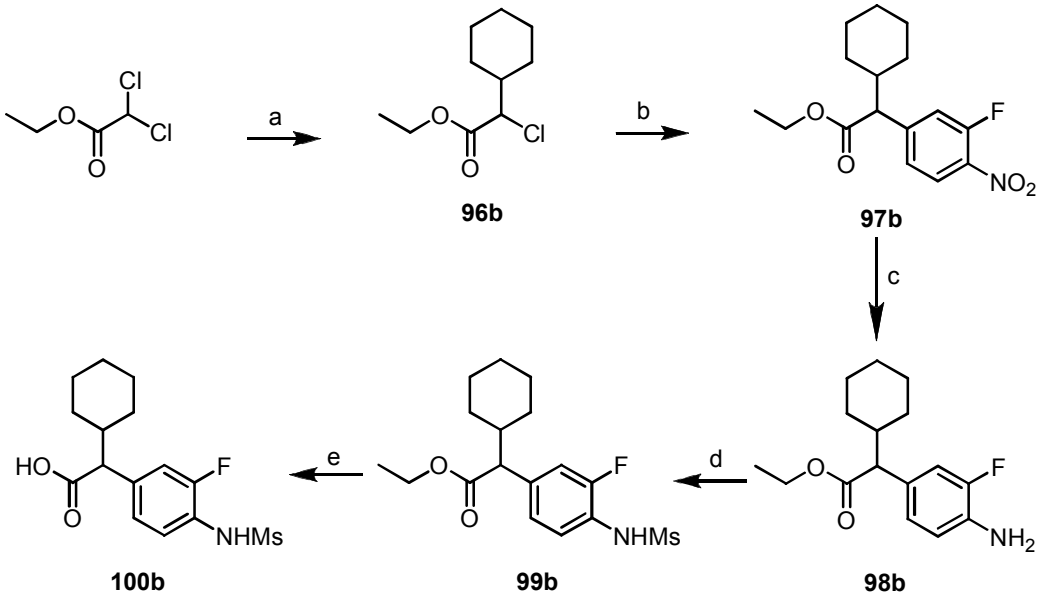

Scheme 21. Synthesis of 2-cyclohexyl-2-(3-fluoro-4-(methylsulfonamido)-phenyl)acetic acid **(100b).**

*Step a: Synthesis of ethyl 2-chloro-2-cyclohexylacetate (**96b**)*

100 mL of 1M BH_3-THF complex (100 mmol) were added to 170 mL of dry THF under a blanket of nitrogen at room temperature. 12.3 mL of cis-1,5-cyclooctadiene (100 mmol) were added dropwise to this mixture within a period of 5 minutes, and the temperature rose to 45°C. The reaction mixture was heated under reflux over a period of 1.5 h, again cooled to 45°C, and 10.1 mL of cyclohexene (100 mmol) were added and stirring was continued for a further 2 h at 45°C. After the reaction mixture had been cooled in an ice bath, 12.2 mL of ethyldichloroacetate (100 mmol) in 50 mL of tert-butanol were added, stirring was continued for a further 15 minutes and 1M potassium tert-butylate (100 mmol, 100 mL) was added dropwise within a further 15 minutes. The reaction mixture was then stirred over a period of 15 minutes, 33 mL of 3M sodium acetate solution (100 mmol) were added and 22.5 mL of 30% strength aq. H_2O_2 solution (750 mmol) were added dropwise. The mixture was stirred at room temperature over a period of 30 minutes, then salted out with NaCl, the organic phase dried over $MgSO_4$ and the solvent removed under reduced pressure. Following washing of the residual solid matter with tert-butylmethyl ether, cyclohexane/tert-butylmethyl ether (9:1), tert-butylmethyl ether, and EA, there were obtained 7.6 g (37.4%) of product.

*Step b: Synthesis of ethyl 2-cyclohexyl-2-(3-fluoro-4-nitrophenyl) acetate (**97b**)*

8.2 g of potassium tert-butoxide were dissolved in 70 mL of DMF and cooled to -5°C. To this, a mixture of ethyl 2-chloro-2-cyclohexylacetate (36.6 mmol, 7.5 g) and 1-fluoro-2-nitrobenzene (36.6 mmol, 3.9 mL) was gently added dropwise and stirring was continued for a further 20 minutes. The reaction mixture was set to pH 4 with 16% strength aq. HCl, diluted with 25 mL of water, and extracted with EA (3 x 50 mL). After combining the organic phases, they were washed with water and sat. aq. NaCl

solution, dried over $MgSO_4$, and concentrated in vacuo. The resulting residue was purified by column chromatography (eluent: 10% EA in n-hexane) and yielded 5.5 g (49%) of the desired product.

*Step c: Synthesis of ethyl 2-(4-amino-3-fluorophenyl)-2-cyclohexylacetate (**98b**)*

Ethyl 2-cyclohexyl-2-(3-fluoro-4-nitrophenyl)acetate was dissolved in a 1:1 mixture of EtOH and EA (420 mL) and 10% Pd/C was added. The mixture was stirred at room temperature under hydrogen gas until the starting material had been consumed. Following removal of the solvent and drying, 5 g of the desired product were obtained (quantitative conversion).

*Step d: Synthesis of ethyl 2-cyclohexyl-2-(3-fluoro-4-(methylsulfonamido)-phenyl)acetate (**99b**)*

The amino compound ethyl 2-(4-amino-3-fluorophenyl)-2-cyclohexylacetate (5 g, 179 mmol) was dissolved in a mixture 1: 1 of 15 mL of pyridine and dichloromethane, cooled under a blanket of nitrogen to 0°C, and 2 mL of methanesulfonyl chloride (26.8 mmol) were added, and stirring of the reaction mixture was continued at 0°C over a period of 1 h. To the reaction mixture there were added, with ice cooling, 15 mL of water, and the mixture was set to pH 1 with 16% strength HCl. Following extraction of the mixture with dichloromethane (3 x 50 mL), the organic phases were combined, dried over $MgSO_4$ and concentrated in vacuo. Purification of the crude product was carried out by column chromatography (eluent: 50% EA in n-hexane) and yielded 5.4 g (85.4%) of product.

*Step e: Synthesis of 2-cyclohexyl-2-(3-fluoro-4-(methylsulfonamido)phenyl)acetic acid (**100b**)*

The phenylacetate (15.2 mmol, 5.4 g) was dissolved in a mixture of 30 mL of THF and 15 mL of water, 1.09 g of LiOH (45.7 mmol) were added and the mixture was heated under reflux over a period of 6 h and stirring was continued over a period of 12 h at room temperature. To the reaction mixture there were added 15 mL of water and the phases were separated. The aqueous phase was acidified with HCl and extracted with dichloromethane (3 x 50 mL) a number of times. The combined organic phases were dried over $MgSO_4$, concentrated, and the residue purified by means of column chromatography (eluent: 50% EA in n-hexane). Yield 1.05 g (21%).

4.4.2. Synthesis of 2-(3-fluoro-4-(methylsulfonamido)phenyl)-2-phenylacetic acid (100c)

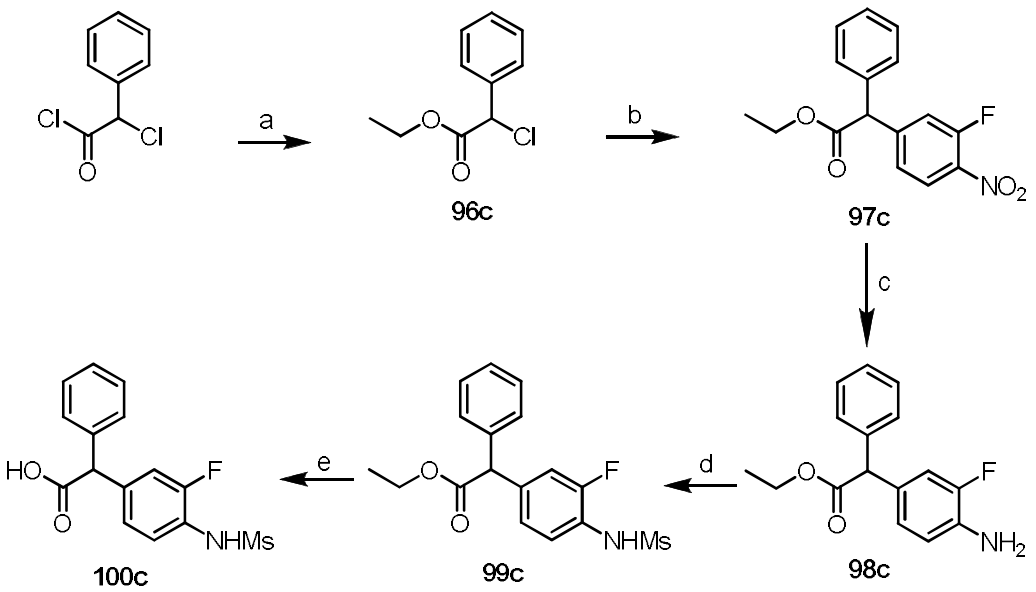

Scheme 22. Synthesis of 2-(3-fluoro-4-(methylsulfonamido)phenyl)-2-phenylacetic acid **(100c)**.

*Step a: Synthesis of ethyl 2-chloro-2-phenylacetate (**96c**)*

To a solution of triethylamine (63.5 mmol, 8.7 mL) in methanol there was added dropwise, at 0°C, α-chlorophenylacetyl chloride (53 mmol, 7.6 mL), and the reaction mixture was then stirred over a period of 3.5 h at room temperature. The reaction mixture was then added to 100 mL of water and extracted with EA (3 x 100 mL). Following the combination of the organic phases, they were dried over $MgSO_4$ and concentrated in vacuo to give 8.76 g (83%) of product.

*Step b: Synthesis of ethyl 2-(3-fluoro-4-nitrophenyl)-2-phenylacetate (**97c**)*

9.8 g of potassium tert-butylate were dissolved in 90 mL of DMF and cooled to -5°C. To this, a mixture of ethyl 2-chloro-2-phenylacetate (43.8 mmol, 8.7 g) and 1-fluoro-2-nitrobenzene (43.8 mmol, 4.6 mL) was gently added dropwise and stirring was continued for a further 20 minutes. The reaction mixture was set to pH 4 with aq. 16% strength. HCl, diluted with 25 mL of water, and extracted with EA (3 x 50 mL). Following combination of the organic phases, they were washed with water and sat. aq. NaCl solution, dried over $MgSO_4$ and concentrated in vacuo. The resulting residue was purified by column chromatography (eluent: 10% EA in n-hexane) and yielded 5.9 g (45%) of the desired product.

*Step c: Synthesis of ethyl -2-(4-amino-3-fluorophenyl)-2-phenylacetate (**98c**)*

Ethyl 2-phenyl-2-(3-fluoro-4-nitrophenyl)acetate was dissolved in a 1:1 mixture of EtOH and EA (465 mL) and and 10% Pd/C was added. The mixture was stirred at room temperature under hydrogen gas until the starting material had been consumed. Following removal of the solvent and drying, 5.2 g (98%) of product were obtained.

*Step d: Synthesis of ethyl 2-phenyl-2-(3-fluoro-4-(methylsulfonamido)-phenyl)acetate (**99c**)*

The amino compound ethyl 2-(4-amino-3-fluorophenyl)-2-phenylacetate (5.2 g, 19 mmol) was dissolved in 15 mL of pyridine, cooled under a blanket of nitrogen to 0°C, and 2.2 mL of methanesulfonyl chloride (28.5 mmol) were added and the reaction mixture was further stirred at 0°C over a period of 1 h. To the reaction mixture there were added, with ice cooling, 15 mL of water, and the mixture was set to pH 1 with aq. 16% strength. HCl. Following extraction of the mixture with dichloromethane (3 x 50 mL), the organic phases were combined, dried over $MgSO_4$ and concentrated in vacuo. Purification of the crude product was carried out by column chromatography (eluent: 50% EA in n-hexane) and yielded 5.8 g (87%) of the desired product.

Step e: Synthesis of 2-phenyl-2-(3-fluoro-4-(methylsulfonamido)-phenyl)acetic acid ***(100c)***

Ethyl 2-phenyl-2-(3-fluoro-4-(methylsulfonamido)-phenyl)acetate (16.5 mmol, 5.8 g) was dissolved in a mixture of 32 mL of THF and 16 mL of water, 1.18 g of LiOH (49.5 mmol) were added, and the mixture was heated under reflux over a period of 15 h. To the reaction mixture there were added 15 mL of water and the phases were separated. The aqueous phase was acidified with aq. HCl and extracted with dichloromethane (3 x 50 mL). The combined organic phases were dried over $MgSO_4$, concentrated, and the residue purified by means of column chromatography (eluent: 50% EA in n-hexane). Yield 3.3 g (61.3%).

4.4.3. Synthesis of (3-fluoro-4-methanesulfonylamino-phenyl)-(3-fluoro-phenyl)-acetic acid (100d)

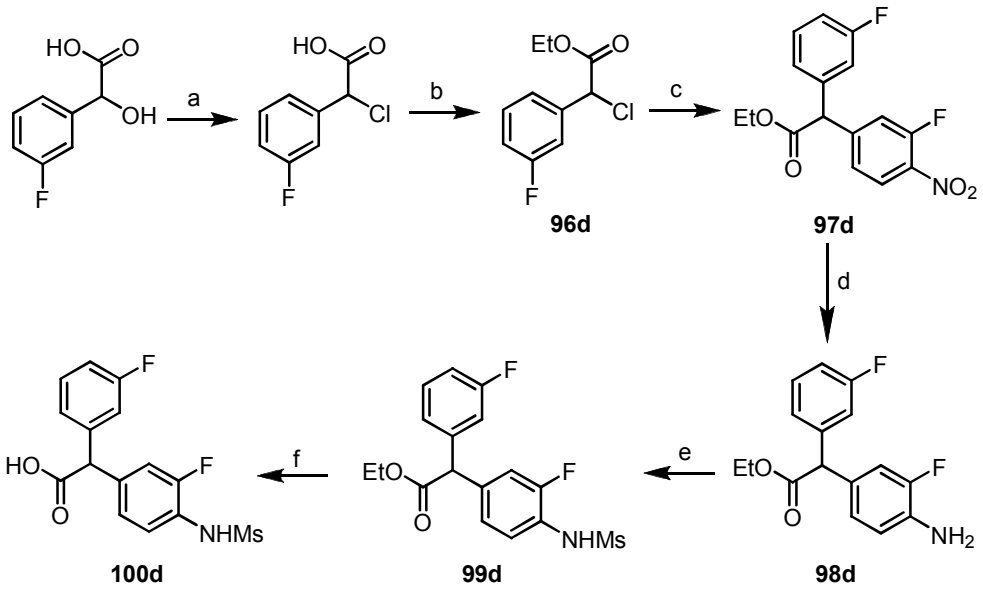

Scheme 23. Synthesis of (3-Fluoro-4-methanesulfonylamino-phenyl)-(3-fluoro-phenyl)-acetic acid **(100d)**.

Step a: Synthesis of 2-chloro-2-(3-fluorophenyl)acetic acid

2-(3-Fluorophenyl)-2-hydroxyacetic acid (12 g, 70.5 mmol), was dissolved in THF (120 mL). Thionyl chloride (10 g, 84.6 mmol) was added to it. Catalytic amount of DMF (1 mL) was added to the reaction mixture. The reaction mixture was stirred at ambient temperature for overnight. The organic solvent was removed under reduced pressure; the residue was diluted with water (200 mL) and extracted with dichloromethane (2 x 200 mL). The combined organic layer was dried over anhydrous magnesium sulfate and concentrated under reduced pressure to afford desired product. Yield: 12 g (crude).

*Step b: Synthesis of ethyl 2-chloro-2-(3-fluorophenyl)acetate (**96d**)*

2-Chloro-2-(3-fluorophenyl)acetic acid (12 g, crude) was dissolved in benzene (240 mL). Ethanol (120 mL) and sulphuric acid (2 mL) was added to it. The reaction mixture

was refluxed for 4 hours using Dean stark apparatus. TLC (5% EA-Hexane, R_f= 0.7) showed complete consumption of starting material. The organic solvent was removed under reduced pressure and the residue was diluted with water (200 mL). The aqueous part was extracted with 20% EA in hexane (3 x 200 mL). The combined organic layer was dried over anhydrous magnesium sulfate and concentrated under reduced pressure to afford a yellow residue, which was purified by column chromatography (eluent: 2% EA in hexane) to afford a light yellow liquid compound. Yield: 8.2 g (60%).

*Step c: Synthesis of ethyl 2-(3-fluoro-4-nitrophenyl)-2-(3-fluorophenyl)acetate (**97d**)*

To a stirred suspension of potassium tert-butoxide (8.5 g, 75.75 mmol) in DMF (50 mL), a mixture of ethyl 2-chloro-2-(3-fluorophenyl)acetate (8.2 g, 38 mmol) and 1-fluoro-2- nitrobenzene (5.34 g, 38 mmol) in DMF (30 mL) was added at –30 ^{o}C. The reaction mixture was stirred for 30 minutes at the same temperature. TLC (10% EA-Hexane, R_f= 0.6) showed complete consumption of starting material. Reaction mixture was diluted with water (800 mL) and extracted with 20% EA in hexane (3 x 200 mL). Then the organic layer was dried over anhydrous magnesium sulfate. The removal of organic solvent under reduced pressure afforded a brown liquid compound, which was purified by column chromatography (eluent: 2% EA in hexane) to afford a light brown liquid compound. Yield: 3.2 g (26%)

*Step d: Synthesis of ethyl 2-(4-amino-3-fluorophenyl)-2-(3-fluorophenyl)acetate (**98d**)*

In a 250 mL round bottomed flask ethyl 2-(3-fluoro-4-nitrophenyl)-2-(3-fluorophenyl)acetate (3.2 g, 10 mmol) was dissolved in EA (50 mL). Palladium on charcoal (150 mg, 10% Pd) was added under nitrogen atmosphere. It was stirred under atmospheric hydrogen pressure for 12 hours. TLC (20% EA in hexane, R_f = 0.3) showed complete conversion of starting material. The reaction mixture was filtered

over celite bed and the bed was washed with EA (3 x 50 mL). The organic layer was concentrated to afford a yellow residue, which was purified through column chromatography (eluent: 10% EA in hexane) to afford the pure amine compound. Yield: 2.3 g (79%).

*Step e: Synthesis of ethyl 2-(3-fluoro-4-(methylsulfonamido)phenyl)-2-(3-fluorophenyl)acetate (**99d**)*

Ethyl 2-(4-amino-3-fluorophenyl)-2-(3-fluorophenyl)acetate (2.3 g, 7.8 mmol) was dissolved in dichloromethane (35 mL). Pyridine (1.9 mL, 23.4 mmol) was added to it. Methanesulfonyl chloride (1.1 g, 9.4 mmol) was added drop wise to the reaction mixture at 0^{o}C and stirred for 16 hours at ambient temperature. TLC (20% EA in hexane, R_f = 0.2) showed complete consumption of starting material. The reaction mixture was diluted with dichloromethane (100 mL) and washed with water (3 x 50 mL). The organic layer was then dried over anhydrous $MgSO_4$ and concentrated to afford a solid compound, which was purified through column chromatography (eluent: 15% EA in hexane) to afford the pure compound. Yield: 2.8 g (96%). ^{1}H NMR ($CDCl_3$, 400 MHz): δ 7.55 (t, 1H), 7.30-7.35 (q, 1H), 6.98-7.18 (m, 5H), 6.50 (s, 1H), 4.21-4.27 (q, 2H), 3.04 (s, 3H), 1.28 (t, 3H).

*Step f: Synthesis of 2-(3-fluoro-4-(methylsulfonamido)phenyl)-2-(3-fluorophenyl)acetic acid (**100d**)*

Ethyl 2-(3-fluoro-4-(methylsulfonamido)phenyl)-2-(3-fluorophenyl)acetate (2.8 g, 7.5 mmol), was dissolved in THF (30 mL). Aqueous LiOH solution (1M, 23 mL, 23 mmol) was added drop wise at 0^{o}C to it. The reaction mixture was then stirred at ambient temperature for 16 hours. TLC (30 % EA-Hexane, R_f = 0.05) showed complete consumption of starting material. The solvent was removed under reduced pressure and

residue was diluted with water (70 mL). The aqueous layer was washed with EA (70 mL) and aqueous part was acidified with 2N HCl up to pH = 3 - 4. The acidified aqueous part was then extracted with EA (3 x 150 mL). The combine organic part was dried over anhydrous $MgSO_4$ and concentrated under reduced pressure to afford a white solid compound. Yield: 1.8 g (70%). ^{1}H NMR (DMSO-d_6, 400 MHz): δ 12.99 (bs, 1H), 9.58 (s, 1H), 7.08 - 7.41 (m, 7H), 5.16 (s, 1H), 3.01 (s, 3H); Mass (M+1): 342; HPLC purity: 96.99%.

4.4.4. Synthesis of (3-fluoro-4-methanesulfonylamino-phenyl)-*o*-tolyl-acetic acid (100f)

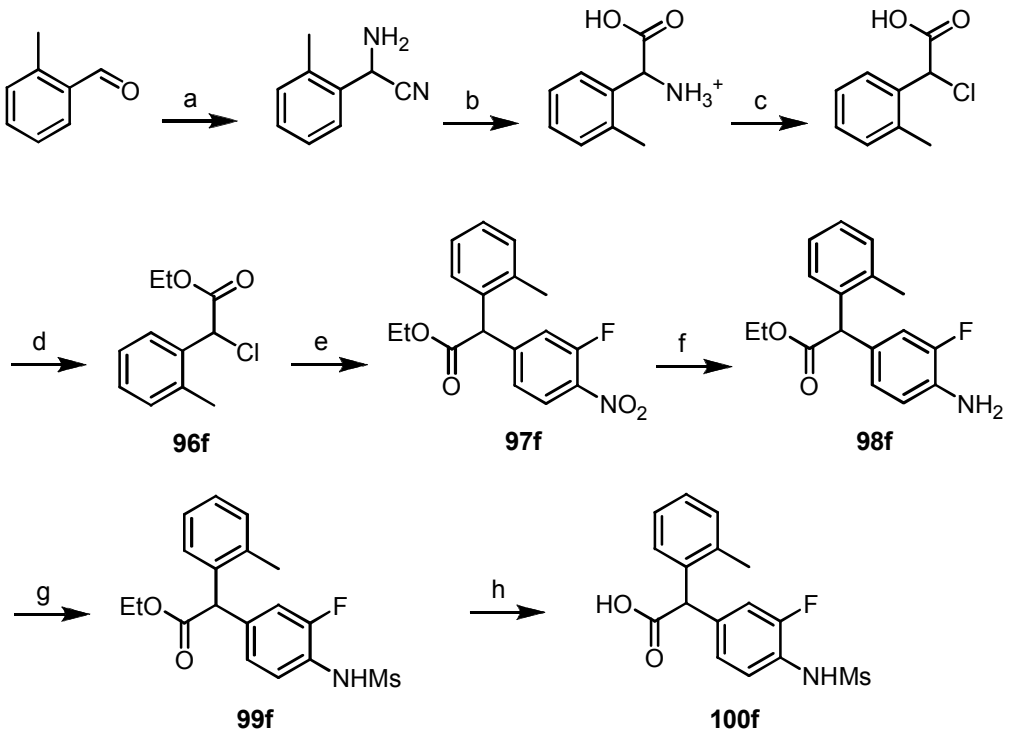

Scheme 24. Synthesis of (3-fluoro-4-methanesulfonylamino-phenyl)-*o*-tolyl-acetic acid **(100f)**.

Step a: Synthesis of 2-amino-2-o-tolylacetonitrile

Sodium cyanide (6.12 g, 124.8 mmol) was dissolved in water (25 mL) and ammonium chloride (7.35 g, 137.3 mmol) was added to it. 2-Methylbenzaldehyde (15 g, 124.8 mmol) in MeOH (25 mL) was added to the reaction mixture and stirred it at ambient temperature for two days. TLC (5% EA-Hexane, R_f = 0.4) showed complete consumption of starting material. Water (100 mL) and benzene (100 mL) was added to the reaction mixture and stirred for 10 minutes. The separated organic layer was dried over anhydrous $MgSO_4$ and concentrated under reduced pressure to afford a yellow liquid desired compound. Yield: 17 g (crude).

Step b: Synthesis of carboxy(o-tolyl)methanaminium

2-Amino-2-o-tolylacetonitrile (17 g, crude) was dissolved 6N HCl (110 mL) and refluxed for 20 hours. HCl was removed under reduced pressure. The residue was diluted with EtOH (2 x 200 mL) and concentrated under reduced pressure. Finally EA (250 mL) was added to it and stirred at 70^{o}C for 1 hour. A solid came out upon cooling and it was filtered through glass-sintered funnel to afford yellow crystalline solid compound. Yield: 13 g (crude).

Step c: Synthesis of 2-chloro-2-o-tolylacetic acid

Carboxy(*o*-tolyl)methanaminium (12 g, 59.5 mmol) was dissolved in HCl (240 mL) and it was cooled to –5^{o}C. Sodium nitrite solution (7.8 g, 113 mmol) in water (36 mL) was added drop wise over the period of 30 minutes. After complete addition, reaction mixture was stirred at ambient temperature for 3 hours. TLC (in EA R_f= 0.3) showed complete consumption of starting material. The aqueous part was extracted in EA (3 x 250 mL). The organic layer was washed with water (2 x 200 mL) and finally with brine (200 mL). The washed organic layer was dried over anhydrous $MgSO_4$ and

concentrated under reduced pressure to afford a yellow solid compound. Yield: 8.5 g (crude).

Step d: Synthesis of ethyl 2-chloro-2-o-tolylacetate (96f)

2-Chloro-2-*o*-tolylacetic acid (8 g, 43.5 mmol) was dissolved in benzene (160 mL). EtOH (80 mL) and H_2SO_4 (2 mL) was added to it. The reaction mixture was refluxed for 4 hours. TLC (in 5% EA-Hexane, R_f = 0.7) showed complete consumption of starting material. The organic solvent was removed under reduced pressure and the residue was diluted with water (200 mL). The aqueous part was extracted with 20% EA in hexane (3 x 200 mL). The combined organic layer was dried over anhydrous $MgSO_4$ and concentrated under reduced pressure to afford a yellow residue, which was purified by column chromatography (eluent: 2% EA in hexane) to afford a light yellow liquid compound. Yield: 6.6 g (72%). ^{1}H NMR ($CDCl_3$, 400 MHz): δ 7.17- 7.49 (m, 4H), 5.59 (s, 1H), 4.16- 4.30 (m, 2H), 2.42 (s, 3H), 1.24 (t, 3H).

*Step e: Synthesis of ethyl 2-(3-fluoro-4-nitrophenyl)-2-o-tolylacetate (**97f**)*

To a stirred suspension of potassium tertiary butoxide (7.0 g, 62 mmol) in DMF (30 mL), a mixture of ethyl 2-chloro-2-*o*-tolylacetate (6.6 g, 31 mmol) and 1-fluoro-2-nitrobenzene (4.38 g, 31 mmol) in DMF (40 mL) was added at –30°C. The reaction mixture was stirred for 30 minutes at the same temperature. TLC (10% EA-Hexane, R_f = 0.6) showed complete consumption of starting material. Reaction mixture was diluted with water (700 mL) and extracted with 20% EA in hexane (3 x 250 mL). Then the organic layer was dried over anhydrous $MgSO_4$. The removal of organic solvent under reduced pressure afforded a yellowish compound, which was purified by column chromatography (eluent: 2% EA in hexane) to afford a yellow liquid compound. Yield:

3.3 g (33.5%). ^{1}H NMR ($CDCl_3$, 400 MHz): δ 7.99 (t, 1H), 7.13-7.25 (m, 5H), 5.22 (s, 1H), 4.20- 4.25 (q, 2H), 2.25 (s, 3H), 1.25 (t, 3H).

*Step f: Synthesis of ethyl 2-(4-amino-3-fluorophenyl)-2-o-tolylacetate (**98f**)*

In a 500 mL round bottomed flask ethyl 2-(3-fluoro-4-nitrophenyl)-2-*o*-tolylacetate (3.3g, 10.4 mmol) dissolved in EA (45 mL). Palladium on charcoal (160 mg, 10% Pd) was added under nitrogen atmosphere. It was stirred under atmospheric hydrogen pressure for 12 hours. TLC (20% EA in hexane, R_f= 0.3) showed complete conversion of starting material. The reaction mixture was filtered over celite bed and the bed was washed with EA (3 x 100 mL). The organic layer was concentrated to afford a yellow residue, which was purified through column chromatography (eluent: 10% EA in hexane) to afford the pure amine compound. Yield: 2.4 g (80%). ^{1}H NMR ($CDCl_3$, 400 MHz): δ 7.19-7.27 (m, 4H), 6.89 (d, 1H), 6.82 (d, 1H), 6.72 (t, 1H), 5.07 (s, 1H), 4.19-4.24 (q, 2H), 3.69 (s, 2H), 2.28 (s, 3H), 1.26 (t, 3H).

*Step g: Synthesis of ethyl 2-(3-fluoro-4-(methylsulfonamido)phenyl)-2-o-tolylacetate (**99f**)*

Ethyl 2-(4-amino-3-fluorophenyl)-2-*o*-tolylacetate (2.4 g, 8.35 mmol) was dissolved in dichloromethane (40 mL). Pyridine (2 mL, 25 mmol) was added to it. Methanesulphonyl chloride (0.78 mL, 10 mmol) was added drop wise to the reaction mixture at 0^{o}C and stirred for 16 hours at ambient temperature. TLC (20% EA in hexane, R_f = 0.2) showed complete conversion of starting material. The reaction mixture was diluted with dichloromethane (100 mL) and washed with water (3 x 70 mL). The organic layer was then dried over anhydrous $MgSO_4$ and concentrated to afford a solid compound, which was purified through column chromatography (eluent: 15% EA in hexane) to afford the desired compound. Yield: 2.9 g (95%). ^{1}H NMR

($CDCl_3$, 400 MHz): δ 9.60 (s, 1H), 7.34 (t, 1H), 7.04-7.20 (m, 5H), 5.32 (s, 1H), 4.12 - 4.19 (m, 2H), 3.02 (s, 3H), 2.21 (s, 3H), 1.16 (t, 3H).

*Step h: Synthesis of 2-(3-fluoro-4-(methylsulfonamido)phenyl)-2-o-tolylacetic acid **(100f)***

Ethyl 2-(3-fluoro-4-(methylsulfonamido)phenyl)-2-*o*-tolylacetate (2.9 g, 7.9 mmol), was dissolved in THF (45 mL). Aqueous lithium hydroxide solution (1M, 24 mL, 24 mmol) was added drop wise at 0^oC to it. The reaction mixture was then stirred at ambient temperature for 16 hours. TLC (30% EA-Hexane, R_f= 0.05) showed complete consumption of starting material. The solvent was removed under reduced pressure and residue was diluted with water (80 mL). The aqueous layer was washed with EA (150 mL) and aqueous part was acidified with 2N HCl up to pH = 3 - 4. The acidified aqueous part was then extracted with EA (3 x 80 mL). The combine organic part was dried over anhydrous $MgSO_4$ and concentrated under reduced pressure to afford a white solid compound. Yield: 2.2 g (82%). ^1H NMR (DMSO-d_6, 400 MHz): δ 12.86 (bs, 1H), 9.58 (s, 1H), 7.33 (t, 1H), 7.05-7.23 (m, 6H), 5.22 (s, 1H), 3.01 (s, 3H), 2.22 (s, 3H); Mass (M+1): 338; HPLC purity: 95.73%.

4.4.5. Synthesis of (3-fluoro-4-methanesulfonylamino-phenyl)-*m*-tolyl-acetic acid (100g)

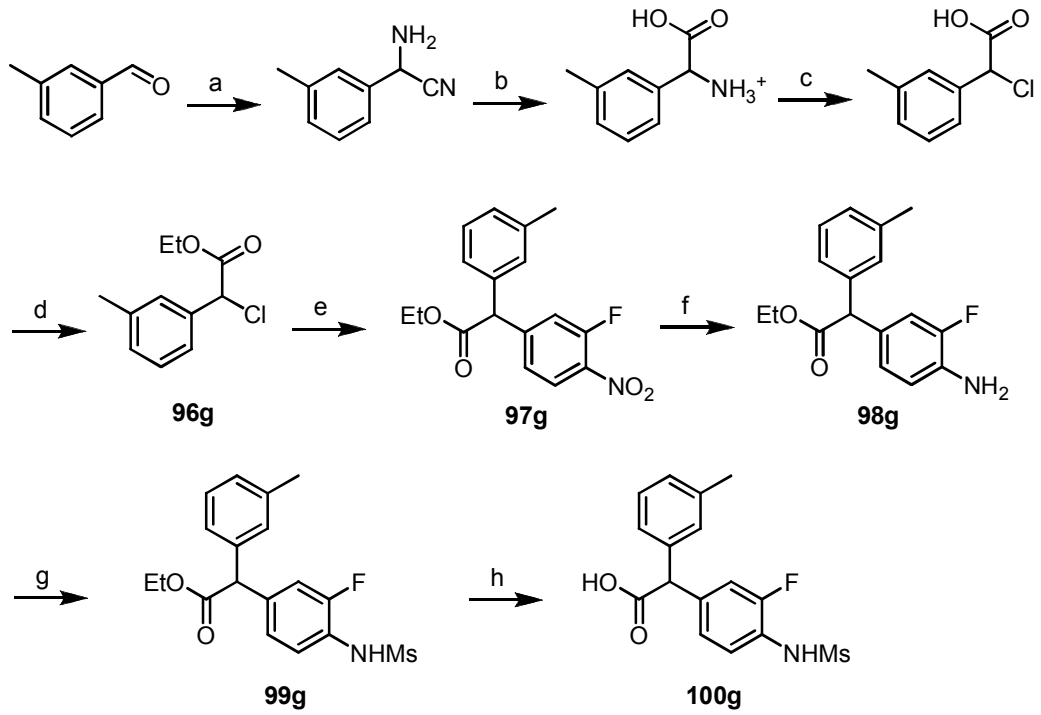

Scheme 25. Synthesis of (3-fluoro-4-methanesulfonylamino-phenyl)-*m*-tolyl-acetic acid **(100g)**.

Step a: Synthesis of 2-amino-2-m-tolylacetonitrile

Sodium cyanide (6.12 g, 124.8 mmol) was dissolved in water (25 mL) and ammonium chloride (7.35 g, 137.3 mmol) was added to it. 3-Methylbenzaldehyde (15 g, 124.8 mmol) in MeOH (25 mL) was added to the reaction mixture and stirred it at ambient temperature for two days. TLC (5% EA-Hexane, R_f = 0.4) showed complete consumption of starting material. Water (100 mL) and benzene (100 mL) was added to the reaction mixture and stirred for 10 minutes. The separated organic layer was dried over anhydrous $MgSO_4$ and concentrated under reduced pressure to afford a yellow liquid compound.Yield: 17 g (crude).

Step b: Synthesis of carboxy(m-tolyl)methanaminium

2-Amino-2-*m*-tolylacetonitrile (17 g, crude) was dissolved in 6N HCl (250 mL) and refluxed for 20 hours. HCl was removed under reduced pressure. The residue was diluted with EtOH (2 x 200 mL) and concentrated under reduced pressure. Finally EA (250 mL) was added to it and stirred at 70^{o}C for 1 hour. A solid came out upon cooling and it was filtered through glass-sintered funnel to afford yellow crystalline solid. Yield: 13 g (crude).

Step c: Synthesis of 2-chloro-2-m-tolylacetic acid

Carboxy(*m*-tolyl)methanaminium (12 g, 60 mmol) was dissolved in HCl (240 mL) and it was cooled to –5^{o}C. Sodium nitrite solution (7.8 g, 113.6 mmol) in water (36 mL) was added drop wise over the period of 30 minutes. After complete addition, reaction mixture was stirred at ambient temperature for 3 hours. TLC (in EA R_f= 0.3) showed complete consumption of starting material. The aqueous part was extracted in EA (3 x 200 mL). The organic layer was washed with water (2 x 100 mL) and finally with brine (200 mL). The washed organic layer was dried over anhydrous $MgSO_4$ and concentrated under reduced pressure to afford a yellow solid. Yield: 8.5 g (crude).

*Step d: Synthesis of ethyl 2-chloro-2-m-tolylacetate (**96g**)*

2-Chloro-2-*m*-tolylacetic acid (8.5 g, 46.2 mmol) was dissolved in benzene (170 mL). EtOH (85 mL) and H_2SO_4 (2 mL) was added to it. The reaction mixture was refluxed for 4 hours. TLC (in 5% EA-Hexane, R_f = 0.7) showed complete consumption of starting material. The organic solvent was removed under reduced pressure and the residue was diluted with water (200 mL). The aqueous part was extracted with 20% EA in hexane (3 x 200 mL). The combined organic layer was dried over anhydrous $MgSO_4$ and concentrated under reduced pressure to afford a yellow residue, which was purified

by column chromatography (eluent: 2% EA in hexane) to afford a light yellow liquid compound. Yield: 6.2 g (63%).

*Step e: Synthesis of ethyl 2-(3-fluoro-4-nitrophenyl)-2-m-tolylacetate (**97g**)*

To a stirred suspension of potassium *tert*- butoxide (6.54 g, 58.3 mmol) in DMF (40 mL), a mixture of ethyl 2-chloro-2-*m*-tolylacetate (6.2 g, 29.15 mmol) and 1-fluoro-2-nitrobenzene (4.12 g, 29.15 mmol) in DMF (30 mL) was added at –30^{o}C. The reaction mixture was stirred for 30 minutes at the same temperature. TLC (10% EA-Hexane, R_f = 0.6) showed complete consumption of starting material. Reaction mixture was diluted with water (700 mL) and extracted with 20% EA in hexane (3 x 200 mL). Then the organic layer was dried over anhydrous $MgSO_4$. The removal of organic solvent under reduced pressure afforded a yellowish compound, which was purified by column chromatography (eluent: 2% ethyl acetate in hexane) to afford a yellow liquid compound. Yield: 5 g (54%). ^{1}H NMR ($CDCl_3$, 400 MHz): δ 8.00 (t, 1H), 7.06-7.28 (m, 6H), 4.98 (s, 1H), 4.18-4.26 (m, 2H), 2.33 (s, 1H), 1.25 (t, 3H).

*Step f: Synthesis of ethyl 2-(4-amino-3-fluorophenyl)-2-m-tolylacetate (**98g**)*

In a 500 mL round bottomed flask ethyl 2-(3-fluoro-4-nitrophenyl)-2-*m*-tolylacetate (5 g, 15.75 mmol) was dissolved in EA (75 mL). Palladium on charcoal (250 mg, 10% Pd) was added under nitrogen atmosphere. It was stirred under atmospheric hydrogen pressure for 12 hours. TLC (20% EA in hexane, R_f= 0.3) showed complete conversion of starting material. The reaction mixture was filtered over celite bed and the bed was washed with EA (3 x 100 mL). The organic layer was concentrated to afford a yellow residue, which was purified through column chromatography (eluent: 10% EA in hexane) to afford the pure amine. Yield: 3.8 g (84%). ^{1}H NMR ($CDCl_3$, 400 MHz): δ

7.19 (t, 1H), 7.07 (t, 3H), 6.96 (d, 1H), 6.86 (d, 1H), 6.69 (t, 1H), 4.83 (s, 1H), 4.15-4.21 (q, 2H), 3.66 (s, 2H), 2.31 (s, 3H), 1.24 (t, 3H).

Step g: Synthesis of ethyl 2-(3-fluoro-4-(methylsulfonamido)phenyl)-2-m-tolylacetate ***(99g)***

Ethyl 2-(4-amino-3-fluorophenyl)-2-*m*-tolylacetate (3.8 g, 13.22 mmol) was dissolved in dichloromethane (60 mL). Pyridine (3.4 mL, 39.66 mmol) was added to it. Methanesulfonyl chloride (1.8 g, 15.87 mmol) was added drop wise to the reaction mixture at 0^{o}C and stirred for 16 hours at ambient temperature. TLC (20% EA in hexane, R_f = 0.2) showed complete conversion of starting material. The reaction mixture was diluted with dichloromethane (200 mL) and washed with water (3 x 200 mL). The organic layer was then dried over anhydrous $MgSO_4$ and concentrated to afford a solid compound, which was purified through column chromatography (eluent: 15% EA in hexane) to afford the pure desired compound. Yield: 4.5 g (93%). ^{1}H NMR ($CDCl_3$, 400 MHz): δ 9.59 (s, 1H), 7.34 (t, 1H), 7.21-7.25 (m, 2H), 7.07-7.16 (m, 4H), 5.17 (s, 1H), 4.11- 4.16 (q, 2H), 3.01 (s, 3H), 2.27 (s, 3H), 1.17 (t, 3H).

Step h: Synthesis of 2-(3-fluoro-4-(methylsulfonamido)phenyl)-2-m-tolylacetic acid ***(100g)***

Ethyl 2-(3-fluoro-4-(methylsulfonamido)phenyl)-2-*m*-tolylacetate (4.5 g, 12.3 mmol), was dissolved in THF (70 mL). Aqueous lithium hydroxide solution (1M, 37 mL, 37 mmol) was added drop wise at 0^{o}C to it. The reaction mixture was then stirred at ambient temperature for 16 hours. TLC (30% EA-Hexane, R_f= 0.05) showed complete consumption of starting material. The solvent was removed under reduced pressure and residue was diluted with water (150 mL). The aqueous layer was washed with EA (150 mL) and aqueous part was acidified with 2N HCl up to pH = 3 - 4. The acidified

aqueous part was then extracted with EA (3 x 100 mL). The combine organic part was dried over anhydrous $MgSO_4$ and concentrated under reduced pressure to afford a white solid. Yield: 3.9 g (80%). ^{1}H NMR (DMSO-d_6, 400 MHz): δ 12.81(bs, 1H), 9.55 (s, 1H), 7.32 (t, 1H), 7.06-7.24 (m, 5H), 5.04 (s, 1H), 3.00 (s, 3H), 2.28 (s, 3H); Mass (M+1): 338; HPLC purity: 98.37%.

4.4.6. Synthesis of 2-(3-fluoro-4-methanesulfonylamino-phenyl)-3-phenyl-propionic acid (100i)

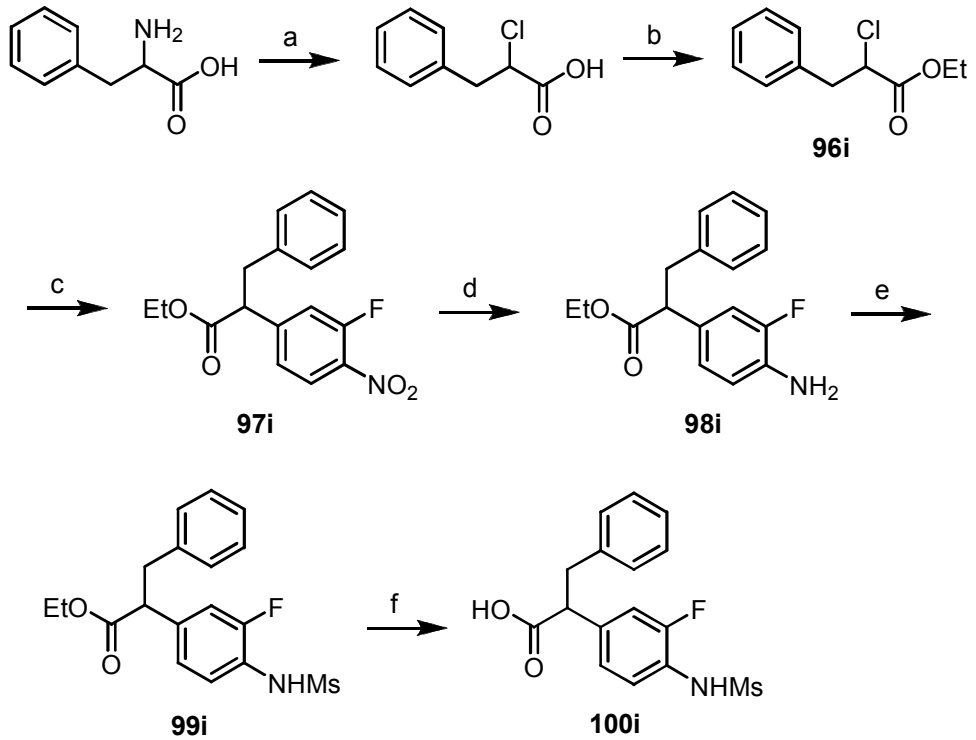

Scheme 26. Synthesis of 2-(3-fluoro-4-methanesulfonylamino-phenyl)-3-phenyl-propionic acid **(100i)**.

Step a: Synthesis of 2-chloro-3-phenylpropanoic acid

2-Amino-3-phenylpropanoic acid (10 g, 60.5 mmol) was dissolved in conc. HCl (200 mL) and was cooled to –5°C. Sodium nitrite solution (7.9 g, 115 mmol) in water (30 mL) was added drop wise over the period of 30 minutes. After complete addition reaction mixture was stirred at ambient temperature for 2 hours. TLC (in 50% EA-Hexane, R_f= 0.4) showed complete consumption of starting material. The aqueous part was extracted in EA (3 x 200 mL). The overall organic layer was washed with water (2 x 200 mL) and finally with brine (200 mL). The washed organic layer was dried over anhydrous $MgSO_4$ and concentrated under reduced pressure to afford a yellow liquid. Yield: 12 g (crude).

*Step b: Synthesis of ethyl 2-chloro-3-phenylpropanoate (**96i**)*

2-Chloro-3-phenylpropanoic acid (12 g, 65 mmol) dissolved in benzene (240 mL). EtOH (120 mL) and H_2SO_4 (2 mL) was added to it. The reaction mixture was refluxed for 4 hours using Dean-stark apparatus. TLC (20 % EA in hexane, R_f= 0.6) showed complete consumption of starting material. The organic solvent was concentrated under reduced pressure and the residue was diluted with water (200 mL). The aqueous layer was extracted with 30% EA in hexane (3 x 200 mL). The overall organic layer was dried over anhydrous $MgSO_4$ and concentrated under reduced pressure to get a yellowish residue, which was purified by column chromatography (eluent: 2% EA in hexane) to afford a light yellow liquid compound. Yield: 10g (87%). ^{1}H NMR ($CDCl_3$, 400 MHz): δ 7.23-7.35 (m, 5H), 4.81 (q, 1H), 4.11 (q, 2H), 3.10-3.34 (m, 2H), 1.14 (t, 3H).

*Step c: Synthesis of ethyl 2-(3-fluoro-4-nitrophenyl)-3-phenylpropanoate (**97i**)*

To a stirred suspension of potassium *tert*-butoxide (14.3 g, 127 mmol) in DMF (90 mL), a mixture of ethyl 2-chloro-3-phenylpropanoate (13.5 g, 63.5 mmol) and 1-fluoro 2-

nitrobenzene (7.12 g, 63.5 mmol) in DMF (50 mL) was added at –30°C. The reaction mixture was stirred for 30 minute at the same temperature. TLC (10% EA-Hexane, R_f= 0.4) showed complete consumption of starting material. Reaction mixture was diluted with water (1.5 L) and extracted with 20% EA in hexane (3 x 250 mL). Then the organic layer was dried over anhydrous $MgSO_4$. The removal of organic solvent under reduced pressure afforded a yellowish compound, which was purified by column chromatography (eluent: 2% EA in hexane) to afford a light brown solid. Yield: 14.5 g (72%). ^{1}H NMR ($CDCl_3$, 400 MHz): δ 6.64-7.24 (m, 8H), 3.96 (q, 2H), 3.77 (t, 1H), 3.18(q, 1H), 2.90 (q, 1H), 1.02 (t, 3H).

*Step d: Synthesis of ethyl 2-(4-amino-3-fluorophenyl)-3-phenylpropanoate (**98i**)*

In a 500 mL round bottomed flask ethyl 2-(3-fluoro-4-nitrophenyl)-3-phenylpropanoate (14.5 g, 45.7 mmol) was dissolved in EA (300 mL). Palladium on charcoal (0.7 g, 10% Pd) was added under nitrogen atmosphere. It was stirred under atmospheric hydrogen pressure for 12 hours. TLC (20% EA in hexane, R_f= 0.4) showed complete conversion of starting material. Reaction mixture was filtered over celite bed and washed with EA (3 x 150 mL). The organic layer was concentrated to afford a yellowish residue, which was purified through column chromatography (eluent: 10% EA in hexane) to afford the pure amine compound. Yield: 12.5 g (95%). ^{1}H NMR ($CDCl_3$, 400 MHz): δ 6.64-7.24 (m, 8H), 5.06 (s, 2H), 3.96 (q, 2H), 3.77 (t, 1H), 3.18(q, 1H), 2.90 (q, 1H), 1.02 (t, 3H).

*Step e: Synthesis of ethyl 2-(3-fluoro-4-(methylsulfonamido)phenyl)-3-phenylpropanoate (**99i**)*

Ethyl 2-(4-amino-3-fluorophenyl)-3-phenylpropanoate (12.5 g, 43.5 mmol) was dissolved in dichloromethane (190 mL). Pyridine (10.5 mL, 130.5 mmol) was added to it. Methanesulfonyl chloride (6 g, 47.85 mmol) was added drop wise to the reaction

mixture at 0-5°C and stirred for 16 hours at ambient temperature. TLC (20% EA in hexane, R_f = 0.2) showed complete conversion of starting material. Reaction mixture was diluted with dichloromethane (200 mL) and washed with water (3 x 200 mL). The organic layer was then dried over anhydrous $MgSO_4$ and concentrated to afford a solid compound, which was purified through column chromatography (eluent: 20% ethyl acetate in hexane) to afford the pure compound. Yield: 13.5 g (85%). ^{1}H NMR ($CDCl_3$, 400 MHz): δ 9.57 (s, 1H), 7.14-7.34 (m, 8H), 3.94-4.04 (m, 3H), 3.25 (q, 1H), 2.97-3.02 (m, 4H), 1.03 (t, 3H).

Step f: Synthesis of 2-(3-fluoro-4-(methylsulfonamido)phenyl)-3-phenylpropanoic acid ***(100i)***

Ethyl 2-(3-fluoro-4-(methylsulfonamido)phenyl)-3-phenylpropanoate (4 g, 11 mmol), was dissolved in THF (60 mL). Lithium hydroxide solution (1M, 33 mL, 33 mmol) was added drop wise at 10-15°C to it. The reaction mixture was then stirred at ambient temperature for 16 hours. TLC (in 30% EA-Hexane, R_f = 0.05) showed complete consumption of starting material. The solvent was removed under reduced pressure and residue was diluted with water (150 mL). The aqueous layer was washed with EA (150 mL) and aqueous part was acidified with 2N aqueous HCl solution up to pH = 3-4. The acidified aqueous part was then extracted with EA (3 x 150 mL). The organic layer was dried over anhydrous $MgSO_4$and concentrated under reduced pressure afforded a white solid compound. Yield: 3 g (81%). ^{1}H NMR ($CDCl_3$, 400 MHz): δ 12.53 (s, 1H), 9.56 (s, 1H), 7.15-7.33 (m, 8H), 3.91 (t, 1H), 3.26 (q, 1H), 3.00 (s, 3H), 2.96 (t, 1H). MS m/z (M+1): 338; HPLC purity 98.27%.

4.5. Synthesis of the A/B-region for 132-135 (Scheme 16)

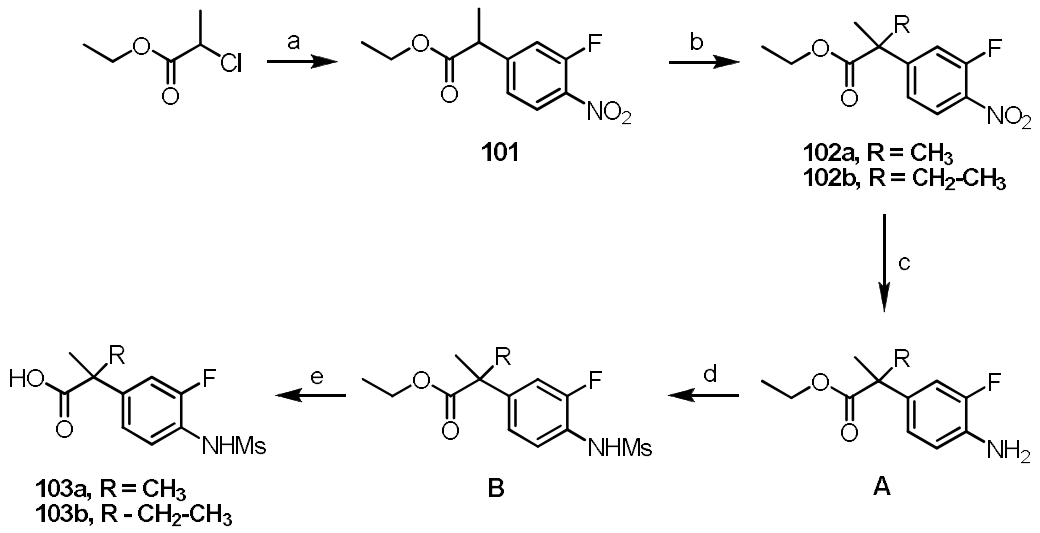

*Step a: Synthesis of ethyl 2-(3-fluoro-4-nitrophenyl)propanoate (**101**)*

3 Equivalents of potassium *tert*-butoxide are suspended in DMF under a blanket of nitrogen and cooled to -40 °C. While maintaining this temperature, a mixture of *o*-fluoronitrobenzene (1 equiv.) and ethyl 2-chloropropionate (1.2 equiv.) is then added and the mixture is stirred over a period of 10 minutes. The reaction mixture is diluted with acetic acid and water at -40°C. The aqueous phase is then extracted a number of times with 20% strength EA in hexane, and the combined organic phases are washed with water and sat. aq. NaCl solution and dried over $MgSO_4$. Purification of the concentrated organic phase is effected by column chromatography (eluent: 10% EA in hexane).

*Step b: Synthesis of **102a/102b***

To a solution of the resulting nitroester (**101**, 1 equiv.) and NaH (0.6 equiv.) in DMF there are slowly added dropwise 0.75 equiv. of alkyliodide at 0°C, and the reaction mixture is stirred over a period of approximately 10 minutes. The reaction mixture is

then diluted with 1N HCl solution and water and extracted with diethyl ether a number of times. The combined organic phases are washed with water and sat. aq. NaCl solution, dried over $MgSO_4$, and concentrated in vacuo. Further purification of the crude product may be carried out by column chromatography (eluent: 10-20% EA in hexane).

*Step c: Synthesis of the general formula **A***

A suspension of the compound of **102a** or **102b** (1 equiv.) and palladium-on-charcoal (10% of Pd) in EtOH is hydrogenated over a period of 1 h under a blanket of hydrogen. The suspension is isolated by filtration, concentrated in vacuo, and purified by column chromatography (eluent: EA/hexane).

*Step d: Synthesis of the general formula **B***

The compound of the general formula **A** (1 equiv.) is used in dichloromethane and pyridine as initial batch and cooled to 0°C. Methane sulfonyl chloride (1.5 equiv.) is added dropwise at 0°C and the reaction mixture is stirred over a period of 2 h at room temperature. After re-cooling the mixture to 0°C, it is acidified with 4N aq. HCl to pH 3. The organic phase is extracted with dichloromethane a number of times. The combined organic phases are washed with water and sat. aq. NaCl solution, dried over $MgSO_4$ and concentrated to dryness. Purification by column chromatography (eluent: EA in hexane) gives the desired product.

*Step e: Synthesis of **103a/103b***

1 Equiv. of the ethyl ester of the general formula **B** is dissolved in a 2:1 mixture of THF/water and stirred over a period of 15 minutes. To this solution there are added 3 equivalents of LiOH likewise dissolved in a 2:1 mixture of THF/water and the

suspension is stirred at 45°C over a period of 2 h. The aqueous phase is set to pH 1 with 4N aq. HCl with cooling and extracted with dichloromethane a number of times. The combined organic phases are dried over $MgSO_4$ and concentrated under reduced pressure.

4.6. Synthesis of the A/B-region for 136-137 (Scheme 17)

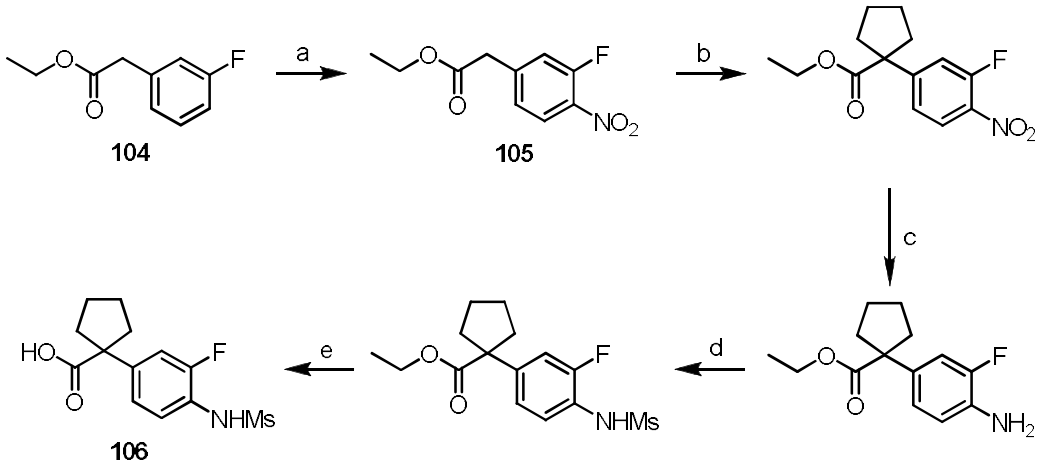

*Step a: Synthesis of ethyl 2-(3-fluoro-4-nitrophenyl)acetate (**105**)*

A mixture of 3-fluorophenyl acetate (**104,** 1 equiv.) and H_2SO_4 (0.261 equiv.) is added dropwise to a solution of nitric acid (1 equiv.) at 0°C and the reaction mixture is stirred over a period of 2 h. The reaction mixture is diluted with ice water and extracted with EA a number of times. The combined organic phases are washed with water, concentrated in vacuo and purified by column chromatography (eluent: EA/hexane).

Step b: Synthesis of ethyl 1-(3-fluoro-4-nitrophenyl)cyclopentanecarboxylate

NaH (10 equivalents) is slowly added to **105** (1 equiv.) dissolved in dry THF, the reaction mixture is stirred over a period of 10 minutes and 1,4-dibromobutane (5 equiv.) is then added. The reaction mixture is heated to room temperature within a period of 30

minutes and diluted with sat. aq. NH_4Cl solution. Following aqueous workup, the resulting crude product is purified by flash chromatography (eluent: EA/hexane).

Step c: Synthesis of ethyl 1-(4-amino-3-fluorophenyl)cyclopentanecarboxylate

A suspension of ethyl 1-(3-fluoro-4-nitrophenyl)cyclopentanecarboxylate (1 equiv.) and palladium-on-charcoal (10% of Pd) in EtOH is hydrogenated under a blanket of hydrogen over a period of 1 h. The suspension is isolated by filtration, concentrated in vacuo, and purified by column chromatography (eluent: EA/hexane).

Step d: Synthesis of ethyl 1-(3-fluoro-4-(methylsulfonamido)phenyl)-cyclopentanecarboxylate

Ethyl 1-(4-amino-3-fluorophenyl)cyclopentanecarboxylate (1 equiv.) is used in dichloromethane as initial batch, cooled to 0°C, and methanesulfonyl chloride (1.5 equiv.) is added dropwise at 0°C and the reaction mixture is stirred at room temperature over a period of 2 h. After re-cooling the mixture to 0°C, it is acidified with 4N aq. HCl to pH 3. The organic phase is extracted with dichloromethane a number of times. The combined organic phases are washed with water and sat. aq. NaCl solution, dried over $MgSO_4$ and concentrated to dryness. Purification by column chromatography (eluent: EA in hexane) gives the desired product.

*Step e: Synthesis of 1-(3-fluoro-4-(methylsulfonamido)phenyl)cyclopentanecarboxylic acid (**106**)*

1 Equivalent of ethyl 1-(3-fluoro-4-(methylsulfonamido)phenyl)-cyclopentanecarboxylate is dissolved in a 2:1 mixture of THF/water and the solution is stirred over a period of 15 minutes. To this solution there are added 3 equivalents of LiOH likewise dissolved in a 2:1 mixture of THF/water, and the mixture is stirred over

a period of 2 h at 45°C. The aqueous phase is set to pH 1 with aq. 4N HCl with cooling and extracted with dichloromethane a number of times. The combined organic phases are dried over $MgSO_4$ and concentrated under reduced pressure.

4.7. Synthesis of C-region amines (Scheme 18)

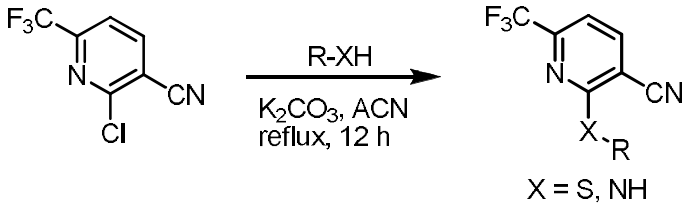

2-Piperidin-1-yl-6-trifluoromethyl-nicotinonitrile (amine addition)

A mixture of 2-chloro-6-trifluoromethyl-nicotinonitrile (1.45 mmol), piperidine (2.90 mmol), and DBU (2.90 mmol) were dissolved in a acetonitrile (10 mL). The mixture was stirred for 15 h at 50°C. The reaction mixture was extracted with EA (30 mL) twice. The combined organic extracts were dried over $MgSO_4$, filtered, and concentrated *in vacuo*. The residue was purified by flash column chromatography on silica gel using EA: hexane (1:15) as eluent to afford the desire product.

2-Cyclohexylsulfanyl-6-trifluoromethyl-nicotinonitrile (thiol addition)

A mixture of 2-chloro-6-trifluoromethyl-nicotinonitrile (1.45 mmol), thiol (2.90 mmol), and DBU (2.90 mmol) were dissolved in a acetonitrile (10 mL). The mixture was stirred for 15 h at 50°C. The reaction mixture was extracted with EA (30 mL) twice. . The combined organic extracts were dried over $MgSO_4$, filtered, and concentrated *in vacuo*. The residue was purified by flash column chromatography on silica gel using EA: hexane (1:15) as eluent to afford the desire product.

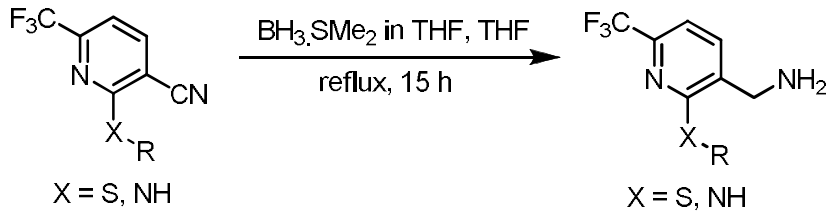

To a solution of SM in THF was added BH_3SMe_2 in THF. The mixture was stirred for 15 hours under reflux condition. After finishing the reaction, the mixture was added water. The reaction mixture was diluted with EA, washed with water, brine and dried over $MgSO_4$, filtered and concentrated. The residue was purified by column chromatography on silica gel to produce the desire C-region amines.

4.8. General procedure for amide coupling (Scheme 19)

To the prepared α-substituted 2-phenylacetic acids (**95**, **100**, **103**, **106**) as A/B-regions (1 equiv.) in THF or DMF was added DIPEA (2.0 equiv.) and HOBt (1.5 equiv.) at ambient temperature. After 10 min, the mixture was added TBTU (1.5 equiv.) and stirred for 1 h. The reaction mixture was added C-region amine (1.2 equiv.) and stirred for overnight. The reaction mixture was diluted with EA, washed with water, brine and dried over $MgSO_4$, filtered and concentrated. The residue was purified by column chromatography on silica gel to produce the final product.

5. References

42. Interational Association for the Study of Pain. 2012, *IASP Taxonomy*, http://www.iasp-pain.org/Taxonomy#Pain, 12 January 2015.

43. Woolf, C. J. *J Clin Invest.* **2010**, 120, 3742-3744.

44. Thienhaus, O.; Cole, B.E. **2002**. *Classification of pain,* In Weiner, R.S. Pain management: A practical guide for clinicians (6 ed.), American Academy of Pain Management.
45. Khairatkar-Joshi, N.; Szallasi, A. *Trends Mol Med.* **2009,** 15, 14-22.
46. Adriaensen, H. *Acta Anaesthesiol Belg.* **1988,** 39, 67-70.
47. Richarz, U.; Jacobs, A.; Spina, E. *Pharmacoepidemiol Drug Saf.* **2012,** 21, 453-462.
48. Mitka, M. *JAMA.* **2003,** 289, 2347-2348.
49. Swift, J. Q.; Roszkowski, M. T. *J Oral Maxillofac Surg.* **1998,** 56, 1081-1085.
50. Hoskin, P. J.; Hanks, G. W. *Drugs.* **1991,** 41, 326-344.
51. Paiotti, A. P.; Marchi, P.; Miszputen, S. J.; Oshima, C. T.; Franco, M.; Ribeiro, D. A. *In Vivo.* **2012,** 26, 381-393.
52. Roth, S. H.; Anderson, S. *Phys Sportsmed.* **2011,** 39, 62-73.
53. Barkin, R. L.; Beckerman, M.; Blum, S. L.; Clark, F. M.; Koh, E. K.; Wu, D. S. *Drugs Aging.* **2010,** 27, 775-789.
54. Roelofs, P. D.; Deyo, R. A.; Koes, B. W.; Scholten, R. J.; van Tulder, M. W. *Spine (Phila Pa 1976).* **2008,** 33, 1766-1774.
55. Frampton, J. E.; Keating, G. M. *Drugs.* **2007,** 67, 2433-2472.
56. Rainsford, K. D. *Subcell Biochem.* **2007,** 42, 3-27.
57. Hilario, M. O.; Terreri, M. T.; Len, C. A. *J Pediatr (Rio J).* **2006,** 82, S206-212.
58. Hunt, R. H.; Harper, S.; Watson, D. J.; Yu, C.; Quan, H.; Lee, M.; Evans, J. K.; Oxenius, B. *Am J Gastroenterol.* **2003,** 98, 1725-1733.
59. Xu, Y.; Oliverson, B. G.; Simmons, D. L. *J Ethnopharmacol.* **2007,** 111, 667-670.
60. Moore, B. C.; Simmons, D. L. *Curr Med Chem.* **2000,** 7, 1131-1144.
61. Silver, R. M.; Edwin, S. S.; Trautman, M. S.; Simmons, D. L.; Branch, D. W.; Dudley, D. J.; Mitchell, M. D. *J Clin Invest.* **1995,** 95, 725-731.

62. Merck, **2003**, *The Merck Manual of Medical Information.* 2nd Home Edition, Whitehouse Station, NJ.

63. Ferrini, F.; Salio, C.; Vergnano, A. M.; Merighi, A. *Pain.* **2007,** 129, 195-209.

64. Caterina, M. J.; Schumacher, M. A.; Tominaga, M.; Rosen, T. A.; Levine, J. D.; Julius, D. *Nature.* **1997,** 389, 816-824.

65. Mandadi, S.; Numazaki, M.; Tominaga, M.; Bhat, M. B.; Armati, P. J.; Roufogalis, B. D. *Cell Calcium.* **2004,** 35, 471-478.

66. Szallasi, A.; Cortright, D. N.; Blum, C. A.; Eid, S. R. *Nat Rev Drug Discov.* **2007**, 6, 357-372.

67. Gharat, L.; Szallasi, A. *Drug Develop Res.* **2007,** 68, 477-497.

68. Vennekens, R.; Owsianik, G.; Nilius, B. *Curr Pharm Des.* **2008,** 14, 18-31.

69. Clapham, D. E.; Julius, D.; Montell, C.; Schultz, G. *Pharmacol Rev.* **2005,** 57, 427-450.

70. Kym, P. R.; Kort, M. E.; Hutchins, C. W. *Biochem Pharmacol.* **2009,** 78, 211-314.

71. Moiseenkova-Bell, V. Y.; Stanciu, L. A.; Serysheva, I. I.; Tobe, B. J.; Wensel, T.G. *Proc. Natl. Acad. Sci. USA.* **2008**, 105, 7451–7455.

72. Gomtsyan, A.; Fatynek, C. R. **2010**, *Vanilloid Receptor TRPV1 in Drug Discovery: Targeting Pain and Other Pathological Disorders*, John Wiley & Sons, Inc., Hoboken, New Jersey.

73. Knotkova, H.; Pappagallo, M.; Szallasi, A. *Clin J Pain.* **2008,** 24, 142-154.

74. Voight, E. A.; Kort, M. E. *Expert Opin Ther Pat.* **2010,** 20, 1107-1122.

75. Jhaveri, M. D.; Elmes, S. J.; Kendall, D. A.; Chapman, V. *Eur J Neurosci.* **2005,** 22, 361-370.

76. Messeguer, A.; Planells-Cases, R.; Ferrer-Montiel, A. *Curr Neuropharmacol.* **2006**, 4**,** 1-15.

77. Hayman, M.; Kam, P. C. A. *Curr. Anaesth. Crit. Care.,* **2008**, 19, 338-343.

78. Pearce, L. V.; Petukhov, P. A.; Szabo, T.; Kedei, N.; Bizik, F.; Kozikowski, A. P.; Blumberg, P. M. *Org Biomol Chem.* **2004,** 2, 2281-2286.

79. Suh, Y. G.; Lee, Y. S.; Min, K. H.; Park, O. H.; Kim, J. K.; Seung, H. S.; Seo, SY; Lee, BY et al. *J. Med. Chem.* **2005**, 48, 5823–5836.

80. Lee, Y.; Hong, S.; Cui, M.; Sharma, P. K.; Lee, J.; Choi, S. *Expert Opin. Ther. Patents.* **2015**, 25, 291-318.

81. Trevisani, M.; Gatti, R.*Open Pain J.* **2013,** 6,108-118.

82. Moran, M. M.; McAlexander, M. A.; Biro, T.; Szallasi, A. *Nat Rev Drug Discov.* **2011,** 10, 601-620.

83. Knotkova, H.; Pappagallo, M.; Szallasi, A. *Clin. J. Pain.***2008**, 24, 142–154.

84. Gavva, N. R.; Bannon, A. W.; Surapaneni, S.; Hovland, D. N.; Lehto, S. G.; Gore, A.; Juan, T.; Deng, H.; Han, B. R.; Klionsky, L.; Kuang, R. Z.; Le, A.; Tamir, R.; Wang, J.; Youngblood, B.; Zhu, D.; Norman, M. H.; Magal, E.; Treanor, J. J. S.; Louis, J. C. *J Neurosci.* **2007,** 27, 3366-3374.

85. Steiner, A. A.; Turek, V. F.; Almeida, M. C.; Burmeister, J. J.; Oliveira, D. L.; Roberts, J. L.; Bannon, A. W.; Norman, M. H.; Louis, J. C.; Treanor, J. J. S.; Gavva, N. R.; Romanovsky, A. A. *J Neurosci.* **2007,** 27, 7459-7468.

86. Wong, G. Y.; Gavva, N. R. *Brain Res Rev.* **2009**, 60, 267-277.

87. Gavva, N. R.; Treanor, J. J. S.; Garami, A.; Fang, L.; Surapaneni, S.; Akrami, A.; Alvarez, F.; Bak, A.; Darling, M.; Gore, A.; Jang, G. R.; Kesslak, J. P.; Ni, L.; Norman, M. H.; Palluconi, G.; Rose, M. J.; Salfi, M.; Tan, E.; Romanovsky, A. A.; Banfield, C.; Davar, G. *Pain.* **2008,** 136, 202-210.

88. Pareek, T. K.; Keller, J.; Kesavapany, S.; Agarwal, N.; Kuner, R.; Pant, H. C.; Iadarola, M. J.; Brady, R. O.; Kulkarni, A. B. *Proc. Natl. Acad. Sci. USA.* **2007,** 104, 660-665.

89. Chizh, B. A.; O'Donnell, M. B.; Napolitano, A.; Wang, J.; Brooke, A. C.; Aylott, M. C.; Bullman, J. N.; Gray, E. J.; Lai, R. Y.; Williams, P. M.; Appleb, J. M. *Pain.* **2007,** 132, 132-141.

90. Tran, P-T.; Kim, H. S.; Ann, J.; Kim, S-E.; Kim, C.; Hong, M.; Hoang, V-H.; Ngo, V. T. H.; Hong, S.; Cui, M.; Choi, S.; Blemberg, P. M.; Frank-Foltyn, R.; Bahrenberg, G.; Stockhausen, H.; Christoph, T.; Lee, J. *Bioorg. Med. Chem. Lett.* **2015**, .

91. (a) Walpole, C.S.; Wrigglesworth, R.; Bevan, S.; Campbell, E.A.; Dray, A.; James, I.F.; Perins, M.N.; Reid, D.J.; Winter, J. *J. Med. Chem*. **1993**, 36, 2362-2372. (b) Walpole, C.S.; Wrigglesworth, R.; Bevan, S.; Campbell, E.A.; Dray, A.; James, I.F.; Masdin, K.J.; Perkins, M.N.; Winter, J. *J. Med. Chem*. **1993**, 36, 2373-2380.

92. Lee, J. H.; Lee, Y.; Ryu, H.; Kang, D. W.; Lee, J.; Lazar, J.; Pearce, L. V; Pavlyukovets, V. A.; Blumberg, P. M.; Choi, S. *J. Comput. Aided Mol. Des.* **2011**, 25, 317-327.

93. Kim, M. S.; Ryu, H.; Kang, D. W.; Cho, S-H.; Seo, S.; Park, Y. S.; Kim, M-Y.; Kwak, E. J.; Kim, Y. S.; Bhondwe, R. S.; Kim, H. S.; Park, S-g. Son, K.; Choi, S.; DeAndrea-Lazarus, I.; Pearce, L. V.; Blumberg, P. M.; Frank, R.; Bahrenberg, G.; Stockhausen, H.; Kögel, B. Y.; Schiene, K.; Christoph, T.; Lee, J. *J. Med. Chem*. **2012**, 55, 8392-8408.

94. Thorat, S. A.; Kang, D. W.; Ryu, H.; Kim, M. S.; Kim, H. S.; Ann, J.; Ha, T-H.; Kim, S. E.; Son, K.; Choi, S.; Blumberg, P. M.; Frank, R.; Bahrenberg, G.; Schiene, K.; Christoph, T.; Lee, J. *Eur. J. Med. Chem.* **2013**, 64, 589-602.

95. Ha, T-H; Ryu, H.; Kim, S-E.; Kim, H. S.; Ann, J.; Tran, P-T.; Hoang, V-H.; Son, K.; Cui, M.; Choi, S.; Blumberg, P. M.; Frank, R.; Bahrenberg, G.; Schiene, K.; Christoph, T.; Frormann, S.; Lee, J. *Bioorg. Med. Chem.* **2013**, 21, 6657-6664.

96. Ryu, H.; Seo, S.; Cho, S-H.; Kim, H. S.; Jung, A.; Kang, D. W.; Son, K.; Cui, M.; Hong, S-h.; Sharma, P. K.; Choi, S.; Blumberg, P. M.; Frank-Foltyn, R.; Bahrenberg, G.; Stockhausen, H.; Schiene, K.; Christoph, T,; Frormann, S.; Lee, J. *Bioorg. Med. Chem. Lett.* **2014**, 24, 4039-4043.

97. Ryu, H.; Seo, S.; Cho, S-H.; Kim, M. S.; Kim, M-Y.; Kim, H. S.; Ann, J.; Tran, P-T.; Hoang, V-H,; Byun, J.; Cui, M.; Son, K.; Sharma, P. K.; Choi, S.; Blumberg, P. M.; Frank-Foltyn, R.; Bahrenberg, G.; Koegel, B-Y.; Christoph, T.; Frormann, S.; Lee, J. *Bioorg. Med. Chem. Lett.* **2014**, 24, 4044-4048.

98. Selvakumar, N.; Reddy, Y. B.; Kumar, G. S.; Iqbal, J. *Tet. Lett*. **2001**, 42, 8395-8398.

99. (a) Stahly, G. P.; Stahly, B. C.; Lilje, K. C. *J. Org. Chem.* **1984**, 49, 579-580. (b) Makosza, M.; Winiarski, J. *J. Org. Chem.* **1984**, 49, 1494-1499.

100. Ryu, H.; Jin, M-K.; Kang, S-U.; Kim, S. Y.; Kang, D. W.; Lee, J.; Pearce, L. V.; Pavlyukovets, V. A.; Morgan, M. A.; Tran, R.; Toth, A.; Lundberg, D. J.; Blumberg, P. M. *J. Med. Chem*. **2008**, 51, 57-67.

101. The 3D structure of the **122** was generated with Concord and energy minimized with a MMFF94s force field and MMFF94 charge until the rms of the Powell gradient was 0.05 kcal $mol^{-1}A^{-1}$ in SYBYL-X 2.0 (Tripos Int., St. Louis, MO, USA). The flexible docking study on our *h*TRPV1 model was carried out using GOLD v.5.2 (Cambridge Crystallographic Data Centre, Cambridge, UK), which uses a genetic algorithm (GA) and allows for full ligand flexibility and partial protein flexibility. The binding site was specified as 8 Å around the capsaicin complexed in the *h*TRPV1 model. The side chains of the nine residues which are important for ligand binding, (i.e., Tyr511, Ser512, Met514, Leu515, Leu518, Phe543, Leu547, Thr550, and Asn551) were allowed to be flexible with 'crystal mode' in GOLD. **122** was docked with the GoldScore scoring function, and the other parameters

remained as default. All the computation calculations were undertaken on an Intel® Xeon™ Quad-core 2.5 GHz workstation with Linux Cent OS release 5.5.

102. Cheng, Y-C.; Prusoff, W. H. *Biochem. Pharmacol.* **1973**, 22, 3099-3108.

Acknowledgements

First of all, I would like to express my deepest gratitude to my supervisor **Professor Jeewoo Lee**, Lab of Medicinal Chemistry, College of Pharmacy, Seoul National University (SNU), Korea for his encouragement, advice, monitoring and research support throughout my studies. In pursuing my Ph.D. research works, I simply appreciate the inspiration and freedom he has given to me. Without his support, I would not have been able to pursue my Ph.D degree and stay in Korea. Besides, supervisor's continuous encouragement, guidance, support and friendly professional attitude, he always played an important role in my entire doctoral study and would also inspiration for my future.

I pay sincere thanks to my Professors in Hanoi University of Pharmacy, Hanoi, Vietnam, specially, Professor Nguyen-Hai Nam, Head of Department of Pharmaceutical Chemistry, for his support and encouragement.

I would like to thank Dr. Kwangsoo Lim, Dr. MyeongSeop Kim, Dr. Yong Soo Kim, Dr. Yongsung Cho, Dr. Rahul S. Bhonwe, Dr. Wei Sun, Dr. Shivaji A. Thorat, Dr. Tae-Hwan Ha, Dr. Sung-Eun Kim for their initial help and continuous support in Lab. My special thanks and gratitude goes to “my sister” JiHyae Ahn for her great help during my entire life in SNU in particular, and in

Korea in general. Her friendly nature and hard work will take her to a good position; I wish her a very good luck for her future life. I would be pleased to thank my friend Ho Shin Kim for his encouragement and help. The members of the Lab of Medicinal Chemistry have contributed immensely to my personal and academic life at SNU. I would like to thank my Vietnamese friends Van-Hai Hoang, Van T. H. Ngo for their friendly, and kinds words which made my days. My colleagues KwangHyun Choi brother, KyeongCheon Kim brother, HyungKyung Park, Hye Jin Yoon, Hobin Lee, Yooran Ki, Suyoung Yoon, Aeran Jung, Sunho Lee brother, Changhoon Kim, Mannkyu Hong, JiSu Beak… deserve special thanks because they helped me a lot for managing the Lab machine, logistic support, conference registration etc. It was a great fun working with them. I would also like to thank the faculty and staff of College of Pharmacy for supporting my academic work.

I would like to express my gratitude to all the members of the SNU Vietnamese students for the community feelings; especially, for their long-lasting supportive hand for me throughout my stay period in Korea. I am grateful to my friends in College of Pharmacy in SNU for their keen interest for the betterment of the community. The sweet memories at every moment during the staying at SNU are unforgettable.

My heartfelt gratitude goes to all of my family members for their unflagging support throughout my life. I would like to acknowledge and show my deepest gratitude to my parents, my parents in law, brothers & sisters for their unconditional love, praying to the Almighty and encouragement. Their full confidence in me and mental support encouraged me a lot to continue this work. They had no idea on the topic of my research, but always helped me to pursue my goals.

My heartiest thanks go to my husband Do The Cuong, who has encouraged me in every stages of this study period. Without his love and intensive care, it would be entirely impossible for me to achieve this grand success.

There are numerous nice wishers too who have shown me their constant support and friendship in various ways, directly or indirectly related to my academic life. I will remember them from the depth of my heart and hope to find a more appropriate place to acknowledge them in the future.